California State University, Monterey Bay

Digital Commons @ CSUMB

Capstone Projects and Master's Theses

Fall 2022

Measuring the Impact of Thermal Stress on Coral Resilience in Hawai'i Using Large-Area Imagery

Caroline Rodriguez

MEASURING THE IMPACT OF THERMAL STRESS ON CORAL

RESILIENCE IN HAWAI'I USING LARGE-AREA IMAGERY

_____

A Thesis

Presented to the

Faculty of

Moss Landing Marine Laboratories

California State University Monterey Bay

_____

In Partial Fulfillment

of the Requirements for the Degree

Master of Science

in

Marine Science

_____

by

Caroline Rodriguez

Term Completed: Fall 2022

CALIFORNIA STATE UNIVERSITY MONTEREY BAY

The Undersigned Faculty Committee Approves the

Thesis of Caroline Rodriguez:

MEASURING THE IMPACT OF THERMAL STRESS ON CORAL

RESILIENCE IN HAWAI'I USING LARGE-AREA IMAGERY

_____
Cheryl Logan, Co-Chair
Department of Marine Science, California State University Monterey Bay

_____
Amanda Kahn, Co-Chair
Moss Landing Marine Laboratories, San Jose State University
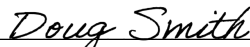

_____
Thomas Oliver
NOAA Pacific Islands Fisheries Science Center, Honolulu

_____
Thomas Connolly
Moss Landing Marine Laboratories, San Jose State University

_____
Doug Smith
CSUMB Interim Dean of Graduate Studies & Research

_____
12/18/2022
Approval Date

ABSTRACT

Measuring the Impact of Thermal Stress on Coral Resilience in
Hawai'i Using Large-Area Imagery
by
Caroline Rodriguez
Master of Science in Marine Science
Moss Landing Marine Laboratories &
California State University Monterey Bay, 2022

Coral reefs worldwide are declining due to several anthropogenic stressors, but rising ocean temperature is the most serious threat to coral reef persistence. Developing models that document changes in coral communities following thermal stress events and forecast trends in reef recovery is crucial in identifying resilient reefs. Traditional approaches to generating the coral vital rates necessary for demographic modeling are time consuming and field intensive; however, by leveraging Structure-from-Motion photogrammetry, we can accurately track populations over time at a large spatial scale. In this study, I assessed the population dynamics of the dominant coral species across the Hawaiian archipelago and investigated the impact of thermal stress on coral populations. The annual growth, survival and recruitment of 3,852 coral colonies (5,636 unique colony-level transitions) for 3 genera was recorded at 16 sites spanning the Hawaiian archipelago across 14 intervals from 2013 to 2019, including 3 bleaching events. These data were used to estimate vital rates (growth, survival, and recruitment) and build integral projection models to determine the impact of thermal stress on population growth. To overcome the inherent challenges in estimating coral reproduction, I modeled recruitment in four different ways and present a comparison of data-rich to data-poor estimation methods. Degree Heating Week output from the NOAA Coral Reef Watch daily global 5km satellite was used to estimate thermal conditions at each site by calculating temperature stress severity (the mean of all maximum thermal anomalies) and frequency (number of thermal stress events per 10 years). I found that all three coral genera, which have different morphologies and life-history strategies, had negative population growth rates. As expected, smaller colonies experienced faster growth, but large colonies had a high probability of shrinking, due to partial mortality. Large, multi-fragmented colonies had high survivorship and it may be advantageous for larger colonies to fragment into smaller pieces to avoid total mortality. Population dynamics were primarily driven by coral growth and survival and should be targeted in future restoration and adaptation projects. Additionally, across all taxa, population growth rates (λ) varied spatiotemporally, but most sites exhibited a declining population growth rate ($\lambda < 1$). While increased severity and frequency of thermal stress events negatively impacted the population growth rate of massive *Porites* corals, there was no signal of this effect on encrusting *Montipora* corals. I demonstrate that despite variations in the responses observed among taxa, there is an overall expected population decline across the Hawaiian archipelago. While most coral population growth rates are higher following bleaching events, signifying recovery, the projected increase in both the severity and frequency of thermal anomalies may overwhelm corals' ability to recover and threaten coral population persistence.

TABLE OF CONTENTS

LIST OF TABLES

LIST OF FIGURES

ACKNOWLEDGEMENTS

INTRODUCTION

Coral reefs protect coastlines from storm surges and erosion, support local economies through tourism, and uphold diverse ecosystems that sustain important fisheries (Wilkinson 2004, Costanza et al. 2014). Coral reefs are the most diverse marine ecosystems and are home to nearly one-quarter of all marine species (Wilkinson 2004); however, reefs worldwide are rapidly declining from a variety of anthropogenic stressors (Pandolfi et al. 2003). Global climate change stressors, such as rising ocean temperatures, ocean acidification, and related epidemics of infectious diseases threaten coral reef persistence (McClanahan et al. 2002, Hughes et al. 2003, Wilkinson 2004, Burke et al. 2011); however, rising ocean temperature is the most serious, medium-term climate change threat (Hughes et al. 2003). The projected increase in the frequency and severity of temperature stress on coral reefs is incredibly rapid and widespread, such that the majority of reefs worldwide are expected to experience thermal stress by 2030-2050 (Donner et al. 2005), potentially leading to widespread mortality. Yet some corals appear to be more heat tolerant than others, suggesting that certain individuals and species are more resilient to temperature change (Baker et al. 2004, Donner et al. 2005, Oliver & Palumbi 2011, Howells et al. 2012, Palumbi et al. 2014, Heron et al. 2016b). Differential responses among taxa or individuals may be due to biological differences including physical characteristics (e.g. colony morphology and tissue thickness) (Loya et al. 2001, Van Woesik et al. 2012, Wooldridge 2014), capacity for adaptation or acclimatization (Coles & Brown 2003, Oliver & Palumbi 2011, Howells et al. 2012, Palumbi et al. 2014, Grottoli et al. 2014, Putnam & Gates 2015, Ainsworth et al. 2016, Jury & Toonen 2019), ability to recover (Marshall & Baird 2000, Loya et al. 2001, McClanahan 2004, Schoepf et al. 2015), or fine-scale environmental differences in microhabitat (Jokiel & Brown 2004, Cunning et al. 2016). Given the number of biological factors that contribute to coral resilience, it is challenging to predict which corals will survive thermal stress events.

Thermal anomalies can lead to coral bleaching, a stress response where the symbiotic relationship between a coral host and its photosynthetic endosymbiotic algae breaks down and the algae are expelled, turning the coral white (Glynn 1984). This process can occur under accumulated temperature stress as minimal as 1-2°C above the summertime mean temperature for a period of a few weeks (Brown 1997) and this can lead to mortality if the heat anomaly persists. Bleaching is often predicted by calculating a Degree Heating Week (DHW) (Liu et al. 2013), which quantifies heat stress accumulation in an area over the past 12 weeks by summing temperature exceeding the bleaching threshold for a particular region (1°C warmer than the highest monthly mean temperature) during that time period (Glynn & D'Croz 1990, Skirving et al. 2020). The units for DHW are degree C-weeks. When heat stress reaches four degree-C weeks, significant coral bleaching is likely; when it reaches eight degree-C weeks, severe, widespread bleaching may occur (Eakin et al. 2010, Heron et al. 2016a).

FACTORS AFFECTING BLEACHING RECOVERY

Corals can recover from short-term bleaching events, but bleaching can negatively impact corals at the individual and population level. Corals cannot survive extended periods without their symbionts because they provide corals with oxygen and more than 90% of their nutrients (Falkowski et al. 1984). Bleaching compromises coral survival and can lead to starvation, diminished algal photosynthetic rates and translocation of nutrients to the coral host, and increased disease susceptibility (Jones 2008, Schoepf et al. 2015, Riegl et al. 2018, Barkley et al. 2018, Eakin et al. 2019). Coral bleaching impacts coral demographics by causing partial (Jones 2008) and total mortality (Baird & Marshall 2002, Roth et al. 2010) and decreasing reproductive output (Arizmendi-Mejía et al. 2015). Corals can tolerate short periods of bleaching or recurrent bleaching events, but they need time to recover and regain their symbionts following a bleaching event. While individual corals can recover in less than two years (Matsuda et al. 2020), reef recovery time varies drastically — rapid recovery has been observed less than seven years following several disturbances in some reefs (Edmunds 2018) while other reefs required nearly 10 years to recover (McClanahan 2014), and other isolated

populations did not fully recover for 12 years (Gilmour et al. 2013). The time needed to recover also depends on several factors, including recruitment conditions, larval supply, and herbivorous grazing pressure (McClanahan 2014, Schoepf et al. 2015, Gouezo et al. 2019), and this makes it difficult to determine which factors drive resilience to thermal stress at the population level. Because population recovery is not fully understood, we cannot accurately predict how long a reef will take to recover from a bleaching event.

Corals exhibit different bleaching responses, and the recovery process varies based on many factors including taxa, morphology, size and environment. While certain genera, such as *Acropora*, *Stylophora*, *Seriatopora*, and *Pocillopora* are highly susceptible to bleaching, others including *Cyphastrea*, *Turbinaria*, *Galaxea*, *Goniopora*, and *Porites* are highly resistant (Marshall & Baird 2000, Loya et al. 2001, McClanahan 2004). Differential susceptibility to bleaching is also linked to both colony morphology and tissue thickness (Loya et al. 2001, Van Woesik et al. 2012, Wooldridge 2014). Branched and corymbose (dense, irregular branching) growth forms and thin tissue layers are more susceptible to bleaching while massive and encrusting growth forms with thick tissue layers are more resistant to thermal stress (Marshall & Baird 2000, Loya et al. 2001, McClanahan 2004, Darling et al. 2012, Wooldridge 2014). Additionally, there is interspecific variation in coral bleaching response (Marshall & Baird 2000, Obura 2001, Brandt 2009, Schoepf et al. 2015, Jury & Toonen 2019).

Different species from the same genus and individual colonies from the same species exhibit different bleaching responses, suggesting that certain individual colonies are able to withstand thermal stress (Jokiel & Coles 1974, Jokiel 2004) due to acclimatization (Coles & Brown 2003, Mieog et al. 2007, Oliver & Palumbi 2011, Putnam & Gates 2015, Ainsworth et al. 2016, Jury & Toonen 2019) or genetic makeup. When the more thermally tolerant colonies reproduce, the population may adapt over time and become less susceptible to bleaching (Palumbi et al. 2014, Grottoli et al. 2014, Putnam & Gates 2015, Ainsworth et al. 2016, Bay et al. 2017). Coral size may also impact bleaching response. Smaller colonies may be more affected by bleaching (Edmunds 2005, 2015), which can cause decreased survival and shift the population size frequency distribution toward larger colonies (Roth et al. 2010) and may reduce genetic variance. Nonetheless, the impact of bleaching on growth may be independent of size

across taxa due to the variability of growth rates among species (Baird & Marshall 2002, Kodera et al. 2020). Finally, environmental conditions and thermal history can be site specific, which can lead to different recovery trajectories at different sites. Natural conditions like habitat and depth can impact coral response to a widespread thermal anomaly and cause patch recovery between sites (Golbuu et al. 2007). Recovery can also vary regardless of similar thermal history. For example, despite exposure to the same repeat bleaching events, reefs at one atoll in the Chagos Archipelago exhibited different recovery trajectories (Sheppard et al. 2008). Differential bleaching responses make it difficult to predict how coral communities will respond to climate change and warrant further investigation.

POPULATION MODELING

Traditional monitoring methods of quantifying coral percent cover do not reveal the drivers of reef recovery like investigating colony-level demographics can. Coral cover alone is limited as an indicator of resilience or recovery because it can only be used to quantify the outcome of disturbance events (Brito-Millán et al. 2019). An innovative method is to measure demographic processes that contribute to population change. Size-dependent, life-history and morphologically focused demographic approaches are useful in revealing the drivers of population structure and recovery and can be used to make projections of coral community trajectories (Brito-Millán et al. 2019, Kodera et al. 2020). Demographic metrics—or vital rates—for corals include survival, growth, and recruitment. The growth rate is the probability of growth (increase in size) given survival and survival is defined as the probability of surviving from one year to the next at a given size. The third vital rate is the probability of recruitment, which is the expected number of recruits of a certain size. When combined, these vital rates regulate population dynamics and can be used to estimate the population growth rate (Savage et al. 2004). These data can also be combined with thermal history and used to model how coral population sizes are expected to change under future climate change projections.

Population modeling approaches that describe the transition of a population from one time point to another can be useful tools to assess population dynamics and project

recovery trajectories. Examples of population models commonly used in ecology are Leslie matrices and Integral Projection Models (IPMs). Leslie matrices project future population growth by using the past population size and the likelihood of an individual transitioning from one age class to another (Caswell 2001); however, Leslie matrices disregard variability among individuals because they use discrete age classes that are arbitrarily chosen and often biologically irrelevant when applied to corals (Easterling et al. 2000, Burgess 2011). While it is logical to divide the life cycle of some organisms (i.e., plants or insects) into discrete classes, coral demographic processes are more strongly linked to size than age (Hughes & Connell 1987), thus, corals are best modeled through continuous functions like size (Merow et al. 2014). Using a demographic model that uses continuous functions rather than discrete classes and treats each individual separately will allow for a more robust assessment of coral population dynamics.

IPMs are a different modeling technique that incorporate information on how an individual's state (i.e., age or size) influences its vital rates to project changes in a population (Merow et al. 2014). Continuous integrals are used to capture the aggregated contributions of each individual to overall population growth (Caswell 2001, Edmunds et al. 2014). Changes in vital rates can have an effect on the population growth rate, which can be analyzed using an elasticity analysis. Elasticity analyses can be used to explain which demographic mechanisms drive population dynamics by estimating the effect of a proportional change in the vital rates on the population growth rate, lambda (λ). For example, an increase in the probability of recruitment and survival may result in higher population growth rates as more individuals are added to the population or are not removed from the population. With these analyses, demographic parameters can be manipulated in silico to determine which vital rates drive the population growth (Caswell 2001) and inform resilience-based management. With demographic metrics such as growth, mortality, and recruitment for a given population of corals, we can determine the processes that are most likely to increase resilience to thermal stress and explore the impacts of environmental factors such as ocean warming on reef population dynamics. As a result, it will be more feasible to project how coral populations will react to increasing frequency and severity of thermal stress events.

CENSUSING POPULATIONS USING PHOTOGRAMMETRY

Photogrammetry is a novel method that can be used to accurately track populations over time at a large spatial scale and collect the demographic data necessary for population modeling. Bleaching is typically detected by individual researchers tracking small reef areas for a short period of time (Jones 2008, Brandt 2009, Roth et al. 2010, Gintert et al. 2018) or using citizen science programs like Reefbase (http://www.reefbase.org). While measuring individual corals' response to increased temperature can elucidate patterns in species-specific recovery, individualistic approaches poorly represent community-level trends and do not explain why bleaching patterns vary between coral communities. To understand how communities will respond to the increasing frequency and intensity of thermal stress events (Donner et al. 2005, Hughes et al. 2018), it is necessary to first understand how coral population dynamics influence community trends. Structure-from-Motion (SfM) photogrammetry is a powerful approach to track and assess demographic processes and bleaching over large areas of the ocean, without having to rely on complex field operations (Burns et al. 2015, Edwards et al. 2017, Kodera et al. 2020). SfM photogrammetry is an automated range imaging technique that processes images from multiple camera angles to create 3D models (Fonstad et al. 2013). The 3D models can be converted into orthorectified 2D imagery, or orthoprojections (Naughton et al. 2015). These orthoprojections can be used to observe colony-level changes over time (Kodera et al. 2020) at large numbers of sites. SfM photogrammetric technology enables biologists to estimate coral demographics including growth, survival, and recruitment with centimeter-scale resolution and accurately quantify population change.

Hawai'i is an ideal system to investigate bleaching susceptibility and resilience using SfM photogrammetry because Hawaiian reefs have experienced four large-scale bleaching events in the last 23 years. Over 60 percent of coral reefs in the United States are in the Hawaiian Archipelago, which is divided into two regions, the Main Hawaiian Islands (MHI) and the Papahānaumokuākea Marine National Monument in the Northwestern Hawaiian Islands (NWHI). The MHI have relatively high coral cover (0.9 - 33%) while the NWHI have relatively low coral cover (4-25%) and three genera, *Porites*,

Pocillopora, and *Montipora*, account for more than 90% of total coral cover in the MHI (Franklin et al. 2013) and NWHI (Kenyon et al. 2006, 2007a b, 2008). Hawaiian reefs have been heavily disturbed over the past three decades, but thermal stress events have not been uniform in intensity or scale. The first documented, large-scale coral bleaching in Hawai'i occurred in 1996, followed by another major bleaching event in the Northwestern Hawaiian Islands (NWHI) in 2002 (Jokiel & Brown 2004) and consecutive bleaching events in 2014 and 2015 in both regions (Hughes et al. 2018, Sale et al. 2019). Throughout the archipelago there has been variation in the extent and intensity of bleaching events, providing a natural experiment for comparing bleaching susceptibilities and assessing resilience following disturbance events.

RESEARCH QUESTIONS

The primary goals of this thesis were to assess population dynamics of the dominant coral species across the Hawaiian Archipelago using SfM photogrammetry and to determine the effect of thermal stress events on coral populations. Specifically, my first research question focused on determining if population growth rates (λ) differed between three genera – *Porites*, *Pocillopora*, and *Montipora*. I expected that the population growth rate (λ) would differ between the three genera due to their morphological differences. I expected that massive *Porites* would likely be the most resistant to thermal stress because despite slow growth, their high fecundity and low mortality (Darling et al. 2012) would enable the population growth rate to increase. Branching *Pocillopora* spp. was hypothesized to be the most susceptible to thermal anomalies (Loya et al. 2001). I predicted that high mortality following bleaching would outweigh fast growth (McClanahan 2004, Barkley et al. 2018) and lead to a decreasing population size. The encrusting *Montipora* spp. grow quickly and are capable of recolonizing an area following disturbance, but can be affected by temperature stress, which causes high mortality (Adjeroud et al. 2009, Darling et al. 2012, Barkley et al. 2018). Therefore, I hypothesized that these populations would initially decline following a bleaching event but stabilize in the long-term.

My second research question investigated which vital rate(s) would most influence the population growth rate to determine appropriate targets for management decisions. Life-history differences between taxa may also affect which vital rates drive the population growth rate. I expected that recruitment would have the largest effect on *Porites* population growth because changes to their high fecundity during episodic spawning events could reduce the population growth. I also expected that growth would have the biggest impact on *Montipora* and *Pocillopora* spp. because their fast growth rate is necessary to maintain the population despite their susceptibility to bleaching.

The different islands in the Hawaiian archipelago have unique thermal histories that may impact coral demographics. For my third research question, I aimed to determine if the frequency and/or severity of thermal stress events correlated to changes in coral population growth. Frequent thermal stress events may enhance coral resilience to temperature stress and allow them to recover faster than corals experiencing infrequent thermal stress events (Thompson & van Woesik 2009), but they may exhibit an increase in mortality (Montero-Serra et al. 2019). These corals may also experience stable or slightly slower growth rates and decreased recruitment due to reallocation of resources to survival (Szmant & Gassman 1990). I hypothesized that decreased survival and recruitment from recurrent temperature anomalies would result in decreased population growth. A history of severe thermal stress events may also lead to a decrease in the population growth rate that may result in the extirpation of the affected populations (Montero-Serra et al. 2018) because severe bleaching events may overwhelm corals already living close to their thermal maximum. I expected that corals exposed to more severe thermal stress events would have a decreased growth rate (Hernández-Pacheco et al. 2011) due to the increase in partial mortality and fission (Edmunds 2015) and decreased survival due the rapid onset of a severe event. I also expected to observe decreased recruitment because partial mortality due to bleaching may result in small, fragmented colonies dominating the population (Hernández-Pacheco et al. 2011) and these smaller colonies are less likely to be reproductive and fragments reduced in size may lose their reproductive ability (Szmant 1991).

METHODS

To determine which biological factors influence coral reef recovery following a bleaching event in Hawai'i, I used repeated fixed site orthoprojections to estimate coral vital rates between 2013 and 2019 for seven of the dominant coral species in Hawai'i from three genera. Although vital rates are crucial in structuring demographic outcomes, few researchers have measured individual coral vital rates at extensive spatial or temporal scales. This is due to the difficulty of tracking the fate of a large number of colonies underwater and this limits the feasibility of conducting demographic analyses at a significant spatial scale (Edwards et al. 2017). To address this problem, I worked with the National Oceanographic Atmospheric Administration (NOAA) Pacific Islands Fisheries Science Center (PIFSC) to develop a workflow that estimates coral vital rates using photogrammetry from SCUBA surveys to determine how vital rates vary across sites and between islands (Rodriguez et al. 2021).

The overall method includes compiling images from SCUBA surveys conducted by the 100 Island Challenge and NOAA PIFSC, generating multi-year 3D models of reefs, aligning the models to visualize the difference between years, generating 2D orthoprojections, and outlining live coral patches of contiguous live tissue in every timepoint. Individual coral colonies were censused in each timepoint, including when a colony broke into numerous patches. The network of patches was used to measure the change in colony size over time (Rodriguez et al. 2021). Using this workflow that I co-led and developed, users can rapidly generate accurate colony-level vital rate estimates across thousands of coral colonies at numerous sites per region compared to tens of colonies at a few sites using traditional *in situ* methods. I used this workflow to generate vital rates and construct an Integral Projection Model (IPM) to determine which vital rates influenced the persistence of certain coral taxa following a bleaching event, at different sites around the Hawaiian Islands. Below, I describe the study system, how vital rates were extracted from orthoprojections and modeled, and the IPM used to estimate coral population growth rates by site, time interval, and genus.

STUDY SYSTEM

Similar to other islands around the Indo-Pacific, Hawaiian archipelago waters show a trend of increasing water temperature and bleaching events. By studying islands experiencing differing degrees of temperature stress, it is possible to investigate the impacts of thermal stress on coral populations. The Hawaiian Islands are an archipelago of islands, atolls, and seamounts. The Hawaiian archipelago provides an ideal study site with islands that span almost 2,500 kilometers, each with a unique thermal history. The entire Hawaiian archipelago features mild air temperatures year-round and infrequent severe storms. The archipelago is divided into two regions: the Main Hawaiian Islands (MHI) and the Papahānaumokuākea Marine National Monument in the Northwestern Hawaiian Islands (NWHI).

Focal sites were selected based on their thermal history (Figure 1), from a larger set of sites curated by NOAA where multiple timepoints of imaging were available. A total of sixteen sites were chosen for this study (Figure 2) because they fall along a gradient of thermal stress event severity and frequency (Figure 3). For severity, Degree Heating Week (DHW) data from the NOAA Coral Reef Watch daily global 5km satellite data from 1985 to January 2020 was used to calculate event severity by averaging the number of DHW events greater than one or greater than four over a ten-year period (Liu et al. 2014, Skirving et al. 2020). Nine sites were chosen along a gradient of event severity, including two sites in the Kahekili Marine Reserve near Kaanapali on the western side of Maui ("MAI") and one site near Olowalu on the southwestern side of Maui (Figure 2). The other sites, four on the Big Island of Hawai'i ("HAW") and two on Oahu ("OAH"), were sampled two to three times between 2015 and 2019. Using the same DHW satellite data, event frequency was calculated by averaging the number of DHW events in a 10-year period. Next, seven additional sites were chosen because they fall along a gradient of thermal stress frequency. One site Pearl and Hermes ("PHR"), two sites on French Frigate Shoals ("FFS"), and Lisianski ("LIS") were all sampled in 2013, 2016, and 2019. One site on Maui, on the Big Island of Hawai`i, and on Kure ("KUR") were only sampled in 2016 and 2019. In total, coral vital rates and population

dynamics were estimated for 16 sites (Figure 2, Supplementary Table 1) and across all sampled years from 2013-2019, for a total of 51 orthoprojections.
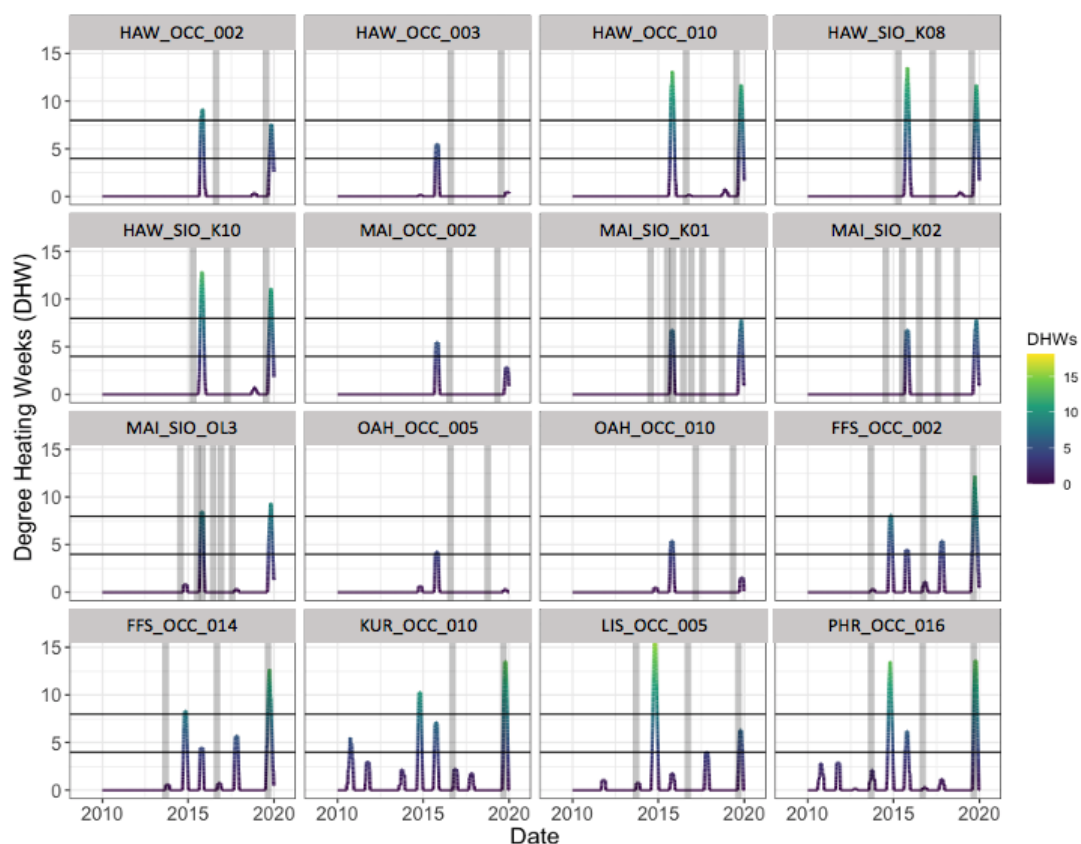
Figure 1. Thermal history of the sixteen fixed sites in the Hawaiian archipelago between 2010 and 2020 in Degree Heating Weeks (DHW). Vertical gray bars represent sample years when photogrammetry images were taken at each site. Horizontal gray bars indicate mild to moderate coral bleaching (DHW ≥ 4) and severe, widespread bleaching (DHW ≥ 8). Site IDs correspond to NOAA National Coral Reef Monitoring Program sites in which OCC refers to NOAA's Oceans and Climate Change Team and SIO refers to sites initially observed by the 100 Island Challenge team at Scripps Institution of Oceanography. Abbreviations: HAW: Big Island of Hawai'i; MAI: Maui; OAH: Oahu; FFS: French Frigate Shoals; KUR: Kure; LIS: Lisianski; PHR: Pearl and Hermes.
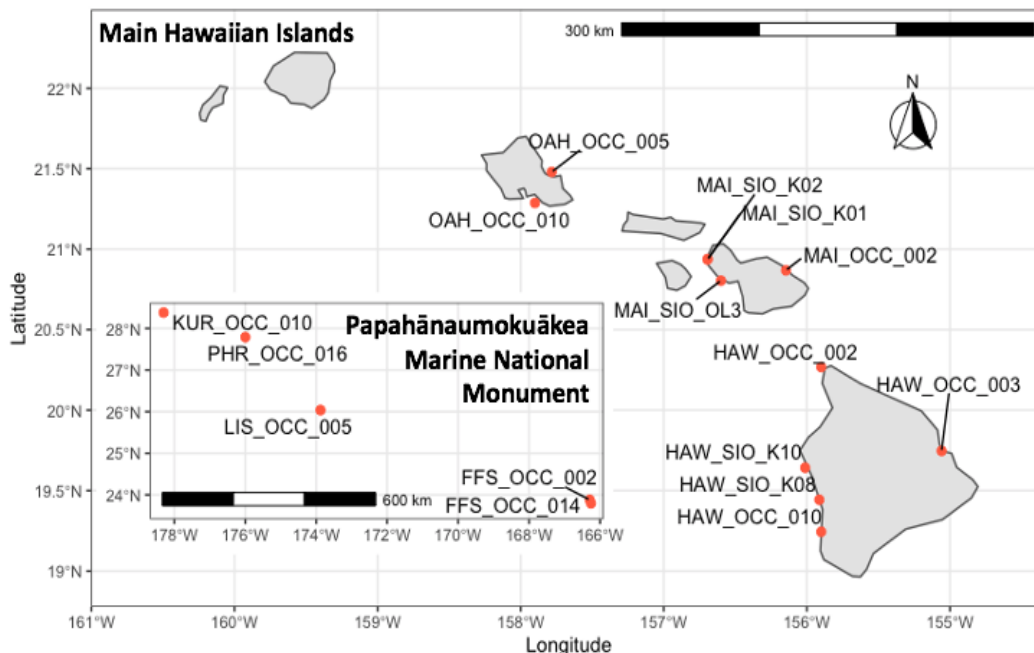
Figure 2. Sixteen fixed sites in the Main Hawaiian Islands and Papahānaumokuākea Marine National Monument used to assess coral population recovery in this study.
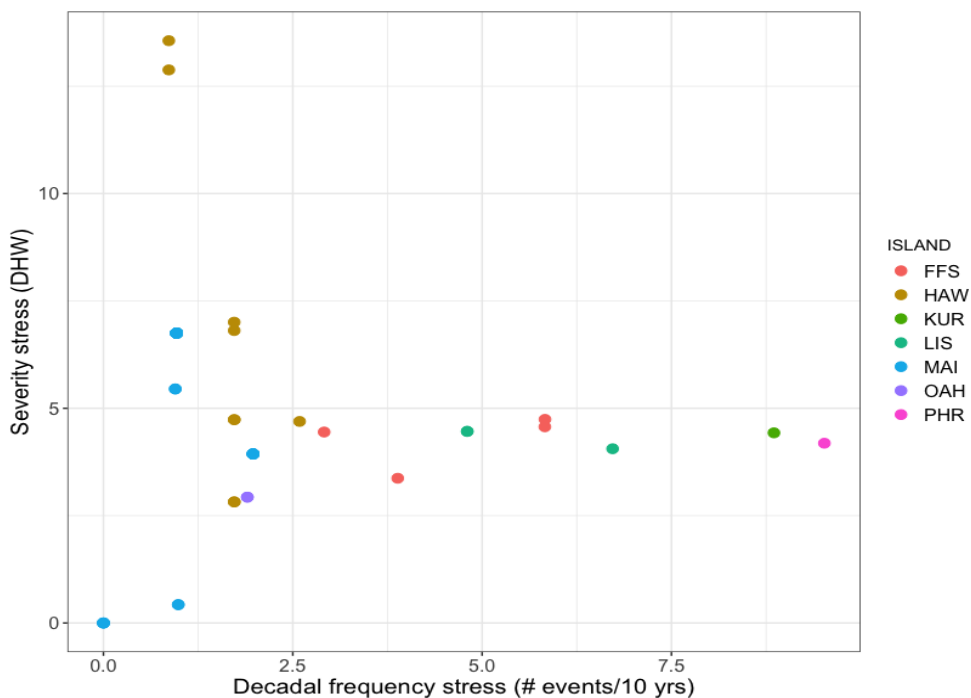
Figure 3. Thermal history of study sites in the Main Hawaiian Islands and Papahānaumokuākea Marine National Monument by thermal stress frequency and severity.

STRUCTURE-FROM-MOTION PHOTOGRAMMETRY

IMAGERY COLLECTION

NOAA PIFSC and the 100 Island Challenge (https://100islandchallenge.org/) collected images at the 16 fixed sites used in this study (Figure 2). Due to the large spatial area that NOAA PIFSC is tasked with studying, *in situ* benthic monitoring is conducted every three years. 100 Island Challenge SCUBA divers placed four reference markers with known scale bars (Ground Control Points, GCPs) on the benthos and collected thousands of images at each study site between February and September from 2013 through 2018 following the methods of the Scripps Institute of Oceanography 100 Island Challenge (Naughton et al. 2015). In brief, SCUBA divers collected images with an 18mm camera lens and 6" dome port. Images were collected from a top-down view with slightly changing angles to capture structurally complex reefs while maintaining a one-meter distance from the substrate. Divers swam in a back-and-forth "mowing the lawn" pattern as this swim pattern ensured that every part of the reef was captured by numerous camera angles (Pizarro et al. 2017). NOAA PIFSC SCUBA divers also collected imagery in 2019 by placing two GCPs on the substrate and swimming in a spiral (Rodriguez et al. 2021), which captures several camera angles and is easier to conduct than the back-and-forth swimming method. NOAA PIFSC scientists post-processed these photos and ensured that they met quality requirements (removing photos of blue water, fins, hands, blurry photos, etc.) and, if needed, edited photo exposure following methodology by (Suka et al. 2019) before use in the 3D models.

IMAGERY PROCESSING

Underwater images were stitched together by NOAA PIFSC and 100 Islands Challenge scientists to form orthomosaics for each site. The photogrammetry software program Agisoft Metashape was used to generate a 3D dense point cloud (DPC) (Naughton et al. 2015), a geometrically accurate 3D model that serves as a detailed reconstruction of the reef. To construct the DPC, overlapping images were processed and

aligned to form a sparse point cloud. The sparse point cloud was scaled by adding Ground Control Points (GCPs) of known length (0.5 meters).

Next, NOAA researchers and I used an identifiable feature in each 3D model to align the DPCs from multiple years at the same site using Viscore software (Petrovic et al. 2014, Naughton et al. 2015). Aligning the 3D models allowed us to census the same coral colonies over time and estimate changes in survival, recruitment, and growth. Because the software is not currently capable of measuring 3D change, the aligned models were exported as 2D orthoprojections (Rodriguez et al. 2021). While 2D reconstructions do not fully account for the complex growth of corals and cannot be used to measure change in volume or surface area, the 2D orthoprojections can be used to track temporal changes in planar area and the linear extension rate.

VITAL RATE EXTRACTION FROM ORTHOPROJECTIONS
ANNOTATE ORTHOPROJECTIONS

Finally, a team of NOAA staff, undergraduate researchers, and I extracted demographic data in ESRI ArcMap by delineating live patches and creating transition tables. We subsampled each 10 to 12-meter plot by randomly distributing 0.5 square meter circular plots on the fixed site photomosaics in ArcMap. First, we identified live corals located inside of the circular plots (Figure 4) using the underlying high-resolution imagery and then outlined all live patches (contiguous coral tissue) of seven of the most common coral species from three genera in the Hawaiian archipelago in the first timepoint. In addition to being the dominant Hawaiian coral species (Kenyon et al. 2006, 2007b a, 2008, Franklin et al. 2013), the chosen target species—*Pocillopora meandrina* and *P. ligulata; Montipora capitata* and *M. patula; Porites lichen, P. lobata,* and *P. lutea*—have different life strategies. Each live coral patch was assigned a unique identification number that was recorded in a table. To calculate maximum diameter, we first created a circular polygon around the delineated patches and measured the diameter of the circle. Metadata (including region, island, latitude/longitude, survey date, plot size and type) were also recorded for each fixed site.
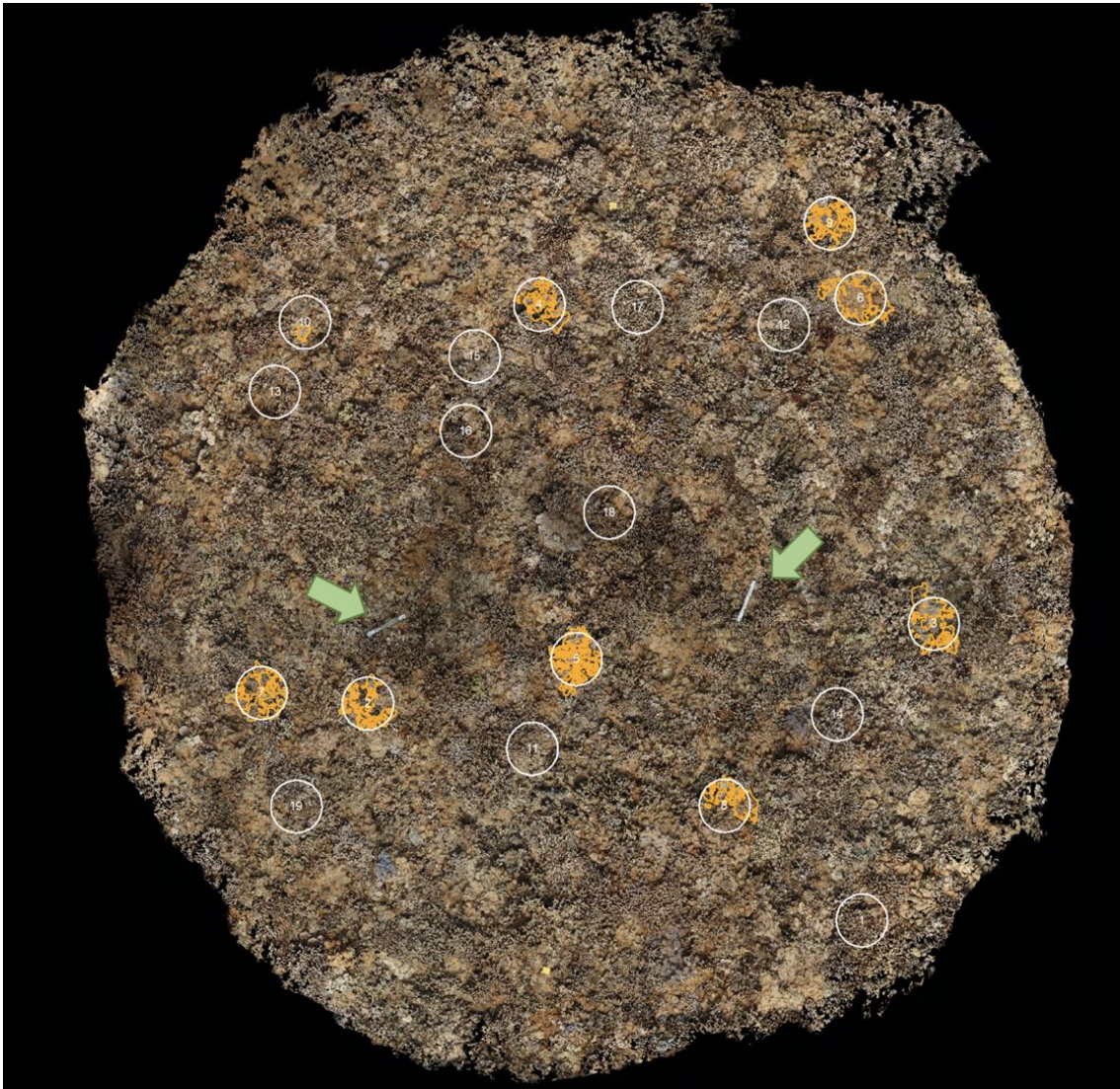
Figure 4. An example of a 2D orthoprojection of a coral reef (OAH_OCC_005) in 2019 with circular plots (white) used to subsample the orthoprojection. Individual coral colonies were outlined (orange) and the perimeter and area of each colony were calculated using ArcMap. Green arrows point to Ground Control Points used to scale the 3D model.

DEMOGRAPHIC MEASUREMENTS

A longstanding challenge for demographic modeling of corals is that it is difficult to model individual coral patches because corals are demographically complex

organisms. Corals are colonial organisms and individual colonies can grow, shrink and undergo fission and fusion. To measure changes in size over time, patches of contiguous live tissue were retraced in subsequent sampling years in ArcMap. The area and perimeter were calculated for each patch. To account for corals breaking into small fragments (fission/partial mortality) and small fragments fusing together (fusion), the network of patches were linked between timepoints based on spatial overlap. The unique patch identification numbers were used to link networks of patches across timepoints. These networks of patches, or the summed area of all patches associated with a single contiguous patch of tissue, were defined as a 'colony.' All IPM modeling was conducted at the colony level.

All of these data were recorded into colony transition tables. Annotations were aggregated by genus/morphological type—encrusting *Montipora*, branching *Pocillopora*, and mounding *Porites*—to reduce error due to the inherent difficulty in identifying colonies to the species level and the added benefit of a larger dataset for more robust population modeling. In total, 1,025 *Montipora* colonies, 264 *Pocillopora* colonies, and 2,790 *Porites* colonies were censused across all sites.

Colony transition tables were exported into R/RStudio to establish the transitions between each year. The unique identification numbers were used to identify the following transition types from year to year: growth, shrinkage, fission, fusion, mortality or recruitment. Growth was defined by an increase in planar area from timepoint one (t, the earliest year) to timepoint two ($t + 1$, a later year) while shrinkage was the opposite. Fission is the process where one coral colony divides into several patches. Any colony in timepoint (t) that linked to more than one patch in the sample circle in timepoint ($t+1$) signified the colony divided into several pieces and underwent fission. Fusion, the process where several coral fragments join together to form one contiguous colony, was defined as n>1 patches in timepoint (t) that are linked to timepoint ($t+1$). A mortality event was defined as a colony in timepoint (t) that lost all live tissue in ($t+1$) or any later year. Recruitment was the opposite; if a colony appeared in timepoint ($t+1$), it signified a recruitment event. For each individual species, change in planar area was calculated by subtracting the linked colony area. The number of recruits per area surveyed based on the total area of annotated circular plots was calculated to determine recruit density. Finally,

the size specific growth rate (growth rate in cm^2/year divided by the colony area in cm^2) and mortality rate (colony fate [alive or dead] per colony area in cm^2) were calculated. In total, I analyzed 1,931 *Montipora* transitions, 309 *Pocillopora* transitions, and 4,184 *Porites* transitions.

DEMOGRAPHIC MODEL CONSTRUCTION

VITAL RATE MODEL FITTING

An IPM is defined by a projection kernel, *K*, which is a function that predicts population growth rate over time. *K* consists of sub-kernels, or functions, representing components of the IPM attributable to different vital rates (e.g., growth, survival, and reproduction). Projection kernels are typically split into sub-kernels to make the model more biologically interpretable. Thus, the first step to building IPMs is fitting demographic models for vital rates to measure the probability of a coral transitioning from one size class to another. These vital rate models were later combined into IPMs. Below I describe how I developed vital rate models for survival, growth (growth and shrinkage/partial mortality), and recruitment. In the subsequent section, I explain how I combined these vital rate functions to create the IPMs to address my research questions.

SURVIVAL

Corals experience two types of mortality: partial mortality and whole colony mortality. Partial mortality occurs when a portion of the colony dies, and results in colony size decreases in timepoint (*t+1*). In contrast, whole colony mortality occurs when all coral polyps in a colony die and no coral tissue remains, resulting in a distinct change in color. To simplify the model, survival was defined as the probability that a coral colony will not undergo whole colony mortality from year (*t*) to year (*t + 1*). Including the number of fragments in the survival model resulted in minimally better model fit but did not survive model simplification using Bayesian Information Criteria. Therefore, colony-level survival was treated as a bimodal variable where the possible outcomes were death (0) or survival (1) and partial mortality was accounted for in the growth variable. The

probability of survival was estimated using a logistic regression where survival was a function of colony size (Ross 2015, Precoda et al. 2018, Kayal et al. 2018). The best model fit was chosen based on lowest Akaike information criterion (AIC) and the results of a stepwise regression with backward elimination using base R packages.

While the enormous temporal scale of this study is a strength of the demographic analysis, it also posed additional challenges. Because the time between sampling events varied by site, it was necessary to annualize survival probability. Colony-level survival was annualized for the site-interval-genus models in the survival sub-kernel in the IPM, described below. For the aggregate genus-region models where many sites and intervals were combined for each genus-region model, survival was annualized in the survival vital rate function. I used the logistic regression from the site-interval-genus models to predict the estimated survival probability for each coral colony. The survival probability was annualized by raising the survival probability to 1 / sampling interval years. Finally, the annualized survival probability was used to refit logistic models for the aggregate genus-region models.

GROWTH

Normal growth and shrinkage occur when coral colonies increase or decrease in size, but remain a single, intact colony. Colony-level growth data were used to fit a model that assessed the annual growth rate depending on the starting and ending size of the coral. However, modeling coral growth was complicated by corals' ability to experience fission, fusion and partial mortality.

Fusion events occur when a larger colony fuses with one or more smaller fragments. Fission typically results in one large fragment and one or more smaller fragments. Fission and fusion can be accounted for in two ways: modeling contiguous coral tissue between timepoints (defined as the 'patch' scale) or modeling all patches associated with a single contiguous patch of tissue from one timepoint to the next (defined as the 'colony' scale). It is possible that colonies undergoing fission and fusion may have distinct growth rates compared to a colony undergoing normal growth, but to avoid adding unnecessary complexity to the model, corals were assessed at the 'colony' level as opposed to the 'patch' level. The planar area measured at year ($t+1$) was taken as

the summed planar area of all of the smaller fragments associated with a single colony in year (t) with the reverse being true for colonies experiencing fusion. To account for possible distinct growth rates, the number of fragments associated with each colony was included as an interaction term in the growth model. This allowed us to assess the relationship between the growth rate and the number of fragments. The best model fit was chosen based on lowest AIC and the results of a stepwise regression with backward elimination using base R packages.

Another aspect of growth that needed to be considered is partial mortality. I observed widespread partial mortality, especially for *Montipora* species and *Porites* species, and these partial mortality events can skew the distribution of growth rates. To account for the substantial partial mortality in Hawai'i, I compared growth vital rate models using a linear regression to models that also included the number of fragments as an interaction term. I found that including the number of fragments to account for fusion, fission, or partial mortality did not significantly improve model fits. Therefore, in my study, growth was simply defined as corals growing or shrinking. To account for the different time intervals between sampling periods, growth and shrinkage were annualized by dividing the change in size by the sampling interval. This was modeled by estimating the probability of each colony undergoing normal growth (p_n) using a linear regression.

After fitting the growth and survival vital rate models, the probability of growth and survival were used to construct the $P(x,x')$ growth and survival sub-kernel. This function describes the probability size distribution with a linear model for surviving corals. Growth was denoted by the transition-specific growth models in brackets and included the transition probabilities for normal growth (p_n) as well as the probability of moving from the (x) to (x') size class with normal growth (g_n). This was multiplied by the probability of survival (p_s).

$$P(x,x') = p_s[p_n g_n]$$

RECRUITMENT

Estimating recruitment rates is challenging because it is difficult to directly observe coral reproduction. Corals reproduce both asexually and sexually via larval dispersal and

determining the extent that a population is open or closed to larval input from other populations determines how fecundity should be estimated. To address the challenge of estimating coral recruitment and determine the most accurate representation of recruitment, I modeled recruitment in four different ways. First, I assumed a fixed-rate recruitment. Second, I tuned the recruitment parameter to the local size structure. Lastly, I estimated the observed site-dependent recruitment using data collected from Structure-from-Motion data (3) and rapid benthic monitoring data collected around the archipelago (4).

1) **Use a recruitment value that results in a stable population growth rate (λ).** To reduce complexity, I first modeled the population as an open system and assumed a fixed-rate recruitment. Previous applications of size-based demographic models to coral populations assumed an open population and that recruitment was decoupled from fecundity (Hughes & Tanner 2000, Edmunds & Elahi 2007). This assumes that most recruits are from habitats outside of the local population. The recruitment parameter for each genus was varied until λ was equal to one. The fecundity kernel was omitted from the projection matrix and a recruitment constant was included. The benefit of this approach to estimating recruitment is that it can be used in data poor systems where little is known about actual recruitment rates. A limitation of modeling recruitment to result in $\lambda = 1$ is that it assumes a stable size distribution and constant recruitment each year in the face of known disturbance events, which is biologically implausible.

2) **Use a recruitment value that results in the observed stable size distribution matching the empirical size distribution.** Next, I modeled a closed population and used the long-term stable size structure from the IPM to tune the recruitment parameter. The closed model assumes that the supply of recruits is a direct cause of reproductive output of the local population. This model also assumes that the number of recruits entering the population at time ($t+1$) is proportional to the total planar surface area of colonies in each year (Ross 2015). The $F(x, x')$ sub-kernel incorporated the number of colonies recruiting back to the population (f) per area of adult colony (x) at year (t).

$$F(x, x') = fx$$

To estimate the recruitment parameter, f, for the closed population, I assumed a stable size distribution and varied f until the stable size distribution (given by the right eigenvector) best fit the size probability density distribution for the study site (Madin et al. 2012). The right eigenvector is one of the predictions of IPMs and is the vector of size-specific values and represents the stable size distribution (Easterling 1998). The estimated recruitment parameter was used to calculate the population growth rate (the dominant eigenvalue λ) for each model. The benefit of this approach is that it utilizes existing data on the current population size structure; however, as with the previous model, it assumes a stable size distribution in the face of several disturbance events.

3) **Use the number of recruits and adult coral area in the 16 fixed sites and assume a site-level stock recruitment relationship.** Unlike previous coral population models, I could leverage the recruits counted in my photogrammetry data to estimate recruitment. For the third recruitment modeling scenario, I assumed an open population and a site-level stock recruitment relationship. This method assumes there is a relationship between the parent corals (spawning biomass) and the resulting number of recruits. I counted the number of recruits (defined as a colony appearing in a later timepoint), it signified a recruitment event) for each site, interval and genus and used this value as the spawning biomass while the total area of adult colonies for each site, interval, and genus was used to represent the parent corals. The site-level stock recruitment parameter was then calculated as the number of observed recruits per area of orthoprojection surveyed divided by the adult area in square centimeters per area of orthoprojection surveyed. To account for the difference in time between sampling events, I annualized the site-level recruitment parameter by dividing by time between sampling events for each site-interval-genus combination. Because the demographic data were collected for each individual site, I assumed that stock recruitment occurred at the site-level; however, it is unlikely that a stock-recruitment relationship is valid at the scale of a 10x10 meter site. In Hawai'i, larval dispersal modeling indicates that many reef tracts seed other reefs on the same island and on adjacent islands (Storlazzi et al. 2017).

4) **Use juvenile density and percent cover from regional benthic monitoring data and assume a sector-level stock recruitment relationship.** For the fourth approach, I assumed an open population and used sector-level observed juvenile densities and

proportional cover to set the recruitment parameter by taxa. Sectors are defined as sub-island, long-term monitoring survey sectors used in National Coral Reef Monitoring Program (NCRMP) monitoring (NOAA Coral Reef Conservation Program 2018). A benefit of this approach is the assumption that the stock recruitment relationship occurs on a more realistic sector-level scale (100s of kilometers; Storlazzi et al. 2017) , rather than over a 10 x10 meter area scale as in the site-level stock recruitment approach described above.

To calculate sector-level coral juvenile density and coral cover, I used previous NCRMP Rapid Ecological Assessment (REA) survey data (NOAA Pacific Islands Fisheries Science Center, 2016). REA surveys are useful in providing a snapshot of reef health at numerous sites during NOAA PIFSC's Reef Assessment and Monitoring Program cruises in the Hawaiian archipelago. The data are a result of shallow water diving surveys conducted in 2010, 2012, 2013, 2015, 2016, and 2019 at random sites near the fixed sites around the Hawaiian Islands. Part of this monitoring included surveying juvenile colonies (< 5 centimeters). I calculated mean juvenile colony density by sector, year, and genus. While these data provide a broad spatial and temporal estimate of juvenile colony density, it is not possible to confirm with certainty which juveniles are true recruits, and which may be fragments of larger, older colonies. With SfM fixed sites, we have the ability to track benthic substrate over time and confirm when a true recruitment event occurred (i.e., a coral appearing in a previously barren space). To resolve this issue, I calculated the proportion of juvenile corals that were true recruits in the SfM plots for each genus. This proportion of true recruits was applied to the mean juvenile colony density to provide a better estimation of true recruitment. Percent cover data was converted to proportional cover and used to represent the spawning biomass. The sector-level stock recruitment parameter was then calculated as the proportional mean juvenile colony density in number of recruits per square centimeters divided by the proportional coral cover.

A regional genus sector-scale stock recruitment parameter was also estimated in a similar way. While the sector-level stock recruitment parameter only utilized juvenile colony density and percent cover data from the sectors in this study (12 sectors), the regional genus sector-scale stock recruitment parameter utilized data from all sectors (30

sectors) in the Main Hawaiian Islands and Northwestern Hawaiian Islands. For the sake of simplicity, I will heretofore refer to this parameter as the all-sectors stock recruitment parameter.

Modeling recruitment in this stepwise approach allowed us to overcome the challenges of directly observing coral recruitment and obtain accurate estimates for coral recruitment to construct a robust IPM. All analyses were conducted in R version 4.0.2. All data and code are available at: https://github.com/coral-line-rodriguez/VitalRates-to-IPM.

BUILDING THE IPM

Vital rate models used to build sub-kernels (growth/survival and recruitment) were combined into IPMs for each taxon-region and each site-interval-genus based on size as the state variable. A size-structured IPM was derived for each taxon-region to calculate the long-term growth rate for each population and determine which vital rates had the largest impact on population growth. A separate IPM was constructed for each coral taxon since coral morphology strongly correlates with demographic characteristics and dictates a coral's ability to thrive or decline in response to environmental disturbances (Darling et al. 2012). A size structured IPM was also derived for each site, genus and time interval to determine the impact of thermal stress on population dynamics across sites with unique thermal histories. The stable size distribution was obtained from the right eigenvector (Easterling et al. 2000). The stable size distribution was used in the second recruitment method. The asymptotic population growth rate was represented by the dominant eigenvalue λ (Easterling et al. 2000). The population growth rate (λ) was calculated for each site-interval-genus and was compared to each site's thermal stress history during the sampling interval (see thermal stress section below).

An IPM is defined by a kernel $K(x,x')$ that is used to project the size distribution forward in time. The kernel represents the probability densities of growth between discrete or continuous stages that depend on the survival and the production of offspring. The probability that a colony of size (x) in year (t) will transition to size (x') in year ($t+1$) was represented by

$$n(x', t + 1) = \int_L^U [K(x, x')] n(x, t) dx$$

$$K(x, x') = P(x, x') + F(x, x')$$

where *n(x', t+1)* is the spatial distribution of colonies at time t+1. The probability of transitioning from x to x' was denoted by the kernel *K(x,x')* and was modeled by integrating over the bounds of the minimum (*L* = lower size limit) and maximum (*U* = upper size limit) colony size for *n(x,t)*, the distribution across size of individuals at time (*t*). The kernel *K(x,x')* was composed of vital rate regressions in sub-kernels. Survival and growth were represented by the *P(x,x')* sub-kernel and recruitment of sexually productive offspring was represented by the, *F(x,x')* sub-kernel (Metcalf et al. 2013). For my analyses, a total of 61 IPMs were built. To determine the differences in population growth rate (λ) between the three dominant genera in the Hawaiian archipelago, 6 aggregate IPMs were built for each genus and region (MHI or NWHI). To assess resilience following disturbance events and determine the effect that thermal stress events have on coral populations, 55 IPMs were constructed for each site, genus, and time interval combination. All analyses were conducted in R version 4.0.2.

STATISTICAL ANALYSIS OF POPULATION GROWTH RATE (Λ)

Each estimate of transition probability and therefore each estimate of the population growth rate was subject to error due to the limited number of individuals that can be sampled. To quantify uncertainty in population growth estimates, error was propagated for each λ calculation. The mean and standard deviation of site-level observed recruitment and all-sectors observed recruitment were used to calculate a mean, lower and upper bounds for each recruitment method. These recruitment values (mean, 5% and 95% confidence intervals) were used to calculate lambda values for each model. Lambda values calculated using the lower and upper confidence intervals were then used to evaluate differences between mean values based on non-overlapping confidence intervals (Alvarez-Buylla & Slatkin 1994).

ELASTICITY ANALYSIS

Elasticity analyses were used to determine the contribution of the kernel components (survival-growth and reproduction) to population growth (λ). To determine which vital rate had the strongest influence on the population growth rate and hence had the most impact on population recovery for each taxon, an elasticity analysis was conducted by making small changes to the growth, fecundity and survivorship functions and determining the sensitivity of λ to each of these changes (Easterling et al. 2000, Caswell 2001). To determine the relative contributions of growth/survival and recruitment separately, the whole IPM elasticity kernel was separated into the growth/survival $P(x,x')$ and recruitment $F(x, x')$ sub-kernels. By partitioning the elasticities, I was able to quantify which component (survival/growth or recruitment) had a larger influence on lambda.

THERMAL STRESS AND POPULATION DYNAMICS

TEMPERATURE STRESS CALCULATIONS

NOAA Coral Reef Watch produces real-time coral bleaching products through the use of real-time and historical satellite sea surface temperature monitoring (Liu et al. 2013, 2014). Coral Reef Watch's Degree Heating Week (DHW) index provides a calculation of cumulative heat stress above the mean monthly maximum at each reef grid cell (5 km^2) that is used to predict bleaching (Liu et al. 2014). Mild to moderate bleaching typically occurs at ≥ 4 DHW and severe bleaching or mortality at ≥ 8 DHW; however, minimal heat stress (DHW < 4) can negatively affect coral cover (Romero-Torres et al. 2020). Thermal conditions were estimated at each island by retrieving DHW records from the NOAA Coral Reef Watch daily global 5km satellite data using data pixels closest to my sampling sites (NOAA Coral Reef Watch, 2018). To account for differences in thermal histories in the NWHI (where five moderate and two major bleaching events have occurred since 1985) and MHI (where only two minor and major

bleaching events have occurred since 2014), DHW records were retrieved for 10 years prior to each sampling day as well as all years before the sampling day (1985 to 2019) and normalized to a decadal estimate to ensure comparability. To quantify thermal history during the sampling period and account for possible negative impacts of mild heat stress (Romero-Torres et al. 2020), a stress event was defined as either > 1 DHW (mild) or ≥ 4 DHW (moderate). Decadal frequency (number of thermal stress events per 10 years) was used to estimate the frequency of thermal stress events for a) 10 years prior to the sampling date, b) all prior years since 1985, c) > 1 DHW and d) ≥ 4 DHW. Severity of these thermal stress events (mean of all maximum thermal stress events for each of the respective metrics calculated for decadal frequency) was used to estimate thermal stress severity for the same four sampling periods. To explore the effect of temperature stress on the population growth rate, a site-interval IPM was derived for each genus. I then assessed the effect of temperature stress (frequency and severity) on the population growth rate (λ).

STATISTICAL ANALYSES

To determine if there is a relationship between the frequency or severity of thermal stress events and coral population dynamics, I correlated the output of the IPM (population growth rate, λ) to each site's thermal stress signature. Lambda values calculated using the all-sectors stock recruitment parameter (4th recruitment method) were used as the response variable while thermal stress severity, thermal stress frequency, genus, region and island were independent variables. I built linear regression models to determine if there was a relationship between the frequency or severity of thermal stress events and the long-term stochastic growth rate (λ) and multiple regression models to determine if the combination of frequent and thermal stress events impacted the population growth rate (λ). To explore the potential for differences among genera, region, and island, mixed-effects models were built using the lme4 package in R (Wood 2011). Genus, region, and island nested within region were held as random effects, and a likelihood ratio test was used to compare the goodness of fit between linear regression, multiple regression, and mixed-effects models. When a variable (main effect or

interaction) in the model was not significant (p value higher than 0.05), I removed the factor from the analysis. Finally, different combinations of thermal stress severity and frequency (10 years, all previous years, > 1 DHW, and ≥ 4 DHW) variables were tested. Final model selection was based on Bayesian Information Criterion (BIC). All multivariate analyses were conducted in R version 4.0.2. All data and code are available at: https://github.com/coral-line-rodriguez/VitalRates-to-IPM.

RESULTS

VITAL RATE MODELS

Growth. Colony-level growth was modeled using a linear regression to examine the relationship between colony size in the first timepoint (t) and timepoint ($t+1$). The growth model included a linear function of colony log10 size and fixed variance (Supplementary Table 2) to describe the probability of growing from the (x) to (x') size class. In the MHI, the intercept (Figure 5) for *Porites* and *Montipora* were similar (0.072 and 0.065), while *Pocillopora* had a higher intercept (0.27) and therefore had a larger initial size. In the NWHI, the intercepts of the three taxa differed where *Pocillopora* had the biggest starting size and the highest intercept (0.34). It is possible that our detection limit was better while annotating the orthoprojections for encrusting *Montipora* and massive *Porites* species or that juvenile branching *Pocillopora* colonies had a larger initial size than the other two taxa. The slopes of the three taxa were similar in both regions. *Porites* colonies had the largest slope in both regions and therefore the fastest growth rate while *Pocillopora* had the lowest slope, signifying the slowest growth rate, in both the MHI and NWHI. Smaller colonies were growing while the largest colonies experienced shrinkage in both regions (Figure 5). In particular, *Pocillopora* colonies were mostly growing across all size classes, especially in the NWHI. In contrast, *Porites* colonies were barely growing in the smallest size classes in both the MHI and NWHI (Figure 5). In all of the following figures, genera are abbreviated in the following manner: POSP = *Porites*, MOSP = *Montipora*, POCS = *Pocillopora*).
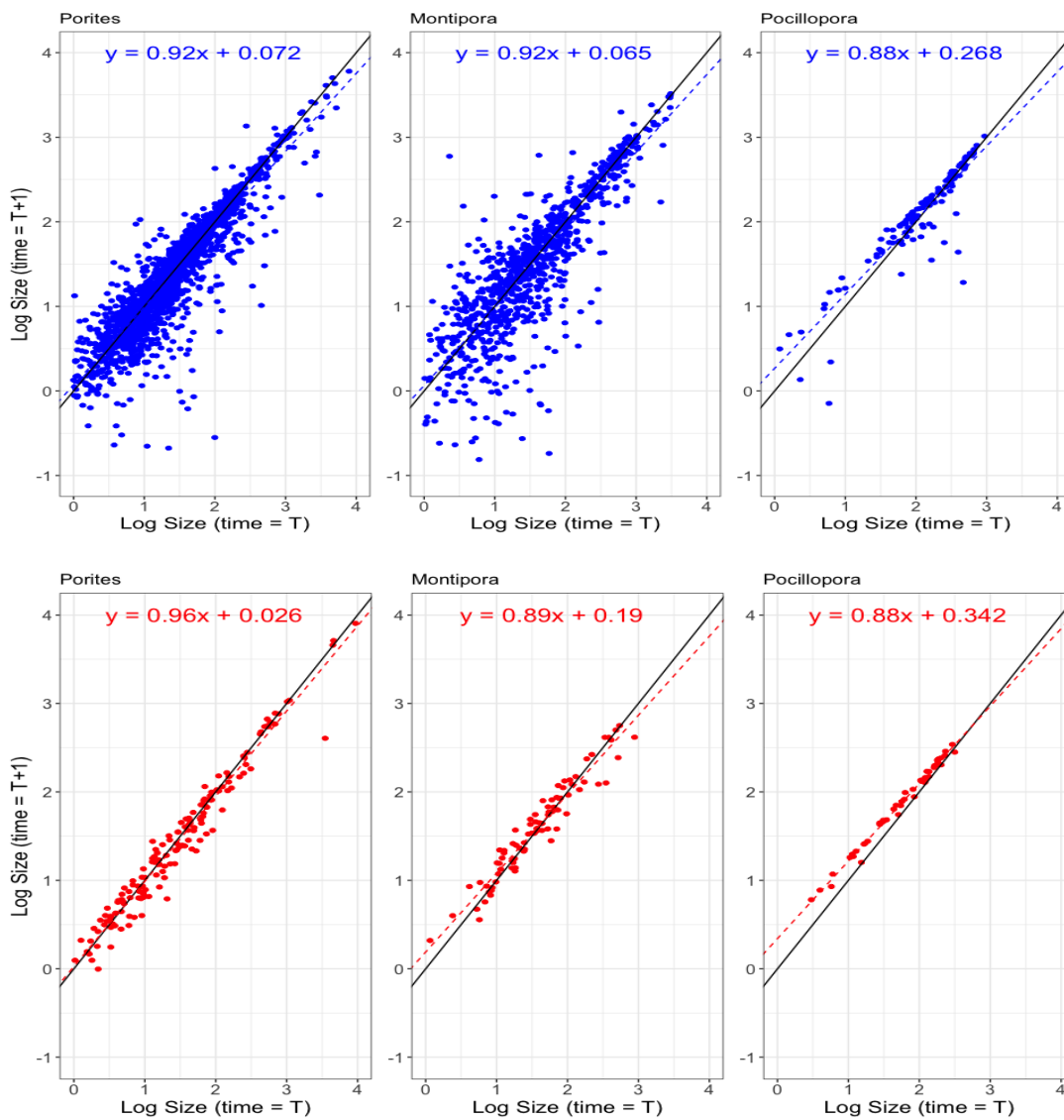
Figure 5. Probability of growth as a function of coral size for three genera in the MHI (top, blue) and NWHI (bottom, red) from 2013-2019. Points represent individual colony data for each genus and the dashed line represents the fitted linear regression. The black line represents stasis or stable population growth ($\lambda =1$).

Survival. Colony-level survival was modeled using a logistic regression (generalized linear model using a binomial function) as a function of colony size in the first timepoint (t). The survival probability was modeled as colony log10 size and background survivorship (Supplementary Table 2). Larger colonies had a higher probability of survival compared to smaller colonies, particularly for *Pocillopora*

colonies in the MHI (slope = 0.98) and *Porites* colonies in the NWHI (slope = 1) (Figure 6). Larger colonies made up of many fragments had high survivorship compared to colonies of the same size with less fragments. When comparing the effect of initial colony size to the probability of survival, there were positive slopes for all genera in both the MHI (*Porites* log-odds slope = 1.13, *Montipora* log-odds slope = 2.02) and NWHI (*Montipora* log-odds slope = 1.2, *Pocillopora* log-odds slope = 2.94).
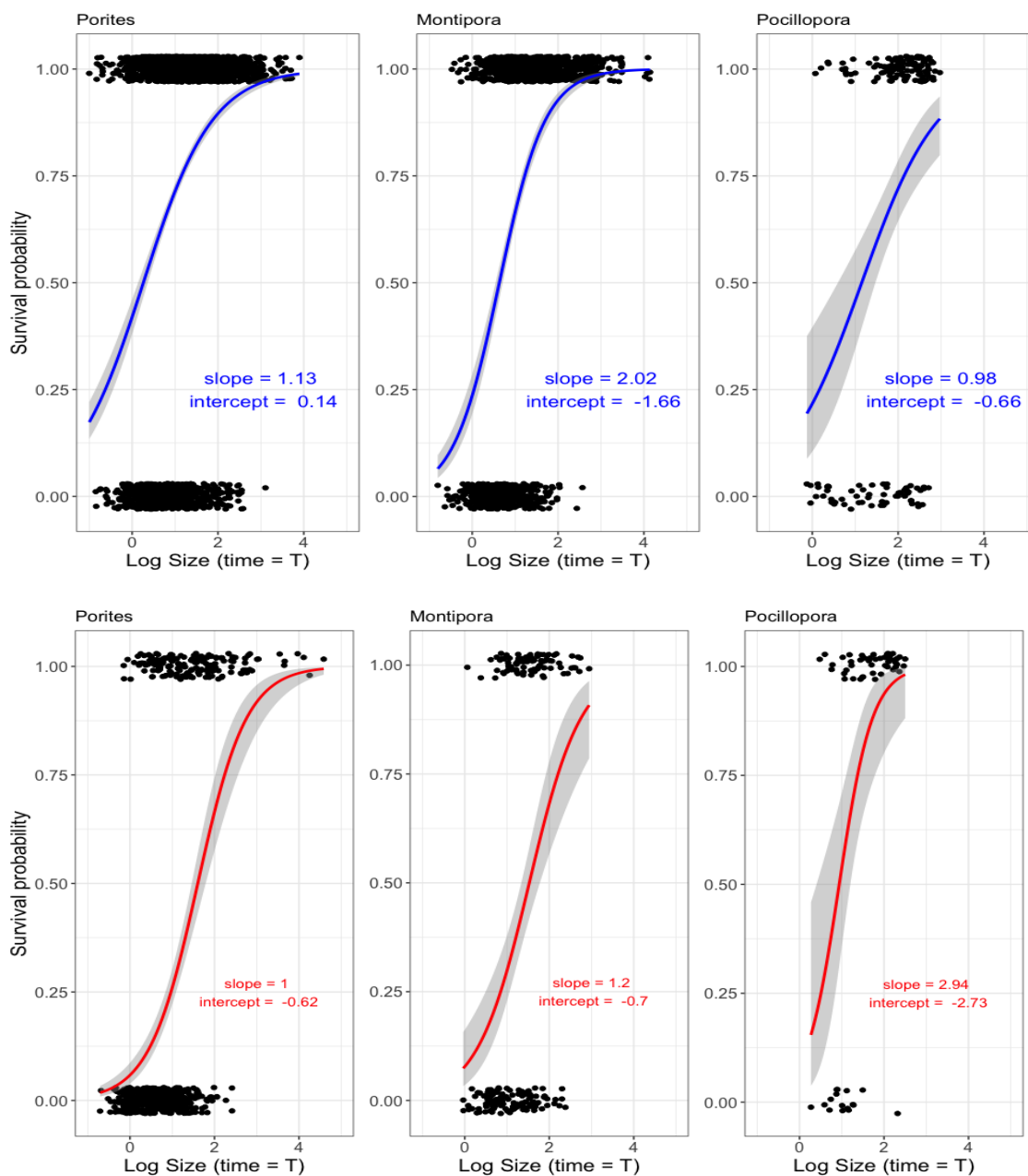
Figure 6. Probability of survival using a logistic regression for three genera (*Porites*, *Montipora* and *Pocillopora*) in the Main Hawaiian Islands (top, blue) and Northwestern Hawaiian Islands (bottom, red) from 2013-2019. Points represent individual colony data.

Recruitment. Due to the complexities of measuring coral fecundity and modeling recruitment (see Methods), recruitment was modeled in four ways.

1) **Use a recruitment value that results in a stable population growth rate (λ).** First, recruitment was optimized by modifying the recruitment parameter to achieve a stable population growth of $\lambda=1$ (Figure 7A). The recruitment constant was estimated as 0.3260 recruits/cm^2 for *Pocillopora*, 0.1669 recruits/cm^2 for *Montipora* and highest for *Porites* recruits/cm^2 (2.2298) (Figure 7A). This method for modeling recruitment was fast and would be particularly useful for modeling population dynamics without any recruitment data. This method would also be useful in comparing the relative differences between lambda in data-poor situations; however, it assumes constant recruitment for all sites, which is unlikely given differing environmental conditions at each site. This approach also assumes that populations are stable, yet this assumption is unlikely due to the history of coral bleaching events in 2014, 2015, and 2019 in both regions as well as 2017 in the Northwestern Hawaiian Islands.

2) **Use a recruitment value that results in the observed stable size distribution matching the empirical size distribution.** The recruitment function was also obtained by matching the stable size structure to the empirical size structure using a sum of squares function (Madin et al. 2012) with the best fit parameters from the survival and growth functions. The recruitment parameter was increased and decreased until the empirical size structure obtained from data collected from the orthoprojections most closely matched the modeled stable size structure (Figure 7B). The recruitment parameter was 0.0055 recruits/cm^2 for *Pocillopora*, 0.001 recruits/cm^2 for *Montipora*, and 0.0041 recruits/cm^2 for *Porites*. The second method is also relatively simple to execute and can be performed without recruitment data; however, the size distribution of the population must be stable over time to meet the assumptions. My data violated the primary assumption because there were several disturbance events during the sampling period.
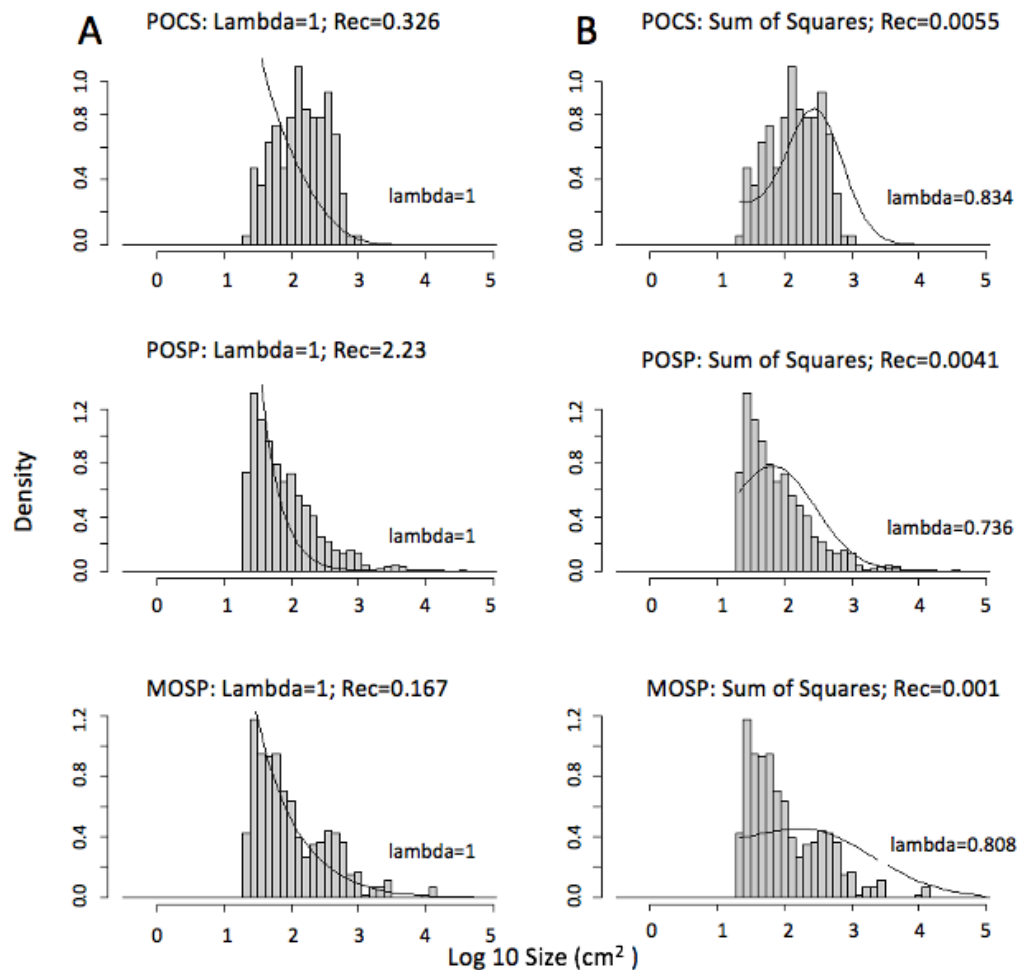
Figure 7. (A) Recruitment estimation using the first method. Colony size distributions (bars) of *Pocillopora*, *Porites*, and *Montipora* and the stable size distribution output from the IPM model (solid line). The recruitment parameter was varied until a lambda of 1 (λ =1) was reached. (B) Recruitment estimation using the second method. Size distributions calculated using data from fixed-site orthoprojections (bars) and the best-fit stable size distribution from the IPM (solid line). The stable size distribution was matched to the empirical size structure by optimizing the recruitment parameter. Note that the population growth rate (λ) decreases for all genera using the best-fit stable size distribution approach for estimating recruitment.

In comparing both the first and second methods, *Montipora* had the lowest recruitment rate and *Pocillopora* had the highest recruitment rate. For both methods, *Porites* had a lower, intermediate recruitment estimate. Recruitment values were two orders of magnitude lower for all species in method 2 compared to recruitment estimates for method 1 (Figure 7).

3) **Use the number of recruits and adult coral area in the 16 fixed sites and assume a site-level stock recruitment relationship.** This approach to estimating the recruitment parameter utilized observed juvenile density data from the 16 fixed orthoprojection sites. The 16 fixed site orthoprojections (hereinafter referred to as "site") used to estimate growth and survival vital rates were also used to calculate a site-level recruitment parameter. This parameter was calculated as the number of recruits per area of adult coral surveyed in each orthoprojection and was calculated for each site-interval-genus combination (Supplementary Table 3) as well as each genus/region (Supplementary Table 4). Using the fixed site data, in the Main Hawaiian Islands, mean site-level recruitment was highest for *Pocillopora* (0.0100 recruits/cm^2) followed by *Montipora* (0.00422 recruits/cm^2), and *Porites* had the lowest calculated recruitment parameter (0.00273 recruits/cm^2). In the Northwestern Hawaiian Islands, mean site-level recruitment was highest for *Montipora* (0.00933 recruits/cm^2) followed by *Porites* (0.00810 recruits/cm^2), while *Pocillopora* had the lowest recruitment (0.00741recruits/cm^2) (Figure 8A). Unlike the previous two methods which only modeled recruitment, this method leveraged the six years and over 2,400 kilometers of space covered by these recruitment data. These data allowed us to confirm true recruitment across a site by corroborating that a coral appeared in a previously open space. Using true recruitment values from orthoprojections instead of estimated values that do not account for vast spatial and temporal scales provided a more realistic recruitment estimate. Nevertheless, this method assumed a stock recruitment relationship occurring at the size of one site (~100 square meters). It is unlikely that there is a strong stock recruitment relationship within a 100 m^2 plot and it is more likely this relationship exists at the scale of a sector (sub-island scale; ~100s of kilometers).
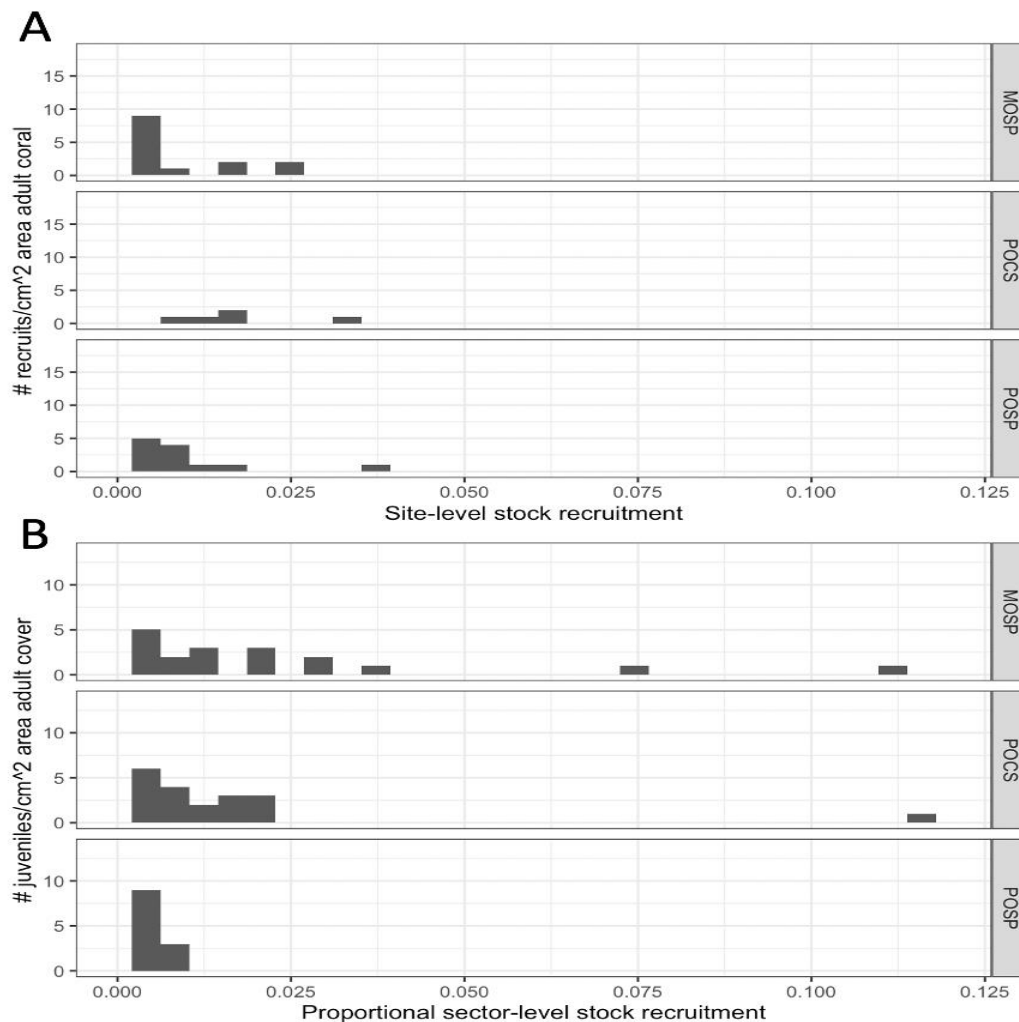
Figure 8. Juvenile density distribution with observed recruits for three genera in the Hawaiian archipelago from 2013-2019. Fixed site data were calculated from 16 sites using repeated orthoprojections (A, recruitment method 3) while the Rapid Ecological Assessment (REA) data were collected by NOAA PIFSC scientific divers using random stratified sampling in the Main and Northwestern Hawaiian Islands (B, recruitment method 4).

4) **Use juvenile density and percent cover from regional benthic monitoring data and assume a sector-level stock recruitment relationship.** Two sector-level (sub-island) recruitment parameters were estimated using juvenile density and percent cover data from regional benthic monitoring data. Rapid Ecological Assessment (REA) data collected in two regions, the Main Hawaiian Islands and Papahānaumokuākea Marine

National Monument in the Northwestern Hawaiian Islands, were utilized to calculate the mean juvenile density per mean coral cover. REA sampling was conducted for six years between 2010 to 2019 compared to the fixed site data, which were mostly collected for two or three years between 2013 and 2019.

First the fixed site data were utilized to calculate the proportion of juvenile corals that were true recruits in order to ground truth the REA data. A verified, or true, recruitment event was defined as a coral appearing in a previously barren space. I utilized the SfM fixed sites to calculate the number of true recruits for each genus. The proportion of juvenile corals that were true recruits for each genus was calculated by taking the number of corals that were true recruits in the SfM and dividing by all juveniles (<5 cm in diameter) in the SfM data (Figure 9). The mean proportion of true recruits was highest for *Pocillopora* (0.813) and was 0.462 for *Montipora*, and 0.325 for *Porites*. This proportion was applied to the mean juvenile colony density REA data to provide a better estimation of true recruitment.
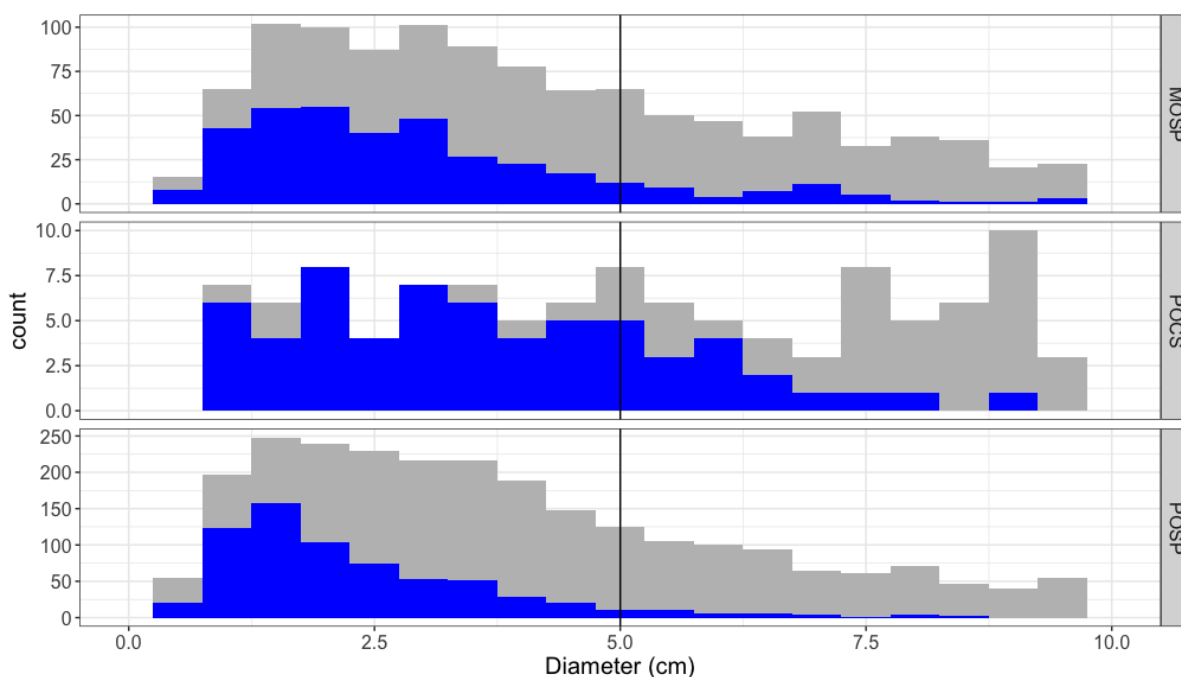
Figure 9. Proportional recruitment based on SfM data for *Montipora* (MOSP), *Pocillopora* (POCS), and *Porites* (POSP). The number of juveniles (gray bars) calculated from SfM data that are estimated to be "true recruits" (blue bars). Any coral smaller than 5 cm in diameter (vertical line) was defined as a juvenile.

The mean proportion of true recruits was applied to the sector-level juvenile density and percent cover data to calculate a proportional sector-level stock recruitment parameter for each site-interval-genus IPM model (Supplementary Table 5) as well as each genus-region model (Table 1), where site signified the 16 fixed sites and region signified the two regions in the archipelago (MHI or NWHI). In the NWHI, the proportional mean sector-level recruitment was highest for *Montipora* (0.044 recruits/cm^2), lowest for *Porites* (0.003 recruits/cm^2), and 0.009 recruits/cm^2 for *Pocillopora*. In the MHI, the proportional mean sector-level recruitment was highest for *Montipora* (0.024 recruits/cm^2), lowest for *Porites* (0.003 recruits/cm^2), and 0.013 recruits/cm^2 for *Pocillopora*. While the sector-level stock recruitment parameter only utilized juvenile colony density and percent cover data from the sectors in this study, the all-sectors stock recruitment parameter utilized data from all sectors in the Main Hawaiian Islands and Northwestern Hawaiian Islands. The all-sectors stock recruitment parameter was calculated for each site-interval-genus IPM model and genus-/region IPM model (Table 1). In the NWHI, the proportional mean all-sectors recruitment was highest for *Montipora* (0.044 recruits/cm^2) and lowest for *Porites* (0.003 recruits/cm^2). Similarly, in the MHI, the highest proportional mean all-sectors recruitment was *Montipora* (0.023 recruits/cm^2) and the lowest all-sectors recruitment was *Porites* (0.005 recruits/cm^2).

Table 1. Sector-level stock recruitment and all-sectors stock recruitment estimates (recruits/cm^2) for *Montipora* (MOSP), *Pocillopora* (POCS), and *Porites* (POSP) and region – Main Hawaiian Islands (MHI) and Northwestern Hawaiian Islands (NWHI) – and the lower and upper confidence intervals (CI).

Genus Code	Region	Mean Sector-Level Rec.	Sector-Level 5% CI	Sector-Level 95% CI	Mean All-sectors Rec.	All-sectors 5% CI	All-sectors 95% CI
MOSP	MHI	0.024	0.007	0.040	0.023	0.004	0.041
MOSP	NWHI	0.044	0.000	0.093	0.044	-0.004	0.093
POCS	MHI	0.013	0.000	0.033	0.013	-0.006	0.033
POCS	NWHI	0.009	0.002	0.017	0.009	0.002	0.017
POSP	MHI	0.003	0.001	0.005	0.005	0.001	0.009
POSP	NWHI	0.003	0.001	0.004	0.003	0.001	0.004

By combining the sector-scale and site-scale estimation of recruitment in the fourth method, I was able to estimate the realized recruitment and reduce the variable to a single, size-relative parameter. This method was also a more realistic estimation of the stock-recruitment relationship for corals because larval dispersal in Hawai'i occurs on the scale of an island or adjacent islands (Storlazzi et al. 2017). The sector (sub-island) scale is therefore a more realistic estimate for larval recruitment; however, while the realized recruitment estimate was enhanced by applying the proportion of true recruitment from SfM data, both sector-level recruitment parameters were not directly measured from the fixed sites like they were for the third recruitment method and could thus be less accurate. In contrast, the first two methods of modeling recruitment, while relatively fast and simple to conduct without any recruitment data, ignored natural variation in recruitment while assuming stable population dynamics, which is unlikely in the face of known disturbance events. Recruitment values for the first method were two orders of magnitude higher than the estimates for method 2, and this could be due to artificially boosting the recruitment parameter to attain a stable population growth. The third and fourth recruitment methods resulted in three relatively similar recruitment parameter estimates. The similarity in recruitment parameter estimates is demonstrated in Figure 10, where blue dots with similar estimates fall along the black diagonal line. Blue dots that plot farther from the diagonal black line are overestimates of one recruitment parameter relative to the other. For example, in Figure 10A, the sector-level estimate is overestimated relative to the site-level estimate. Therefore, I chose to only use the final three recruitment calculations (Figure 10) to construct the region-genus IPMs and the site-interval-genus IPMs and calculate the population growth rate (λ). However, I presented a comparison of data-rich to data-poor recruitment estimation methods here because it may be useful for other IPM studies conducted with limited recruitment data.
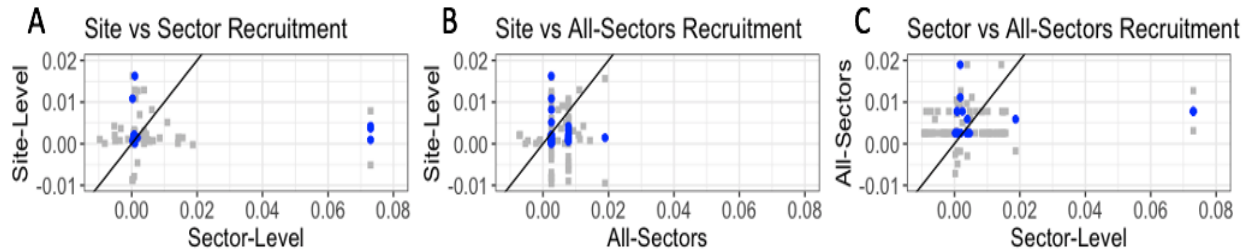
Figure 10. Comparison of three recruitment parameter estimates (recruits/cm²) for the two recruitment methods used in the Integral Projection Models: site-level stock recruitment, sector-level stock recruitment, and all-sectors stock recruitment. Gray squares (jittered for plotting) indicate the recruitment parameter estimate and blue circles compare the differences in estimates between the specified recruitment methods. Recruitment parameter estimates in blue that fall along the black diagonal line mean that the two methods resulted in a similar estimate.

POPULATION GROWTH RATE BY TAXA

My first research question was to determine if population growth rates (λ) differed between three genera – *Porites*, *Pocillopora*, and *Montipora* during the study time period (2013-2019). I expected that the population growth rate (λ) would differ between the three genera due to their morphological differences. Growth and survival parameter estimates (Supplementary Table 2) were used to build integral projection models (IPMs). Unlike the site-level stock recruitment and sector-level recruitment parameters, which were limited in data, it was possible to calculate an all-sectors stock recruitment parameter (recruitment method 4) for every IPM model. The all-sectors stock recruitment parameter also resulted in similar recruitment estimates as the site-level and sector-level estimates (Figure 10). Therefore, for this research question, I used the all-sectors recruitment parameter (recruitment method 4) to calculate regional lambda values.

The population growth rates were different for each taxon in the NWHI, while lambda was similar for *Pocillopora* and *Porites* in the MHI (Figure 11). The population growth rates for *Porites* and *Montipora* in both regions as well as *Pocillopora* in the MHI had lambda values less than 1, indicating that the populations were declining. In contrast, *Pocillopora* species in the NWHI had a lambda greater than 1, signifying populations

were growing. In the MHI, *Montipora* colonies had the highest lambda value (λ =0.954); however, the lambda value was less than 1, signifying population decrease, and the population was declining by 4.6% per year. Lambda values for *Pocillopora* (λ =0.860) and *Porites* (λ =0.864) colonies were lower than *Montipora* and represent a ~14% annual decline. In the NWHI, population growth rates differed by genus. While the population of *Pocillopora* (λ =1.054) increased, the *Montipora* (λ =0.835) population was declining and the *Porites* (λ =0.791) population declined the most. This suggests that the *Porites* population was declining by 20.9% annually.
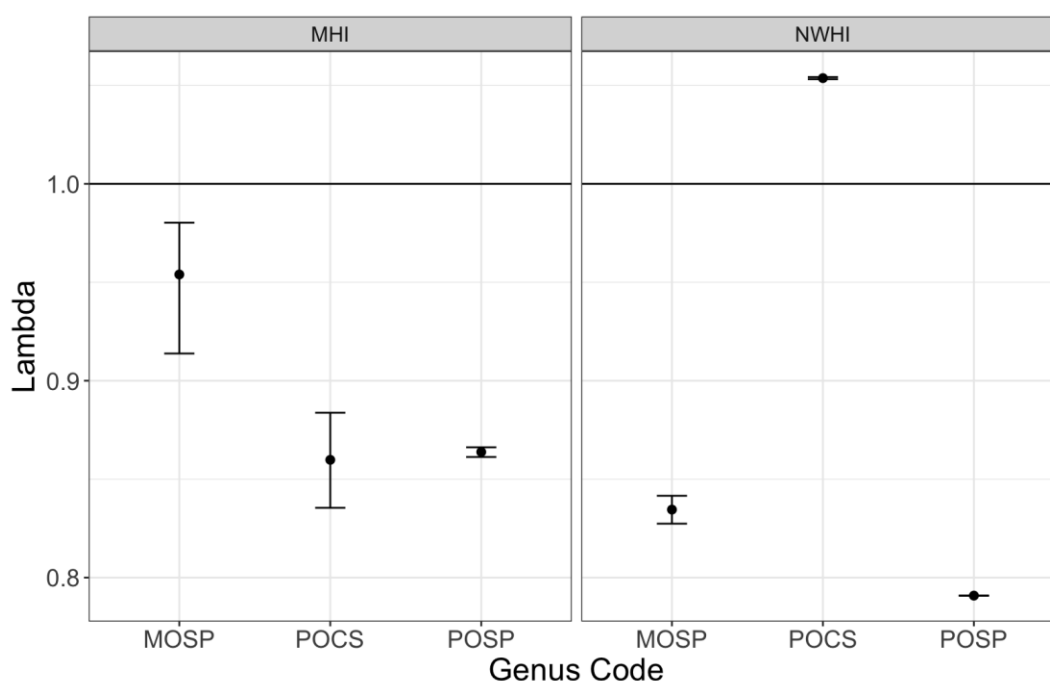
Figure 11. Population growth rates (lambda values, λ) for *Montipora* (MOSP), *Pocillopora* (POCS), and *Porites* (POSP) corals in the Main Hawaiian Islands (left) and Northwestern Hawaiian Islands (right) pooled over sites and time intervals between 2013-2019. Error bars represent 95% confidence intervals.

Plots of the IPM kernel *K(x,x')* are commonly used to represent the summed investigated demographic parameters (survival, growth, recruitment) and can be used to observe the probability of growth/survival and recruitment from time *t* to time *t+1* across all size classes (Figure 12). Across all genera and both regions, there was a shift from a probability of positive growth for smaller colonies to negative growth for larger colonies

(Figure 12, A-E). In general, survivorship increased with coral growth (i.e., larger corals had high survivorship). The highest probability of survival was evident for corals in the largest size classes, but these colonies were decreasing in size. The horizontal band at the bottom of the kernel represents recruitment contribution and showed that the greatest recruitment (the darkest red) was driven by the largest colonies. Thus, colonies from all three genera needed to be large in size to reproduce.
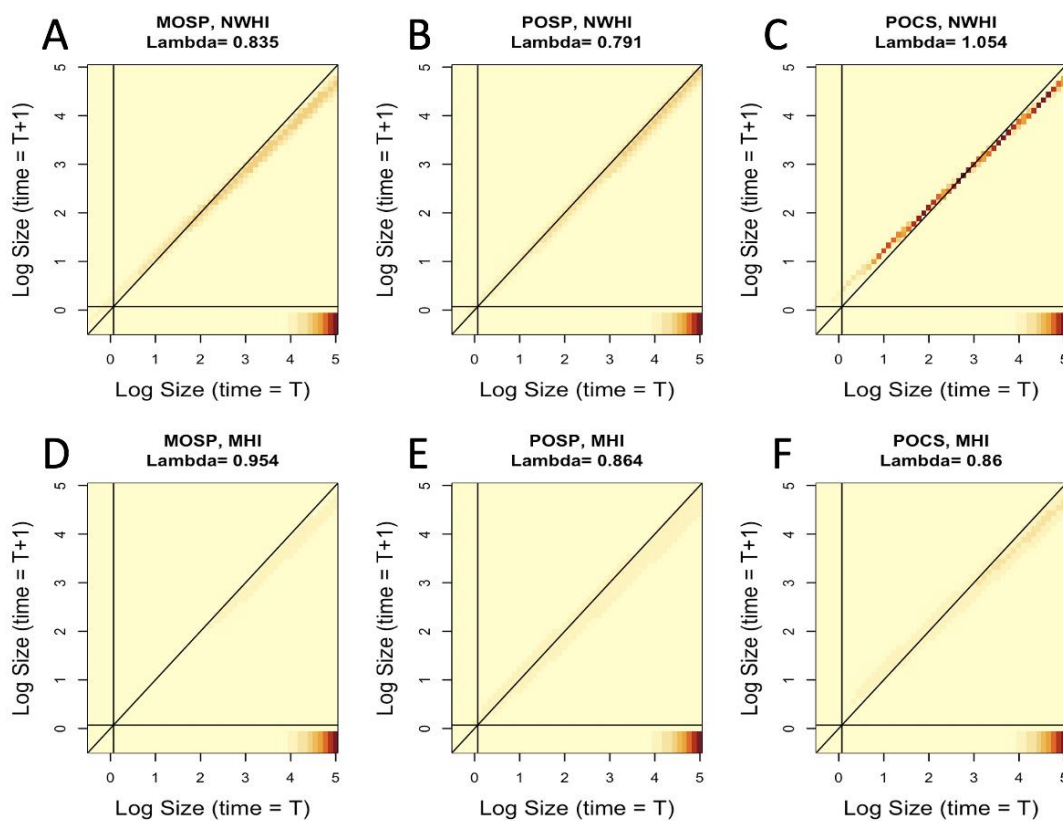
Figure 12. Integral Projection Model kernel for *Montipora* (MOSP), *Porites* (POSP), and *Pocillopora* (POCS) corals in the Hawaiian archipelago from 2013-2019. The dashed black line represents stasis whereas the diagonal band of the kernel surrounding the 1:1 stasis line represents the growth and survival of the population. The horizontal band at the bottom of the plot below the horizontal black line represents coral recruitment. Warmer colors indicate a higher probability of size transitions and survival from one timepoint (*T*) to the next (*T + 1*).

The IPM kernel for *Pocillopora* differed by region (Figure 12C, F). In the NWHI (the only region-genus model with a positive lambda value), size at *t+1* was not related to size at time *t*. This model was also fit with the fewest number of transitions (112 growth + survival transitions; Supplementary Table 2). In the MHI, the largest colonies exhibited the highest probability of growth and survival, where the probability of growth was defined as the probability of increasing or decreasing in size. Smaller colonies had a higher probability of growth while larger colonies were more likely to experience shrinkage.

Large *Porites* colonies had a high probability of survival, especially in the NWHI (Figure 12B, E). In the NWHI, the probability of survival and growth fell along the 1:1 line, indicating a high probability that corals will maintain equilibrium; however, there was a slightly higher probability of shrinkage for the medium and large size classes. In the MHI, colonies were more likely to experience more shrinkage for medium and large size classes. It also appears that the highest recruitment probability stemmed from the largest colonies.

For *Montipora* populations, the highest probability of growth and survival was evident for the largest colonies, especially in the NWHI as indicated by the warmer color (Figure 12A, D). While large colonies had the highest probability of survival, the type of growth that was most probable was shrinkage due to size transitions falling below the 1:1 stasis line. Similar to *Pocillopora* and *Porites*, the highest recruitment probability stemmed from the largest colonies.

POPULATION SENSITIVITY

My second research question asked which vital rate(s) would most influence the population growth rate. Elasticity analyses show which vital rates within the IPM have the greatest impact on lambda (λ) and further highlighted the differences between taxa. Similar to IPM kernels, results from an elasticity analysis can be visualized as a kernel plot. In this case, high (dark red) values indicate areas with a greater contribution to the population growth rate and were evident for the growth and survival portions of the IPMs

(Figure 13), indicating that population dynamics were driven primarily by growth and survival. Elasticity values did vary by size class for the different genera and regions, but generally medium to large corals surviving and maintaining stasis had the largest impact on lambda.
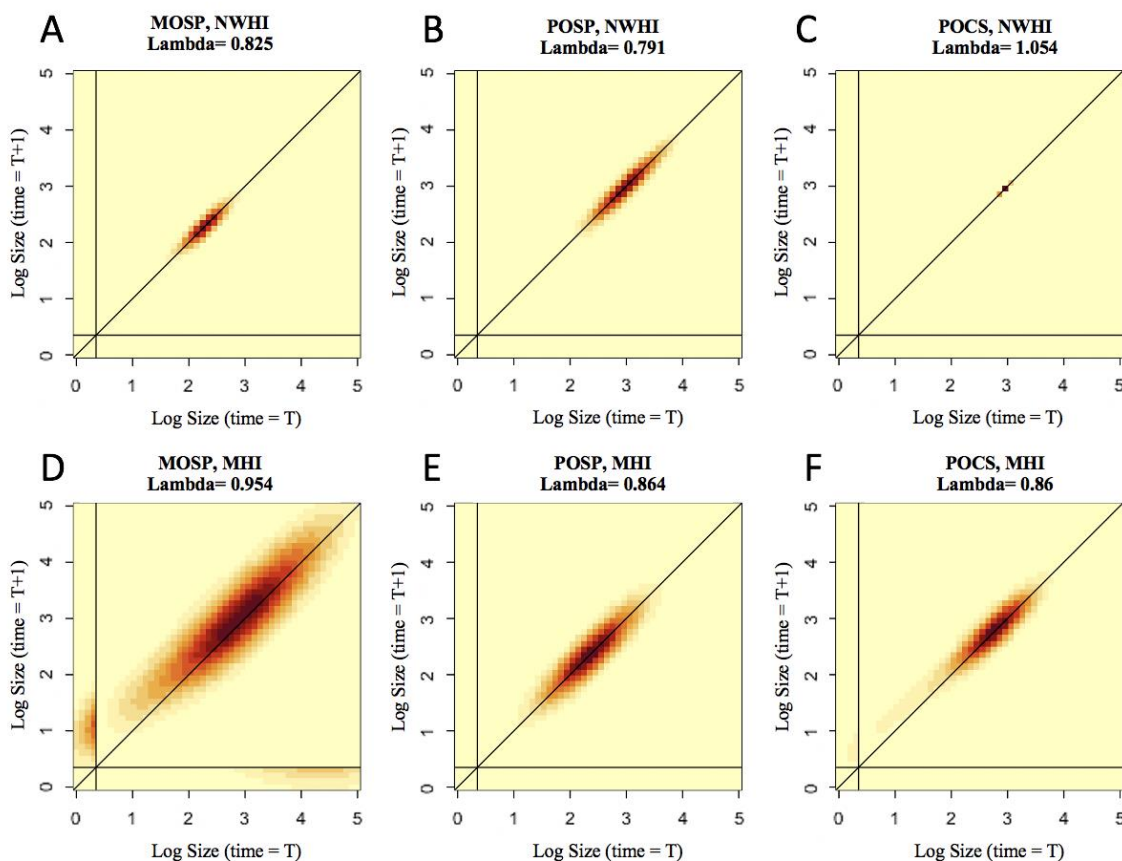
Figure 13. Elasticity of the IPM kernel, plotted as a natural log to increase visibility, for *Montipora* (MOSP), *Porites* (POSP), and *Pocillopora* (POCS) corals. The black line represents no change in size over time. The area along the black diagonal line indicates the growth and survival portions of the kernel. The horizontal band at the bottom below the horizontal black line reflects the recruitment sub-kernel. The vertical band on the left side reflects growth of recruits. Warmer colors indicate a greater contribution to the population growth rate.

Medium to medium-large sized corals about 2.5 - 3.5 cm^2 surviving and maintaining their size had the largest impact on the population growth rate for *Pocillopora* (Figure 13 C, F). Therefore, losing medium sized colonies would have a

large impact on population growth for *Pocillopora*. The elasticity analysis in the NWHI did not show which vital rates drive changes in lambda and was therefore inconclusive, likely due to insufficient IPM models as a result of the lack of *Pocillopora* colonies in all but one NWHI site. For *Porites* (Figure 13 B, E), the population growth also depended primarily on the growth and survival of medium sized colonies. In the MHI, the contribution of growth/survival to lambda was dominated by transitions in the medium size range, while it was dominated by transitions in the medium-large size range in the NWHI. This means that in the MHI, the survival of medium sized colonies about 2 - 3 cm^2 most affected lambda while in the NWHI, medium-large *Porites* colonies around 3 - 3.5 cm^2 dying would negatively impact the population growth rate. The population elasticity of *Montipora* (Figure 13 A, D) indicated that population growth was driven by changes in the growth and survival of medium to large sized colonies. In the NWHI, individuals from medium sizes (2 - 3 cm^2) maintaining stasis and surviving contributed the most to the population growth rate. While population growth predominantly depended on coral growth in the MHI, for large adult colonies (2.5 - 3.5 cm^2), recruitment was an important factor that affects population growth, which was evidenced by the higher (darker colors) along the x axis below the horizontal line on the elasticity plots (Figure 13).

As seen in the whole IPM kernel elasticity plots (Figure 13), the growth/survival function made a greater contribution to λ (warmer colors) than the recruitment function (no shading) in all species. To determine the relative contributions of growth/survival and recruitment separately, the whole IPM elasticity kernel was separated into the growth/survival $P(x,x')$ and recruitment $F(x, x')$ sub-kernels. Estimating the IPM sub-kernels elasticities separately allowed us to determine the percent contribution of each sub-kernel, where the total elasticity sums to 1. Growth and survival contributed over ~95 - 99% to the population growth rate, whereas recruitment contributed only 0.000079 – 4.65% to lambda (Table 2). While recruitment contributes less to lambda, the contribution varies from 20 to over a million times less than the contribution from growth and survival (Table 2). Growth and survival are ~122 - 1.2 million times more important than recruitment in the NWHI (Table 2) and have a larger contribution to lambda compared to the MHI.

Table 2. IPM sub-kernel elasticities for growth/survival (eP), recruitment (eR), and the ratio of growth/survival to recruitment (eP:eR) for all three genera.

Region	Elasticity	*Montipora*	*Porites*	*Pocillopora*
MHI	eP	0.954	0.996	0.978
	eR	0.0465	4.05e-3	0.0217
	eP:eR	20.5	245.9	45.1
NWHI	eP	0.992	0.999	0.999
	eR	8.10e-3	7.87e-07	6.62e-4
	eP:eR	122.5	1,269,377	1,509

While growth and survival had the largest impact on lambda for all regions and genera, the population growth rate also depended on recruitment from medium-sized *Montipora* colonies in the NWHI (about 2 cm^2) and across all of the largest size classes (about 2 - 5 cm^2) in the MHI (Figure 14). For the reproduction component of the kernel for *Porites*, recruitment was important for medium colonies. Similarly, the contribution of recruitment to λ was dominated by medium sized *Pocillopora* corals.
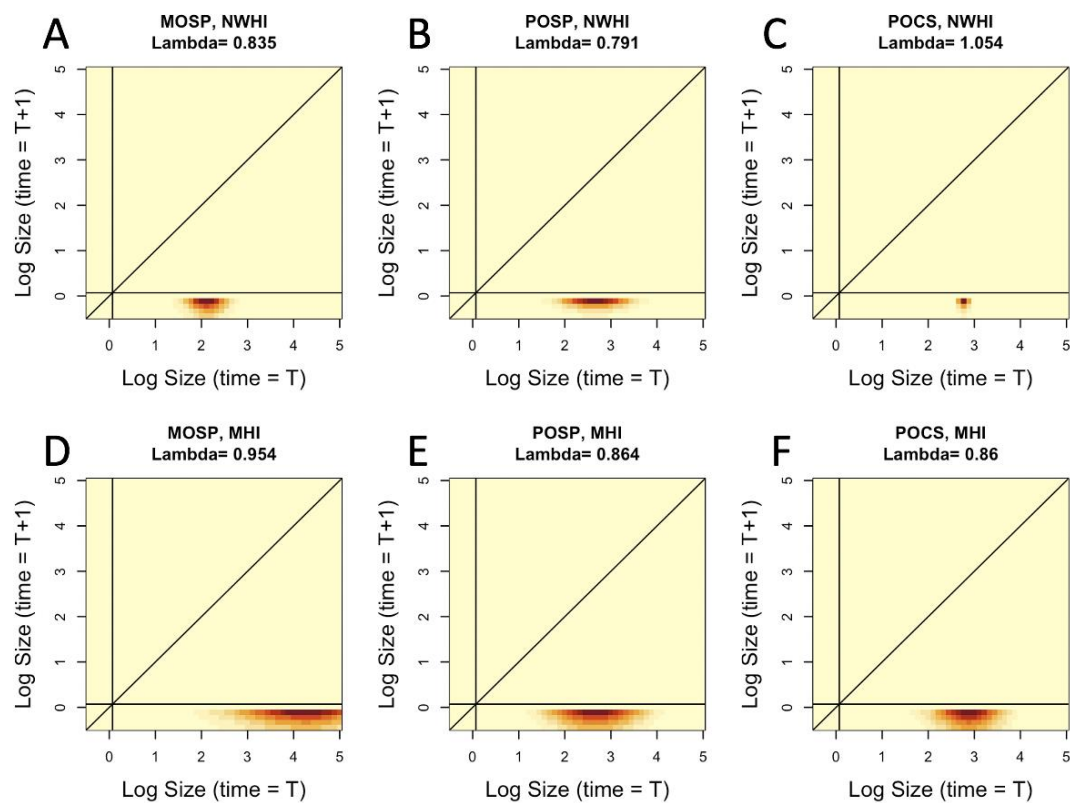
Figure 14. Recruitment elasticity of the IPM kernel only, plotted as logarithmic scale to increase visibility. The warmer colors indicate greater probability of size transitions from one year to the next. The horizontal band at the bottom reflects the recruitment sub-kernel.

POPULATION GROWTH RATE BY SITE AND INTERVAL

Population growth rates were calculated for each site, interval and genus combination using three different recruitment parameterizations: site-level stock recruitment, sector-level stock recruitment, and all-sectors stock recruitment (Supplementary Table 6). Lambda values varied temporally (Figure 15). Across all three lambda calculations using the different recruitment methods, lambda values were less than 1 in 2015 following the repeat 2014-2015 bleaching events. Lambda values for most sites in the Main Hawaiian Islands (MHI) started to increase in 2016 and rose above 1 in 2017 for *Montipora* corals. In the MHI, the population growth rate dropped below 1 in 2018 for *Montipora* and *Porites* species. There were limited data for *Pocillopora* species between 2014 to 2017, but lambda values also declined in 2018 in the MHI.

MHI Site-Interval-Genus Population Growth Rates

NWHI Site-Interval-Genus Population Growth Rates
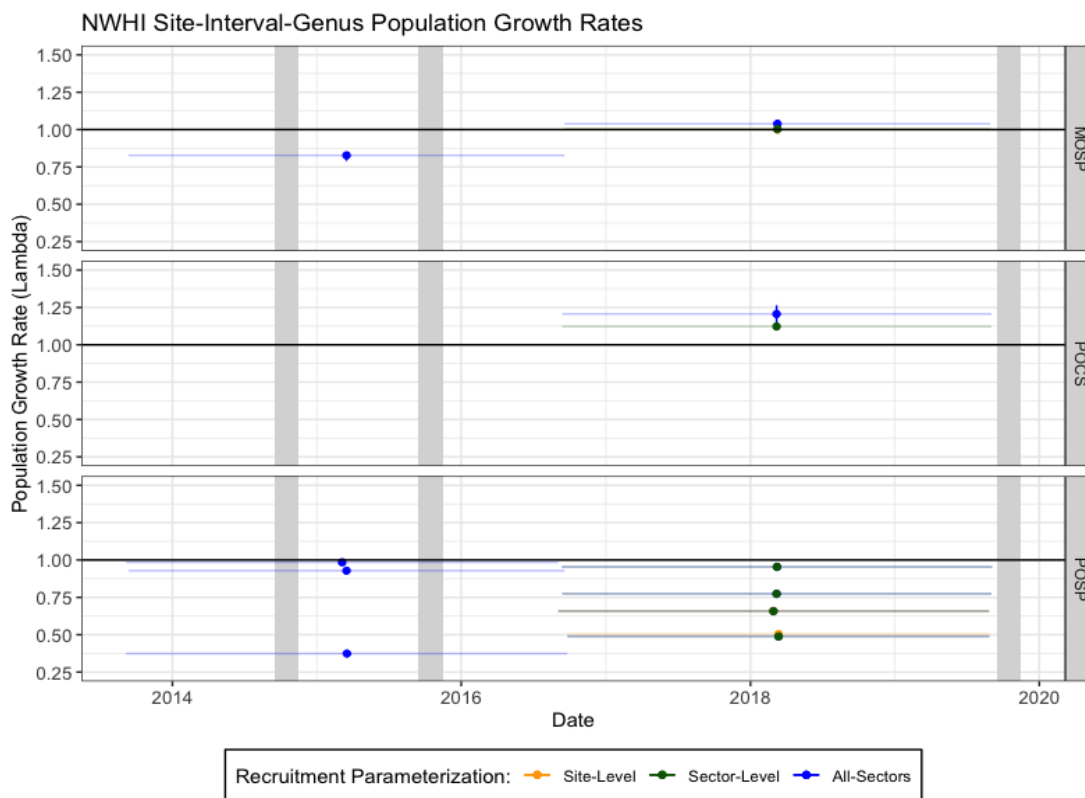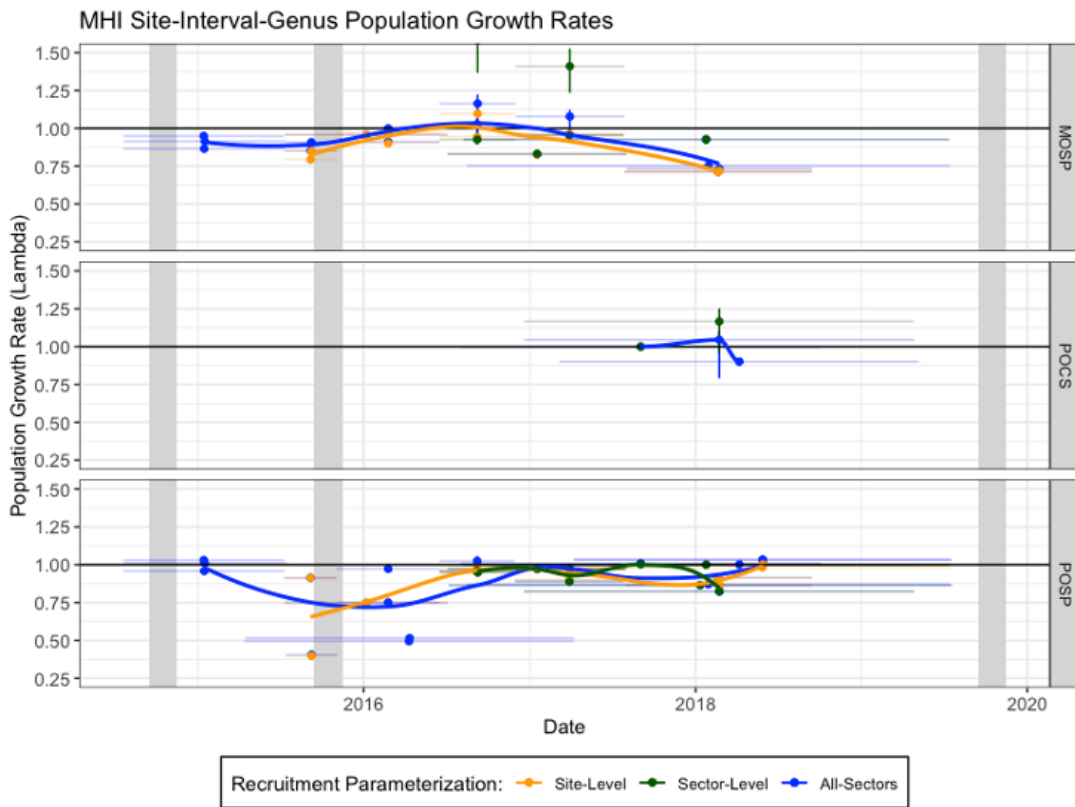
Figure 15. Population growth rates calculated for each site, interval, and genus [*Montipora* (MOSP), *Pocillopora* (POCS), and *Porites* (POSP)] using three different recruitment parameters between 2013 to 2019. The vertical gray lines indicate the bleaching events in 2014, 2015 and 2019. Horizontal bars demonstrate the time interval between sampling events while vertical bars indicate error. The locally weighted polynomial trend was estimated for the MHI using each recruitment parameterization and is plotted as an orange, green or blue line.

In the Northwestern Hawaiian Islands (NWHI), all lambda values were less than 1 in the 2014 - 2017 time interval for both Montipora and Porites, but lambda rose to around 1 in the 2016 - 2019 time interval for Montipora corals (Figure 15, Supplementary Table 6). Similar to the MHI, there were limited *Pocillopora* data in the NWHI, but lambda values were above 1 in the 2016 - 2019 time interval, representing a positive population growth rate. Overall, there was a similar trend as the MHI for *Montipora* corals in the NWHI where lambda values were lower following the 2014-2015 repeat bleaching events and higher during the 2016-2019 recovery period. In contrast, *Porites* corals in the NWHI had declining population growth in both the 2013-2016 bleaching interval and the 2016-2019 recovery interval.

The population growth rate varied by site (Supplementary Table 6). Assuming a site-level stock recruitment, Kahekili, Maui (MAI_SIO_K01) and Kona, Hawai'i (HAW_SIO_K08) had the highest population growth rate ($\lambda = 1.10$ and $\lambda = 1.00$), respectively. The population in Maui was increasing by 10% while the population in Hawai'i was maintaining stasis. The lowest lambda values were calculated for Olowalu, Maui ($\lambda = 0.40$) and French Frigate Shoals ($\lambda = 0.50$). Assuming all-sectors stock recruitment, French Frigate Shoals (FFS_OCC_002) had the lowest recorded lambda value (0.374) in 2013-2016 followed by Olowalu, Maui (MAI_SIO_OL3) in 2015 ($\lambda = 0.404$), which represent a 62.6% and 59.6% annual decline, respectively. In contrast, coral populations in Kure and Kahekili, Maui (MAI_SIO_K01) exhibited the highest lambda values ($\lambda = 1.21$ and $\lambda = 1.16$), respectively.

RELATIONSHIP BETWEEN THERMAL STRESS AND POPULATION GROWTH

My third research question was to determine if the frequency and/or severity of thermal stress events correlated to changes in coral population growth. Linear regressions and multiple regressions were used to determine the effect of temperature on the population growth rate (lambda), while accounting for variability in genus, region, island, frequency of thermal stress events, and severity of thermal stress events. Decadal frequency (number of thermal stress events per 10 years) was used to estimate the frequency of thermal stress events and the mean of all maximum thermal stress events was used to estimate thermal stress severity for 10 years prior to the sampling date, all prior years since 1985, and for mild (> 1 DHW) and moderate (≥ 4 DHW) stress events. There were fewer IPM models built using the site-level and sector-level recruitment parameter compared to the all-sectors stock recruitment parameter and plots comparing the three lambda values revealed similar trends between temperature stress and lambda. Therefore, I used the all-sectors stock recruitment parameter for the thermal stress modeling. Genus, region, and island nested within region were held as random effects, but linear mixed models including random effects were not significantly better than the multiple regression models (p value higher than 0.05 using a Likelihood Ratio Test) and were excluded from the final models (Table 3). Separate models were built for each genus due to differences in lambda values. Due to limited data (N = 2 models), the relationship between thermal stress and lambda was not modeled for *Pocillopora*. In total, I compared 20 models for each genus (Supplementary Table 7). Here I included the top three *Porites* models and three *Montipora* models, none of which had significant explanatory variables (Table 3).

Table 3. Multiple linear regression and linear regression models with the best model fit and highest explanatory power. Significant explanatory variables (p < 0.05) are denoted with an asterisk (*).

Model	Explanatory Variable(s)	BIC	Num df	Adjusted R^2	Regression ANOVA
Porites	Major_Freq_YR10*, Severity_YR10*	-15.854	4	0.272	$p<0.05$*
Porites	Major_Freq_YR10, Severity_AllPriorYears*	-14.680	4	0.243	$p<0.05$*
Porites	Frequency_YR10, Severity_YR10*	-13.097	4	0.202	$p<0.05$*
Montipora	Frequency_YR10	-19.696	3	-0.043	$p = 0.623$
Montipora	Freq_AllPriorYears	-19.634	3	-0.047	$p = 0.664$
Montipora	Severity_AllPriorYears	-19.522	3	-0.053	$p = 0.763$

I found that thermal stress severity and thermal stress frequency significantly predicted the population growth rate for *Porites* corals using a multiple regression (Figure 16). Including the variables major decadal thermal stress frequency (DHW $\geq$ 4) and thermal stress severity for 10 years ("Severity_YR10") explained 27% of the variance in lambda (Table 4, adjusted $R^2 = 0.27$) while major decadal thermal stress frequency ("Major_Freq_YR10") and thermal stress severity for all years since 1985 ("Severity_AllPriorYears") had the second highest adjusted R^2 (24%) (Table 3). For the three *Porites* models with the lowest BIC and highest adjusted R^2, both major temperature stress frequency and severity over the past 10 years significantly impacted lambda (Figure 16). For *Porites* corals, for each increase in major frequency (i.e., an additional DHW $\geq$ 4 event in that 10-year period), lambda was reduced by 0.066 ± 0.026 (Table 4). For each increase in severity of thermal stress (mean of all maximum thermal stress events in the prior 10 years), lambda was reduced by 0.024 ± 0.0098. When there was no temperature stress, the expected lambda was 1.074 ± 0.068 (Table 4).
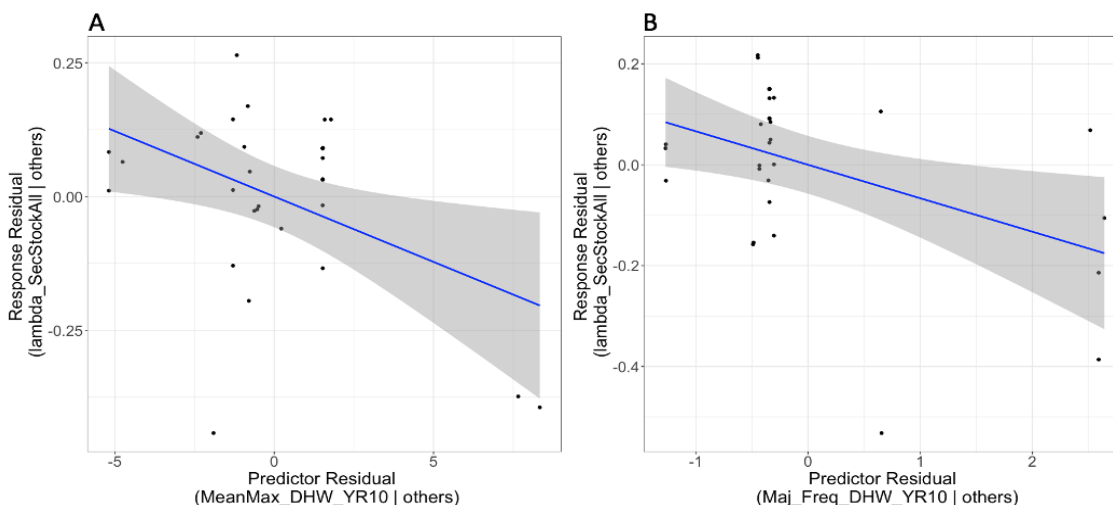
Figure 16. Both the major decadal thermal stress frequency (A) and severity (B) for 10 years significantly predict the *Porites* population growth rate (λ). Individual plots display the relationship between lambda and one predictor variable while controlling for the presence of the other predictor variable and therefore reflect the statistically independent effect of (a) major decadal thermal stress frequency and (b) severity for 10 years. Fitted lines are linear regressions and shaded areas are ± 95% confidence intervals.

Table 4. Multiple-regression model ANOVA table for *Porites* corals with lambda as the response variable. *Denotes factors that are significant at p < 0.05.

Porites model	Coefficient	SE	P value
Intercept*	1.074	0.068	<0.05
Major_Freq_YR10*	-0.066	0.026	<0.05
Severity_YR10*	-0.024	0.0098	<0.05

Adjusted R^2 = 0.27; Regression ANOVA p < 0.05

In contrast, when the same model structure was applied to *Montipora* data, it resulted in a linear regression fit with almost no explanatory power. There was no significant relationship between thermal stress frequency or severity and the population growth rate for *Montipora* corals (Figure 17). The non-significant model with the most explanatory power and lowest BIC included the frequency of thermal stress events for 10

years (p = 0.623). This model was not significantly correlated with lambda (Table 5) and the model only explained 4.3% of the variation in lambda (adjusted R^2 = -0.043).
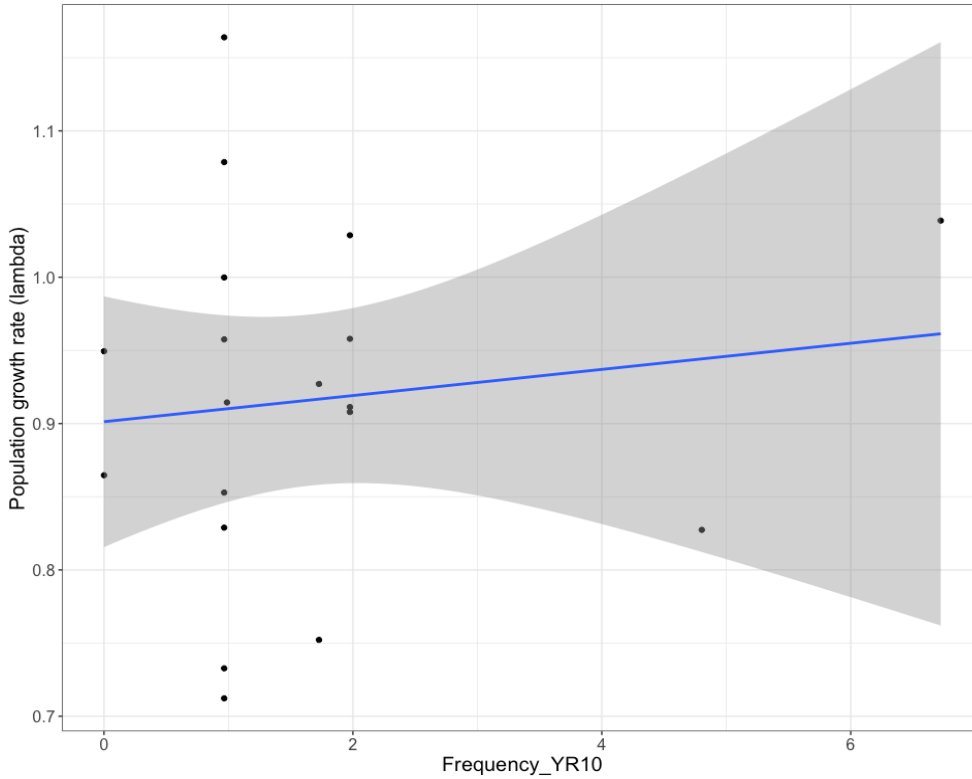
Figure 17. The frequency of thermal stress events does not predict the population growth rate (λ) for *Montipora* corals. Fitted line is a linear regression and the shaded area is the ± 95% confidence intervals.

Table 5. Multiple-regression model ANOVA table for *Montipora* corals with lambda as the response variable. *Denotes factors that are significant at p < 0.05.

Montipora model	Coefficient	SE	P value
Intercept*	0.901	0.041	<0.05
Frequency_YR10	0.009	0.018	0.623

Adjusted R^2 = -0.043; Regression ANOVA p = 0.623

DISCUSSION

This study utilized Structure-from-Motion (SfM) photogrammetry techniques to characterize coral demography for the three most common coral genera across the Main Hawaiian Islands (MHI) and the Papahānaumokuākea Marine National Monument in the Northwestern Hawaiian Islands (NWHI) during a time period (2013 - 2019) that included three thermal stress events. Coral vital rates were used to construct Integral Projection Models (IPM) and calculate population growth rates (λ). These IPMs were used to determine if population growth rates differed between three genera representing three distinct growth forms. I used an elasticity analysis to determine which vital rate drives population dynamics for each genus to provide important information for resource managers. Finally, I modeled whether the frequency and/or severity of thermal stress events correlated to changes in coral population growth.

DIFFERENCES IN POPULATION GROWTH BY TAXA

This study shows that the populations of three coral genera, which have different growth morphologies and life-history strategies, have declining population growth rates. The population of *Porites, Pocillopora*, and *Montipora* in both the MHI and NWHI exhibited negative population growth ($\lambda < 1$) and are declining anywhere from 4.6% to 21% annually, with the exception of the *Pocillopora* population in the NWHI, which exhibited positive population growth ($\lambda > 1$). With the exception of *Pocillopora* in NWHI, population growth rates during the study period were extremely low (0.791 - 0.954) for all genera. These low lambda values mean that populations are declining from 20.9 to 4.9% annually, respectively, and all morphological types are in danger of extirpation. The population growth rate for *Porites* was very low (0.791 - 0.864) in both regions and both populations are likely to experience rapid decline. To the best of my knowledge, there are no comparative studies that measure population growth across the Hawaiian archipelago, but studies examining long-term changes in coral cover in the MHI found that overall, coral cover remained stable, with some variation at the site level (Rodgers et al. 2015). However, the finding of stable coral cover referenced a period of

time (1999 to 2012) when there were no bleaching events in the MHI compared to my study, which included two thermal anomalies. While coral cover may decrease following a bleaching event (Couch et al. 2017), coral cover varies over time due to other acute disturbances as well (Rodgers et al. 2015). While the time period of my study included mostly disturbance-free years, the largest disturbance ever recorded for Hawaiian reefs occurred near the beginning of my study period. It is still concerning that the long-term population growth across almost the entire archipelago is declining.

I predicted there would be a positive population growth for massive *Porites*, but populations in both regions had high growth rates, high partial mortality, and low recruitment for an overall negative population growth rate. I expected that massive *Porites* corals would exhibit minimal growth. Although growth rates were similar across the archipelago, *Porites* had the fastest growth rate in the NWHI and the same growth rate as *Montipora* in the MHI. Colonies of *Porites* were likely to maintain their size, and this same trend was observed for the smallest size classes. In the NWHI, medium to large colonies exhibited a high probability of survival and were likely to remain the same size; however, larger colonies also had a higher probability of shrinkage. This corresponds to the widespread partial mortality observed for *Porites* colonies in both regions (Dr. Thomas Oliver, personal communication). *Porites* populations in both regions also had the lowest observed recruitment from both the site-level stock recruitment calculation and the all-sectors stock recruitment calculation. Corals with massive morphologies are thought to have a physiological advantage during thermal stress events that increases their viability during recurrent thermal stress events (Van Woesik et al. 2012, Cant et al. 2021); however, my results demonstrate that massive *Porites* had declining population growth rates and may be in danger. While coral species with a massive growth form are known to have low mortality, similar to my results, the limited recruitment observed may be driving the declining population growth.

The *Pocillopora* population in the MHI experienced minimal growth and intermediate recruitment and exhibited negative population growth. In the MHI, there was minimal shrinkage across all size classes and small *Pocillopora* colonies are expected to increase in size, compared to the other taxa, where small colonies were more likely to experience stasis. *Pocillopora* corals are often referred to as "weedy" corals and

are known to have fast growth rates (Loya et al. 2001, Baird & Marshall 2002, Darling et al. 2012); however, in my study, *Pocillopora* corals had slightly slower growth rates compared to the other taxa. Larger colonies had a higher probability of survival but were also more likely to experience decreasing size, as observed with the other two taxa. In the MHI, there was intermediate recruitment compared to *Porites* and *Montipora* corals. Despite slightly slower growth and moderate recruitment, the IPM for *Pocillopora* in the MHI yielded a substantial population decline. Branching morphologies like *Pocillopora* with faster or weedy life histories (Loya et al. 2001, Darling et al. 2012) often demonstrate higher mortality rates following thermal stress events that decimate the population, as seen in my results. The *Pocillopora* population in the NWHI was the only population with an increasing population ($\lambda > 1$), but both the kernel and elasticity matrix plots were inconclusive because size was not related from one timepoint to the next in the kernel plots and does not show which vital rates have the greatest impact on lambda in the elasticity plot. This is due to insufficient vital rate transition data (Supplementary Table 2) due to the scarcity of Pocilloporids in the Northwestern Hawaiian Islands, which were only observed at Kure Atoll. Therefore, it is unlikely that the population growth rate for *Pocillopora* corals is increasing in the NWHI.

I expected corals with an encrusting growth form to experience rapid growth and high mortality that would lead to a stable population growth ($\lambda = 1$), but *Montipora* populations in both regions are declining ($\lambda < 1$). Growth rates differed by region. Colonies in the MHI are experiencing faster growth compared to the other taxa while *Montipora* colonies in the NWHI exhibited slower growth rates. The probability for survival increased with colony size in both regions, but larger corals were more likely to shrink in size, which corresponds to the widespread observed partial mortality. Recruitment was very high for the site-level stock recruitment calculation (Supplementary Table 4) and the all-sectors stock recruitment calculation (Table 1) in both regions. Nonetheless, the high recruitment *Montipora* corals are experiencing may not be enough to offset the higher probability of shrinkage, especially in the largest size classes in the MHI, which could be driving the negative population growth in both regions. It is possible that *Montipora* corals are allocating physiological resources towards recruitment at the expense of growth (Stearns 1989).

Across all taxa, smaller colonies are experiencing faster growth while larger colonies have a high probability of shrinkage and survival. Smaller, juvenile corals grow faster than larger colonies (Borgstein et al. 2020, Schlecker et al. 2022) and as expected, smaller colonies in all regions grew faster. This finding supports the current coral restoration practice of micro-fragmentation-fusion, where large colonies are broken into small pieces to increase overall coral growth rate and the fast-growing fragments are outplanted on reefs close together to encourage fusion (Forsman et al. 2015). Furthermore, I found that smaller colonies experienced high mortality. This means that restoration practitioners would need to outplant many small colonies to offset the higher mortality of small fragments. Large colonies also had a high probability of shrinkage (decreasing area) due to partial mortality. Partial mortality occurs when a portion of a colony dies and results in a smaller colony size in a later timepoint. I observed widespread partial mortality in *Montipora* and *Porites* colonies in both regions, but fusion was also common for these taxa. Fusion, which leads to an increase in colony size, may offset the shrinkage as a result of partial mortality and could explain the faster growth rates for *Montipora* and *Porites*. Even though larger colonies are shrinking, the probability of survival was also higher for larger colonies. This could be a physiological strategy based on the allocation theory predicting that tradeoffs occur between vital rates due to energetic constraints acting at the physiological level (Stearns 1989). Therefore, it may be advantageous for larger colonies to break into smaller pieces to avoid whole colony mortality, but changes in the size structure of colonies have major implications for demographic performance.

The size structure of a population impacts both recruitment and susceptibility to future thermal stress events. The finding that there was a higher probability of recruitment from the largest size classes was not unexpected considering the largest colonies in a population contribute disproportionately to reproduction (Hall & Hughes 1996). However, in my study, I observed numerous small colonies and small fragments from partial mortality. The extensive shrinkage and fragments observed across the archipelago could lead to decreased recruitment as the size of corals gets smaller. The increase in the number of smaller corals, which reproduce less than their larger counterparts, could further contribute to population decline. The viability of coral

populations is dependent on larval supply, which adds genetic diversity and enhances recovery from disturbance events (Noreen et al. 2009). Therefore, possible shifts towards smaller, fragmented corals could lead to even lower population growth rates. Furthermore, the combination of a potentially shifting population size structure and thermal stress events could exacerbate the impact on community recruitment. In addition to contributing less to recruitment, smaller colonies suffer greater reproduction impacts in response to disturbance (Johnston et al. 2020). Disturbances such as a thermal stress event can significantly compromise coral reproductive output for extended periods (Levitan et al. 2014). Smaller colonies—or fragments, which were observed throughout the archipelago—suffer greater reproduction impacts over a longer period of time than larger colonies (Johnston et al. 2020). A change in population structure towards smaller colonies and an increase in future thermal anomalies, could have an even greater deleterious impact on coral recruitment.

One of the biggest challenges of this project was estimating recruitment due to the difficulties in observing and quantifying coral recruitment considering that corals reproduce both sexually and asexually and release massive numbers of eggs and sperm in broadcast spawning events. In this study, I modeled recruitment in four different ways to try to identify the most accurate estimate of recruitment. The first two methods were better for data-poor situations while the last two methods utilized field data collected from NOAA Pacific Islands Fisheries Science Center (PIFSC). The first method involved changing the recruitment parameter to achieve a stable population growth rate ($\lambda = 1$) while in the second method, I altered the recruitment parameter to achieve a matching observed stable size distribution and empirical stable size distribution. Both of these methods are simple, fast, and useful in data-poor situations, but are not ideal in areas affected by disturbances because both assume either constant recruitment or stable population growth. The first method also resulted in a recruitment parameter that was several magnitudes higher than the other estimates and likely overestimated coral recruitment. These inflated recruitment values were likely driven up by the incorrect assumption that population growth rate was stable ($\lambda = 1$) whereas the population was actually decreasing ($\lambda < 1$). Therefore, the stable size distribution method (second method) may provide a more accurate estimate for recruitment in situations lacking

observational data. The last two methods used field data at two different scales. The third method utilized the number of recruits observed in the study sites while the fourth method used juvenile density data from regional benthic monitoring conducted across the entire Hawaiian archipelago. Leveraging a large dataset of recruitment data provided a more accurate representation of real-life conditions on the reefs compared to the first two methods. While the last methods resulted in similar recruitment parameter estimates, the third method assumed a stock-recruitment relationship existed at the scale of a single 10 x 10-meter site. This assumption is highly unlikely given that many Hawaiian reef tracts seed other reefs on the scale of an island or adjacent islands (Storlazzi et al. 2017). The sector-scale (sub-island) utilized in the fourth method best reflects this scale and provides a more realistic estimate of larval recruitment in Hawai'i. Therefore, I show that the last two methods using recruitment data from the field produced reliable recruitment estimates, particularly compared to the first method, which resulted in a recruitment estimate several magnitudes higher than the other three methods. While the sector-level stock recruitment estimate from the fourth method may provide the most robust estimate of coral recruitment in Hawai'i, the stable size distribution method (second method) is an alternate way to estimate recruitment in a data-poor scenario.

POPULATION SENSITIVITY TO CERTAIN VITAL RATES

Elasticity analyses showed that coral population dynamics are primarily driven by growth and survival for all genera across the Hawaiian archipelago. I expected that life-history differences between taxa would affect which vital rates drive the population growth. However, across all taxa and regions, growth and survival made a large contribution (95-99%) to the population growth rate and, in general, medium to large corals surviving and maintaining stasis most impacted lambda. The exception to this trend was observed in the MHI where the population growth rate was driven by *Montipora* corals increasing in size. This could be due to *Montipora* corals there exhibiting extensive partial mortality. Larger colonies made up of numerous fragments had lower rates of whole-colony mortality relative to colonies of the same size with fewer

fragments. Given the higher survivorship of multi-fragmented colonies, it could be advantageous for colonies to fragment into smaller pieces both to avoid total mortality and increase the probability of small fragments growing into a larger size class. The idea that the survival of medium-large colonies drives population dynamics supports the current understanding that survival and reproductive potential increase with colony size (Hall & Hughes 1996, Raymundo & Maypa 2004). Therefore, larger corals surviving and maintaining their size (i.e., not shrinking or experiencing partial mortality) influence all other demographic processes and contribute the most to population growth.

Growth and survival had a greater impact on population growth compared to recruitment and the importance of recruitment varied by region. Analyzing the relative contributions of growth/survival and recruitment separately revealed that recruitment had a minimal effect on population growth in the NWHI and for *Porites* in both regions (<1%) and was anywhere from around 122 to 1 million times less important than growth/survival. Growth and survival may be driving population growth for *Porites* and all taxa in the NWHI because if corals are maintaining their size and surviving despite exposure to thermal stress, recruitment may not be as critical in maintaining the population. In addition, corals in the NWHI may allocate their energy towards growth and survival at the expense of recruitment. These factors combined could make recruitment less significant for population dynamics in the NWHI. In contrast, in the MHI, recruitment could have a significant impact on the population growth rate. In the MHI, *Montipora* recruitment contributed nearly 5% to lambda. While recruitment was ~20x less important than growth/survival of medium-large *Montipora* colonies, from a management perspective, it is easier to stimulate recruitment compared to halting large colony mortality. Therefore, for *Montipora* corals, recruitment could have a significant impact on population growth. Across the archipelago, recruitment is important for medium-large sized colonies with the exception of *Montipora* corals in the MHI where the population growth depends on the largest colonies reproducing.

IPM analyses and the associated elasticity analysis give us the ability to perform fine-scale investigations of species demography and identify which vital rate has the strongest influence on recovery trajectories. Elasticity analyses can then be utilized to inform management strategies and guide management efforts. In my study, the

population dynamics for all three taxa are driven by growth and survival of medium to medium-large colonies. Therefore, conservation efforts should prioritize enhancing factors that positively affect survivorship of medium to medium-large corals, such as protecting species diversity (Clements & Hay 2019) and enhancing nutrition – which would only be economically viable in *ex situ* mariculture (Toh et al. 2014). Although recruitment does not drive changes in lambda in the NWHI, stimulating recruitment in the MHI will likely impact the population growth rate and this impact would likely be more significant for *Montipora* corals. For example, restoration groups could artificially outplant small coral fragments to encourage growth by fusion, which enhances survival (Kikuzawa et al. 2021). Other potential reproductive interventions include supportive breeding via captive rearing and release, or capturing gametes and larvae for future release into the wild (National Academies of Sciences, Engineering 2019).

While elasticity analyses can be used to determine the contribution of survival/growth and reproduction to population growth, they do not tell us the sensitivity of parameters to perturbation. Perturbation analyses explain how sensitive the population growth rate is to changes in vital rates. By quantifying the proportional changes in lambda when individual vital rates are varied, it is possible to identify which demographic process has the largest impact on population growth rates and quantify that impact. Future work should use a perturbation analysis in addition to an elasticity analysis to provide well-informed answers to management questions. These analyses could be used to determine which vital rates are the most important, which vital rates need to be reduced or increased to maximize population growth, and which specific demographic process should be targeted to conserve the population. This would be particularly useful for projecting the consequences of decreased survival or growth due to thermal stress on coral population dynamics.

EFFECT OF THERMAL STRESS ON POPULATION GROWTH

I anticipated that increasing frequency and severity of thermal anomalies would negatively impact coral populations and lead to declining populations. For *Porites*, this

relationship was evident. In contrast, I found no clear signal of effect of severity or frequency of thermal stress on lambda for *Montipora* and did not analyze this relationship for *Pocillopora* due to limited data. I also expected that the more frequent stress events in the NWHI would lead to lower lambda values; however, region did not predict the population growth rate. This was unexpected given that NWHI had a more "active" history of frequent thermal stress events with bleaching events occurring in 1997, 2002, 2004, 2005, 2014, 2015, and 2017 versus 2014 and 2015 in the MHI. This could be a result of acclimatization to more frequent thermal anomalies, where an organism undergoes phenotypic changes in response to environmental stress that results in a change in the organism's tolerance. In this way, acclimatization can increase survival and allow for a population to adapt (Coles & Brown 2003).

Encrusting growth forms like *Montipora* and massive morphologies like *Porites* are often both considered resistant to bleaching and often experience low mortality following bleaching events (Marshall & Baird 2000, Loya et al. 2001, McClanahan 2004, McCowan et al. 2012, Darling et al. 2012). One hypothesis is that less complex morphologies like sub-massive and encrusting corals may provide a physiological advantage during thermal stress events (Van Woesik et al. 2012). Nonetheless, the differing trends observed in my study could be due to morphological or taxonomic differences. While I expected that increasing frequency and severity of thermal stress would negatively impact encrusting populations, previous population simulations of extended, recurrent thermal disturbance elicited a stable population growth for encrusting corals (Cant et al. 2021). The ability of encrusting corals to quickly recolonize an area following a disturbance event combined with their fast growth could overcome high mortality rates and permit encrusting corals to maintain a stable population growth rate, despite the projected increase in thermal stress severity and frequency. Even though I expected that increased thermal stress events would negatively impact lambda, in my study, the massive growth form, which is considered stress tolerant, was more susceptible to thermal stress than the encrusting growth form. If this pattern holds true for other massive corals, the results for susceptible taxa like branching *Pocillopora* could be more concerning. Repeating this study with additional mounding or stress tolerant taxa would improve our ability to conclude whether all stress tolerant corals are negatively affected

by frequent and severe thermal anomalies. While both genera in my study do have different growth forms, they also belong to different families, with *Montipora* corals in the Acroporidae family and *Porites* corals in the Poritidae family. Mizerek, Baird, & Madin (2018) found that coral family explained more variation in bleaching response than morphological or physiological traits but including colony growth form with coral family increased predictability dramatically. Therefore, it is not possible to claim the different response observed was due to morphology or taxa alone. Variation in bleaching susceptibility is further confounded by differences in growth rates (Baird & Marshall 2002), tissue thickness (Dimond et al. 2012, Wooldridge 2014), colony size and age (Loya et al. 2001), and thermal tolerance of symbionts (Grottoli et al. 2014, Kenkel & Matz 2017, Thomas et al. 2019).

For massive *Porites* corals, the frequency of major thermal stress events (Degree Heating Weeks ≥ 4) negatively impacts lambda. When DHW reaches 4°C -weeks, minor to moderate coral bleaching is likely. This indicates that when frequent coral bleaching is occurring, the population growth rate suffers whereas when DHW < 4 in repeated events and bleaching is likely absent, the population growth rate is unaffected. For severity, any type of thermal stress event (DHW > 1) negatively impacts lambda. Therefore, even if coral bleaching is not likely to occur, *Porites* corals are harmed by severe thermal anomalies. It is also possible that a different threshold (e.g., DHW > 2 or DHW > 3) would have a much greater impact on lambda compared to DHW > 1. Bleaching events have been increasing in frequency in both regions of Hawai'i in the last decade and the frequency and intensity of mass bleaching events around the globe is predicted to increase (Hughes et al. 2018). If these predicted frequent bleaching events are lower in intensity (i.e., DHW < 4) in both regions, *Porites* populations may decline, but to a lesser extent than if the frequent bleaching events were also severe in nature.

I also showed that the significant effects of thermal stress frequency on population growth rate come from a short period of time (10 years), while the effect of severe events can stem from recent events or be spread out over a much longer timespan (1985 to 2019). The recent increase in the frequency of bleaching events in the last ten years and corresponding population growth rate decrease indicates that these recent events are likely leading to declining *Porites* populations in both regions. Both recent and longer-

term severe events negatively impact population growth. Severe events over the last ten years may be occurring too frequently for corals to adequately recover before the next severe event. In addition, severe events that happened long ago can lead to mass mortality that can nearly terminate a population. This could lead to a cascading effect where individual colonies are first removed from the population due to mortality. Then, there is both a smaller spawning stock as well as reduced colony fitness and decreased reproduction for the colonies that survive, especially if losses stem from the medium-large sized colonies (Grottoli et al. 2014, Schoepf et al. 2015). With decreased reproductive output, the population continues to stagnate, and population growth is minimal for several years. Thus, severe bleaching events from many years' past can cause long-lasting impacts.

Major frequent thermal stress events that occurred within the last ten years negatively impact lambda, but any type (magnitude or timing) of severe event led to declining *Porites* populations. Our concern may not be how frequently these events are occurring, but rather their severity. Yet with climate change, these are accelerating and increasing simultaneously and as baseline thermal anomalies continue increasing in severity, future repeat events will likely be more severe (Hughes et al. 2018). Fortunately, the rate of corals' adaptation to temperature may be sufficient to prevent extinction of some coral populations – barring rapid environmental change, which can lead to adaptive collapse (Bay et al. 2017). Resilience strategies such as identifying and targeting resilient corals for assisted gene flow will be critical to ensuring the continuation of corals in Hawaii.

As demonstrated in this study, we can draw conclusions about how changes in heat stress severity and frequency are associated with lambda, but these metrics may not be the best predictors of population growth rate. My linear regression and multiple linear regression models had low R-squared values (Table 3), but it is difficult to predict biological processes and even more challenging to predict how complex organisms like corals will respond to disturbance events. It is possible that other temperature metrics with higher temporal and spatial resolution not tested in my study might have greater predictive power (Safaie et al. 2018). Although these results demonstrate the impact of frequent and severe thermal stress events, the impact to lambda may be specific to short

term events. More frequent photomosaic sampling would allow us to better estimate acute effects of thermal stress. While my study represents one of the largest spatial and temporal datasets for corals, it lacks high temporal resolution. Photogrammetry is a cost-effective method to collect demographic data from repeated sampling (Burns et al. 2015), but cost and scale still limit our ability to sample yearly or monthly, particularly at the scale of the entire Hawaiian archipelago. Machine learning and cloud-based tools like CoralNet could be used to automate 2D image analysis from benthic photo transects (Beijbom et al. 2012) and overcome the significant data processing time necessary for processing and annotating the 3D models created from SfM photogrammetry. Alternately, more frequent sampling could be conducted at a smaller scale (i.e., island-scale) to measure the impacts of acute stress.

To estimate corals' recovery time at the scale of the entire archipelago, future research should also model additional environmental variables other than temperature. For example, high levels of anthropogenic nutrients can increase bleaching susceptibility (Wiedenmann et al. 2012, Donovan et al. 2020), while moderate doses of anthropogenic nutrients can have no impact on coral growth and fish-mediated nutrients positively affect coral growth (Allgeier et al. 2020). Other environmental variables that have the potential to influence coral recovery include turbidity and sedimentation, which can reduce mortality during thermal stress (Anthony et al. 2007, Sully & van Woesik 2020), dissolved oxygen (Albright 2018), wind conditions and wave action (Jokiel & Brown 2004, Harrison et al. 2019) and salinity (Hoegh-Guldberg & Smith 1989, Gegner et al. 2017).

To better model the acute effects of thermal stress, future work could examine the time since the last disturbance as well as other metrics of thermal stress. I expect that a shorter time to the last thermal stress event (i.e., recent event) and that less time since the last severe event (i.e., DHW $\geq$ 8) would be associated with a low lambda value. Modeling the acute effects of thermal stress could reveal the short-term impacts of temperature stress on coral population dynamics. Determining the impact that time has on lambda would allow us to better estimate corals' recovery time. In addition to the time to last disturbance, future research should include the high-frequency temperature variability (i.e., daily temperature range) – the difference between maximum and minimum

temperatures for each day – which has been shown to be the most influential factor in predicting bleaching prevalence (Safaie et al. 2018). Future studies would also benefit from explicitly modeling the impact of widespread bleaching on population dynamics. While I modeled mild heat stress (DHW > 1) and major heat stress (DHW ≥ 4), NOAA Coral Reef Watch uses DHW ≥ 8 as a threshold for severe, widespread bleaching. If we limit the temperature stress metric to severe, widespread stress, we may see a higher correlation between increasing thermal stress and declining population growth. Other variables that should be included include the sea surface temperature (SST) anomaly – the daily climatological difference in SST – and Coral Bleaching HotSpots – the occurrence and magnitude of instantaneous heat stress/areas that have exceeded the maximum monthly mean SST by at least one degree Celsius. These variables, in combination with thermal stress severity and frequency measured in DHW, would give a more robust analysis of the impact of thermal stress on coral populations.

LIMITATIONS OF IPM MODELING

IPMs are powerful mathematical tools to assess population dynamics and project population sizes under future climate scenarios (Burgess 2011, Bruno et al. 2011, Madin et al. 2012, Edmunds et al. 2014, Montero-Serra et al. 2018, Kayal et al. 2018, Cant et al. 2021); however, there are several challenges with implementing an IPM for a coral population.

In this study, I modeled recruitment in four different ways. The first two methods (tuning the recruitment parameter to achieve a stable population growth and tuning the recruitment parameter to match the empirical size structure to the stable size distribution), can both be utilized in studies lacking observed recruitment data. Nevertheless, both of these methods are limited by the assumption that populations remain stable during disturbance events and do not account for stochasticity. Future work could utilize Bayesian state-space framework (Nickols et al. 2019) to account for environmental stochasticity.

Additionally, my surveys were conducted over a large timescale, but the time between censuses varied between sites. Normalizing by time interval for the survival portion of the IPM was relatively simple for the site-interval-genus models and was achieved by dividing by the time interval in the survival IPM sub-kernel, but this presented a challenge for the region-genus models. I addressed this challenge by annualizing survival in the vital rate function by using the logistic regression model to predict estimated survival and using the annualized survival probability to refit logistic regression models for the aggregate region-genus models. To improve IPM model building, future work should consider using a binomial mixed model for survival with time interval and site added as random effects to improve survival model fits.

Finally, while there is an urgent need for demographic approaches to evaluate the consequences of declining coral abundance, IPMs demand a data-heavy approach that limits their usability (Edmunds & Riegl 2020). IPMs also demand large quantities of fecundity data. While this limitation can be partially resolved through my detailed recruitment modeling approach, collecting observed recruitment data from Structure-from-Motion orthoprojections is extremely time-consuming and modeling the recruitment parameter without field data is less accurate. Considering the operational challenges inherent in collecting long-term demographic data, an IPM framework may not be possible for smaller coral monitoring organizations that lack access to extensive operations budgets.

MODELING THE IMPACT OF CLIMATE CHANGE ON MARINE BIODIVERSITY

The utility of the emerging technologies and novel modeling techniques described in this paper have wide applications outside of the scope of coral ecology. Structure-from-Motion (SfM) photogrammetry is a non-invasive tool that can be used to measure changes in coral demographics across a large spatial scale. SfM photogrammetry also has wide applications in marine research and can be used to better understand the patterns and changes in marine biodiversity in response to anthropogenic pressures (Burns 2016,

Ferrari et al. 2016, Couch et al. 2017, Fox et al. 2019, Magel et al. 2019). As demonstrated in this study, the demographic data collected from SfM can be used to parameterize population models, including IPMs. This research advances modeling techniques by promoting the use of IPMs for non-model populations and adds to the limited studies that apply IPMs to stony corals (Burgess 2011, Madin et al. 2012, Edmunds et al. 2014, Kayal et al. 2018, Scavo Lord et al. 2020, Cant et al. 2021). In addition, the iterative approach I used to parameterize my IPM models improved model output accuracy for demographically complex organisms like corals. Nevertheless, potential IPM applications are not limited to corals. My approaches to parameterizing an IPM could be applied to other sessile benthic species with complex demographic characteristics such as sponges, anemone, bryozoans, and tunicates.

Demographic approaches can also be used to investigate the impact of climate change stressors on population dynamics. Ocean warming is negatively impacting marine ecosystems around the globe (Hoegh-Guldberg & Bruno 2010) and it is important to understand the mechanisms by which thermal stress impacts the life history of marine organisms like phytoplankton, sea grasses, invertebrates, and sea birds (Polovina et al. 2008, Doney et al. 2009, Hoegh-Guldberg & Bruno 2010, Bennett et al. 2022). Demographic modeling can also be used to test hypotheses regarding the effects of intensifying environmental stressors like extreme weather events, hypoxia, sea level rise, and ocean acidification on ecological change (Coulson 2012, Edmunds & Riegl 2020). Because demographic approaches are well suited to projecting the fate of marine species in the face of anthropogenic climate change, they can be used to inform resilience management to reduce the impact of local stresses.

Unlike traditional monitoring assessments, demographic approaches can reveal the drivers of population change. Changes in coral communities are often studied by tracking percent coral cover, but this method can mask the underlying causes driving changes in community structure (Brito-Millán et al. 2019). In contrast, elasticity analyses and population models like IPMs can be used to identify which vital rates have the greatest impact on future changes in coral community composition. These results can be used by coral reef practitioners to craft specific interventions that can be utilized in conservation planning and management. Despite the usefulness of demographic

approaches, estimating the population growth rate in conjunction with coral cover could also provide further insight into the drivers of coral community structure. Although it is difficult to directly compare these two methods due to the paucity of coral cover studies undertaken at a similar temporal and spatial scale, my results are similar to other coral cover studies. Previous studies found that coral cover in the NWHI decreased significantly during the back to back bleaching events in 2014 and 2015 (Couch et al. 2017) and moderately between 2012 and 2016 (Brainard et al. 2020). Similar to my results, Brainard et al. (2020) found that benthic cover from 2012 to 2016 was significantly negatively impacted in the MHI. Therefore, documenting changes in both coral cover and the population growth rate will be important for assessing future declines in coral reefs and identifying potential reefs that could be targeted for management actions.

CONCLUSION

This thesis explored the impact of temperature stress on coral population dynamics across the Hawaiian archipelago using repeated imaging through Structure from Motion photogrammetry at fixed-sites. I successfully developed a process to estimate vital rates for individual coral colonies from orthomosaics. My study represents one of the few applications of IPMs for demographically complex organisms like corals and is the largest coral IPM study to date in terms of combined spatial and temporal coverage. This research also presents four different approaches for modeling recruitment and illustrates the benefits and challenges of each method. This modeling effort will be particularly useful for future research projects with limited recruitment data. I found that all three coral genera, which have different morphologies and life-history strategies, had negative population growth rates. As expected, smaller colonies experienced faster growth, but large colonies had a high probability of shrinking, due to partial mortality. Given the high survivorship of multi-fragmented colonies, large colonies fragmenting into smaller pieces may be advantageous for evading total mortality. Across all taxa and both regions, population dynamics were primarily driven by coral growth and survival and could be targeted in future restoration and adaptation projects whereas recruitment had a minimal effect on population growth. This study also demonstrates that increasing severity and frequency of thermal anomalies from climate change is causing population-level decline of *Porites* corals across the Hawaiian archipelago. Modeling efforts can be further improved by using a perturbation analysis to guide management strategies and by incorporating other variables indicative of acute thermal stress or other environmental variables to provide a more robust understanding of the impact of environmental stress on population dynamics. This study highlights how future thermal stress events may negatively impact even the most stress tolerant coral morphological type in an environment where coral populations across the archipelago are declining. By improving our understanding of corals' vulnerabilities to ocean warming, we can better plan for conservation efforts to help preserve these critical ecosystems.

REFERENCES

Adjeroud M, Michonneau F, Edmunds PJ, Chancerelle Y, de Loma TL, Penin L, Thibaut L, Vidal-Dupiol J, Salvat B, Galzin R (2009) Recurrent disturbances, recovery trajectories, and resilience of coral assemblages on a South Central Pacific reef. Coral Reefs 28:775–780.

Ainsworth TD, Heron SF, Ortiz JC, Mumby PJ, Grech A, Ogawa D, Eakin CM, Leggat W (2016) Climate change disables coral bleaching protection on the Great Barrier Reef. Science (80-) 352:338–342.

Albright R (2018) Ocean Acidification and Coral Bleaching. In: *Coral Bleaching: Patterns, Processes, Causes and Consequences*. Springer, Cham, p 295–323

Allgeier JE, Andskog MA, Hensel E, Appaldo R, Layman C, Kemp DW (2020) Rewiring coral: Anthropogenic nutrients shift diverse coral–symbiont nutrient and carbon interactions toward symbiotic algal dominance. Glob Chang Biol 26:5588–5601.

Alvarez-Buylla ER, Slatkin M (1994) Finding Confidence Limits on Population Growth Rates: Three Real Examples Revised. Ecology 75:255–260.

Anthony KRN, Connolly SR, Hoegh-Guldberg O (2007) Bleaching, energetics, and coral mortality risk: Effects of temperature, light, and sediment regime. Limnol Oceanogr 52:716–726.

Arizmendi-Mejía R, Ledoux JB, Civit S, Antunes A, Thanopoulou Z, Garrabou J, Linares C (2015) Demographic responses to warming: reproductive maturity and sex influence vulnerability in an octocoral. Coral Reefs 34:1207–1216.

Baird AH, Marshall PA (2002) Mortality, growth and reproduction in scleractinian corals following bleaching on the Great Barrier Reef. Mar Ecol Prog Ser 237:133–141.

Baker AC, Starger CJ, McClanahan TR, Glynn PW (2004) Corals' adaptive response to climate change. Nature 430:741–741.

Barkley HC, Cohen AL, Mollica NR, Brainard RE, Rivera HE, DeCarlo TM, Lohmann GP, Drenkard EJ, Alpert AE, Young CW, Vargas-Ángel B, Lino KC, Oliver TA, Pietro KR, Luu VH (2018) Repeat bleaching of a central Pacific coral reef over the past six decades (1960–2016). Commun Biol 1:1–10.

Bay RA, Rose NH, Logan CA, Palumbi SR (2017) Genomic models predict successful coral adaptation if future ocean warming rates are reduced. Sci Adv 3.

Beijbom O, Edmunds PJ, Kline DI, Mitchell BG, Kriegman D (2012) Automated annotation of coral reef survey images. Proc IEEE Comput Soc Conf Comput Vis Pattern Recognit:1170–1177.

Bennett S, Alcoverro T, Kletou D, Antoniou C, Boada J, Buñuel X, Cucala L, Jorda G, Kleitou P, Roca G, Santana-Garcon J, Savva I, Vergés A, Marbà N (2022) Resilience of seagrass populations to thermal stress does not reflect regional

differences in ocean climate. New Phytol 233:1657–1666.

Borgstein N, Beltrán DM, Prada C (2020) Variable Growth Across Species and Life Stages in Caribbean Reef Octocorals. Front Mar Sci 7:1–11.

Brainard R, Conklin E, Delaney D, Duke W, Falinski K, Geiger E, Grabowski T, Hall R, Heenan A, Heinen De Carlo E, Kimball J, Koike H, Lameier M, Levine A, Maurin P, Minato RSR, Oleson K, Oliver T, Parrish F, Richmond B, Schemmel E, Schroeder B, Swanson D, Teneva L, Timmers M, Uchimura R, Vargas-Angel B, Williams I, Young C (2020) Coral reef condition: A status report for the Hawaiian Archipelago.

Brandt ME (2009) The effect of species and colony size on the bleaching response of reef-building corals in the Florida Keys during the 2005 mass bleaching event. Coral Reefs 28:911–924.

Brito-Millán M, Vermeij M, Alcantar E, Sandin S (2019) Coral reef assessments based on cover alone mask active dynamics of coral communities. Mar Ecol Prog Ser 630:55–68.

Brown BE (1997) Coral bleaching: causes and consequences. Coral Reefs 16:129–138.

Bruno JF, Ellner SP, Vu I, Kim K, Harvell CD (2011) Impacts of aspergillosis on sea fan coral demography: modeling a moving target. Ecol Monogr 81:123–139.

Burgess HR (2011) Integral Projection Models and analysis of patch dynamics of the reef building coral *Monstastraea annularis*. Dissertation. University of Exeter. Exeter, UK.

Burke L, Reytar K, Spalding M, Perry A (2011) Reefs at Risk Revisited. Washington, D.C.

Burns JHR (2016) New Insights Into the Biology and Ecology of Hawaiian Corals Enabled by 3D Reconstruction Technology. Dissertation. University of Hawaii Manoa. Manoa, Hawaii.

Burns JHR, Delparte D, Gates RD, Takabayashi M (2015) Integrating structure-from-motion photogrammetry with geospatial software as a novel technique for quantifying 3D ecological characteristics of coral reefs. PeerJ 2015:e1077.

Cant J, Salguero-Gómez R, Kim SW, Sims CA, Sommer B, Brooks M, Malcolm HA, Pandolfi JM, Beger M (2021) The projected degradation of subtropical coral assemblages by recurrent thermal stress. J Anim Ecol 90:233–247.

Caswell H (2001) Matrix Population Models, Second Edition. Sinauer Associates, Inc. Publishers, Sunderland, Massachusetts.

Clements CS, Hay ME (2019) Biodiversity enhances coral growth, tissue survivorship and suppression of macroalgae. Nat Ecol Evol 2019 32 3:178–182.

Coles SL, Brown BE (2003) Coral Bleaching - Capacity for Acclimatization and Adaptation. In: *Advances in Marine Biology*. Southward AJ, Tyler PA, Young CM, Fuiman LA (eds) Academic Press, p 183–212

Costanza R, de Groot R, Sutton P, van der Ploeg S, Anderson SJ, Kubiszewski I, Farber

S, Turner RK (2014) Changes in the global value of ecosystem services. Glob Environ Chang 26:152–158.

Couch CS, Burns JHR, Liu G, Steward K, Gutlay TN, Kenyon J, Eakin CM, Kosaki RK (2017) Mass coral bleaching due to unprecedented marine heatwave in Papahānaumokuākea Marine National Monument (Northwestern Hawaiian Islands). PLoS One 12:1–27.

Coulson T (2012) Integral projections models, their construction and use in posing hypotheses in ecology. Oikos 121:1337–1350.

Cunning R, Ritson-Williams R, Gates RD (2016) Patterns of bleaching and recovery of *Montipora capitata* in Kāne'ohe Bay, Hawai'i, USA. Mar Ecol Prog Ser 551:131–139.

Darling ES, Alvarez-Filip L, Oliver TA, McClanahan TR, Côté IM (2012) Evaluating life-history strategies of reef corals from species traits. Ecol Lett 15:1378–1386.

Dimond JL, Holzman BJ, Bingham BL (2012) Thicker host tissues moderate light stress in a cnidarian endosymbiont. J Exp Biol 215:2247–2254.

Doney SC, Fabry VJ, Feely RA, Kleypas JA (2009) Ocean Acidification: The Other CO_2 Problem. Ann Rev Mar Sci 1:169–192.

Donner SD, Skirving WJ, Little CM, Oppenheimer M, Hoegh-Guldberg O (2005) Global assessment of coral bleaching and required rates of adaptation under climate change. Glob Chang Biol 11:2251–2265.

Donovan MK, Adam TC, Shantz AA, Speare KE, Munsterman KS, Rice MM, Schmitt RJ, Holbrook SJ, Burkepile DE (2020) Nitrogen pollution interacts with heat stress to increase coral bleaching across the seascape. Proc Natl Acad Sci 117:5351–5357.

Eakin CM, Morgan JA, Heron SF, Smith TB, Liu G, Alvarez-Filip L, Baca B, Bartels E, Bastidas C, Bouchon C, Brandt M, Bruckner AW, Bunkley-Williams L, Cameron A, Causey BD, Chiappone M, Christensen TRL, Crabbe MJC, Day O, de la Guardia E, Díaz-Pulido G, DiResta D, Gil-Agudelo DL, Gilliam DS, Ginsburg RN, Gore S, Guzmán HM, Hendee JC, Hernández-Delgado EA, Husain E, Jeffrey CFG, Jones RJ, Jordán-Dahlgren E, Kaufman LS, Kline DI, Kramer PA, Lang JC, Lirman D, Mallela J, Manfrino C, Maréchal JP, Marks K, Mihaly J, Miller WJ, Mueller EM, Muller EM, Toro CAO, Oxenford HA, Ponce-Taylor D, Quinn N, Ritchie KB, Rodríguez S, Ramírez AR, Romano S, Samhouri JF, Sánchez JA, Schmahl GP, Shank B V., Skirving WJ, Steiner SCC, Villamizar E, Walsh SM, Walter C, Weil E, Williams EH, Roberson KW, Yusuf Y (2010) Caribbean Corals in Crisis: Record Thermal Stress, Bleaching, and Mortality in 2005. PLoS One 5:9.

Eakin CM, Sweatman HPA, Brainard RE (2019) The 2014–2017 global-scale coral bleaching event: insights and impacts. Coral Reefs 38:539–545.

Easterling MR (1998) The Integral Projection Model: Theory, Analysis and Application. Dissertation. North Carolina State University. Raleigh, North Carolina.

Easterling MR, Ellner SP, Dixon PM (2000) Size-specific sensitivity: Applying a new structured population model. Ecology 81:694–708.

Edmunds PJ (2015) A quarter-century demographic analysis of the Caribbean coral, *Orbicella annularis*, and projections of population size over the next century. Limnol Oceanogr 60:840–855.

Edmunds PJ (2018) Implications of high rates of sexual recruitment in driving rapid reef recovery in Mo'orea, French Polynesia. Sci Rep 8:16615.

Edmunds PJ (2005) The effect of sub-lethal increases in temperature on the growth and population trajectories of three scleractinian corals on the southern Great Barrier Reef. Oecologia 146:350–364.

Edmunds PJ, Burgess SC, Hollie M. Putnam, Marissa L. Baskett, Lorenzo Bramanti, Nick S. Fabina, Xueying Han, Michael P. Lesser, Joshua S. Madin, Christopher B. Wall, Denise M. Yost, Gates RD (2014) Evaluating the causal basis of ecological success within the scleractinia: an integral projection model approach. Mar Biol 161:2719–2734.

Edmunds PJ, Elahi R (2007) The demographics of a 15-year decline in cover of the Caribbean reef coral *Montastraea annularis*. Ecol Monogr 77:3–18.

Edmunds PJ, Riegl B (2020) Urgent need for coral demography in a world where corals are disappearing. Mar Ecol Prog Ser 635:233–242.

Edwards CB, Eynaud Y, Gareth, Williams J, Pedersen NE, Zgliczynski BJ, Arthur, Gleason CR, Smith JE, Sandin SA (2017) Large-area imaging reveals biologically driven non-random spatial patterns of corals at a remote reef. Coral Reefs 36:1291–1305.

Falkowski PG, Dubinsky Z, Muscatine L, Porter JW (1984) Light and the Bioenergetics of a Symbiotic Coral. Bioscience 34:705–709.

Ferrari R, Bryson M, Bridge T, Hustache J, Williams SB, Byrne M, Figueira W (2016) Quantifying the response of structural complexity and community composition to environmental change in marine communities. Glob Chang Biol 22:1965–1975.

Fonstad MA, Dietrich JT, Courville BC, Jensen JL, Carbonneau PE (2013) Topographic structure from motion: A new development in photogrammetric measurement. Earth Surf Process Landforms 38:421–430.

Forsman ZH, Page CA, Toonen RJ, Vaughan D (2015) Growing coral larger and faster: Micro-colony-fusion as a strategy for accelerating coral cover. PeerJ 2015:e1313.

Fox MD, Carter AL, Edwards CB, Takeshita Y, Johnson MD, Petrovic V, Amir CG, Sala E, Sandin SA, Smith JE (2019) Limited coral mortality following acute thermal stress and widespread bleaching on Palmyra Atoll, central Pacific. Coral Reefs 38:701–712.

Franklin EC, Jokiel PL, Donahue MJ (2013) Predictive modeling of coral distribution and abundance in the Hawaiian Islands. Mar Ecol Prog Ser 481:121–132.

Gegner HM, Ziegler M, Rädecker N, Buitrago-López C, Aranda M, Voolstra CR (2017) High salinity conveys thermotolerance in the coral model *Aiptasia*. Biol Open 6:1943–1948.

Gilmour JP, Smith LD, Heyward AJ, Baird AH, Pratchett MS (2013) Recovery of an isolated coral reef system following severe disturbance. Science (80-) 340:69–71.

Gintert BE, Manzello DP, Enochs IC, Kolodziej G, Carlton R, Gleason ACR, Gracias N (2018) Marked annual coral bleaching resilience of an inshore patch reef in the Florida Keys: A nugget of hope, aberrance, or last man standing? Coral Reefs 37:533–547.

Glynn PW (1984) Widespread Coral Mortality and the 1982–83 El Niño Warming Event. Environ Conserv 11:133–146.

Glynn PW, D'Croz L (1990) Experimental evidence for high temperature stress as the cause of El Niño-coincident coral mortality. Coral Reefs 8:181–191.

Golbuu Y, Victor AS, Penland AL, Idip AD, Emaurois AC, Okaji AK, Yukihira AH, Iwase AA, Van Woesik AR (2007) Palau's coral reefs show differential habitat recovery following the 1998-bleaching event. Coral Reefs 26:319–332.

Gouezo M, Golbuu Y, Fabricius K, Olsudong D, Mereb G, Nestor V, Wolanski E, Harrison P, Doropoulos C (2019) Drivers of recovery and reassembly of coral reef communities. Proc R Soc B Biol Sci 286:20182908.

Grottoli AG, Warner ME, Levas SJ, Aschaffenburg MD, Schoepf V, Mcginley M, Baumann J, Matsui Y (2014) The cumulative impact of annual coral bleaching can turn some coral species winners into losers. Glob Chang Biol 20:3823–3833.

Hall VR, Hughes TP (1996) Reproductive Strategies of Modular Organisms: Comparative Studies of Reef- Building Corals. Ecology 77:950–963.

Harrison HB, Álvarez-Noriega M, Baird AH, Heron SF, MacDonald C, Hughes TP (2019) Back-to-back coral bleaching events on isolated atolls in the Coral Sea. Coral Reefs 38:713–719.

Hernández-Pacheco R, Hernández-Delgado EA, Sabat AM (2011) Demographics of bleaching in a major Caribbean reef-building coral: *Montastraea annularis*. Ecosphere 2:1–13.

Heron SF, Johnston L, Liu G, Geiger EF, Maynard JA, De La Cour JL, Johnson S, Okano R, Benavente D, Burgess TFR, Iguel J, Perez DI, Skirving WJ, Strong AE, Tirak K, Mark Eakin C (2016a) Validation of Reef-Scale Thermal Stress Satellite Products for Coral Bleaching Monitoring. Remote Sens 2016, Vol 8, Page 59 8:1–16.

Heron SF, Maynard JA, van Hooidonk R, Eakin CM (2016b) Warming Trends and Bleaching Stress of the World's Coral Reefs 1985–2012. Sci Rep 6:38402.

Hoegh-Guldberg O, Bruno JF (2010) The impact of climate change on the world's marine ecosystems. Science (80-) 328:1523–1528.

Hoegh-Guldberg O, Smith GJ (1989) The effect of sudden changes in temperature, light and salinity on the population density and export of zooxanthellae from the reef corals *Stylophora pistillata* Esper and *Seriatopora hystrix* Dana. J Exp Mar Bio Ecol 129:279–303.

Howells EJ, Beltran VH, Larsen NW, Bay LK, Willis BL, Van Oppen MJH (2012) Coral

thermal tolerance shaped by local adaptation of photosymbionts. Nat Clim Chang 2:116–120.

Hughes TP, Anderson KD, Connolly SR, Heron SF, Kerry JT, Lough JM, Baird AH, Baum JK, Berumen ML, Bridge TC, Claar DC, Eakin CM, Gilmour JP, Graham NAJ, Harrison H, Hobbs J-PA, Hoey AS, Hoogenboom M, Lowe RJ, McCulloch MT, Pandolfi JM, Pratchett M, Schoepf V, Torda G, Wilson SK (2018) Spatial and temporal patterns of mass bleaching of corals in the Anthropocene. Science 359:80–83.

Hughes TP, Baird AH, Bellwood DR, Card M, Connolly SR, Folke C, Grosberg R, Hoegh-Guldberg O, Jackson JBC, Kleypas J, Lough JM, Marshall P, Nyström M, Palumbi SR, Pandolfi JM, Rosen B, Roughgarden J (2003) Climate Change, Human Impacts, and the Resilience of Coral Reefs. Science (80-) 301:929–933.

Hughes TP, Connell JH (1987) Population dynamics based on size or age? A reef-coral analysis. Am Nat 129:818–829.

Hughes TP, Tanner JE (2000) Recruitment failure, life histories, and long-term decline of Caribbean corals. Ecology 81:2250–2263.

Johnston EC, Counsell CWW, Sale TL, Burgess SC, Toonen RJ (2020) The legacy of stress: Coral bleaching impacts reproduction years later. Funct Ecol 34:2315–2325.

Jokiel P, Coles S (1974) Effects of Heated Effluent on Hermatypic Corals at Kahe Point, Oahu. Pacific Sci 28:1–18.

Jokiel PL (2004) Temperature Stress and Coral Bleaching. In: *Coral Health and Disease*. Springer Berlin Heidelberg, Berlin, Heidelberg, p 401–425

Jokiel PL, Brown EK (2004) Global warming, regional trends and inshore environmental conditions influence coral bleaching in Hawaii. Glob Chang Biol 10:1627–1641.

Jones RJ (2008) Coral bleaching, bleaching-induced mortality, and the adaptive significance of the bleaching response. Mar Biol 154:65–80.

Jury CP, Toonen RJ (2019) Adaptive responses and local stressor mitigation drive coral resilience in warmer, more acidic oceans. Proc R Soc B Biol Sci 286:20190614.

Kayal M, Lenihan HS, Brooks AJ, Holbrook SJ, Schmitt RJ, Kendall BE (2018) Predicting coral community recovery using multi-species population dynamics models. Ecol Lett 21:1790–1799.

Kenkel CD, Matz M V. (2017) Gene expression plasticity as a mechanism of coral adaptation to a variable environment. Nat Ecol Evol 1:1–6.

Kenyon JC, Dunlap MJ, Aeby GS (2008) Community Structure of Hermatypic Corals at Kure Atoll in the Northwestern Hawaiian Islands: Stemming the Shifting Baseline. Atoll Res Bull:1–25.

Kenyon JC, Dunlap MJ, Wilkinson CB, Page KN, Vroom PS, Aeby GS (2007a) Community Structure of Hermatypic Corals at Pearl and Hermes Atoll, Northwestern Hawaiian Islands: Unique Conservation Challenges Within the Hawaiian Archipelago. Atoll Res Bull:1–23.

Kenyon JC, Vroom PS, Page KN, Dunlap MJ, Wilkinson CB, Aeby GS (2006) Community Structure of Hermatypic Corals at French Frigate Shoals, Northwestern Hawaiian Islands: Capacity for Resistance and Resilience to Selective Stressors. Pacific Sci 60:153–175.

Kenyon JC, Wilkinson CB, Dunlap MJ, Aeby GS, Kryss C (2007b) Community Structure of hermatypic corals at Laysan Island and Lisianski Island/Neva Shoal in the Northwestern Hawaiian Islands: a new layer of scientific exploration. Atoll Res Bull:1–23.

Kikuzawa YP, Ng CSL, Sam SQ, Toh TC, Tan KS, Loo PL, Chou LM (2021) Transplanting Coral Fragments in Close Contact Enhances Their Survival and Growth on Seawalls. J Mar Sci Eng 2021, Vol 9, Page 1377 9:1377.

Kodera SM, Edwards CB, Petrovic V, Pedersen NE, Eynaud Y, Sandin SA (2020) Quantifying life history demographics of the scleractinian coral genus *Pocillopora* at Palmyra Atoll. Coral Reefs 39:1091–1105.

Levitan DR, Boudreau W, Jara J, Knowlton N (2014) Long-term reduced spawning in *Orbicella* coral species due to temperature stress. Mar Ecol Prog Ser 515:1–10.

Liu G, Heron SF, Mark Eakin C, Muller-Karger FE, Vega-Rodriguez M, Guild LS, de la Cour JL, Geiger EF, Skirving WJ, Burgess TFR, Strong AE, Harris A, Maturi E, Ignatov A, Sapper J, Li J, Lynds S (2014) Reef-Scale Thermal Stress Monitoring of Coral Ecosystems: New 5-km Global Products from NOAA Coral Reef Watch. Remote Sens 6:11579–11606.

Liu G, Rauenzahn JL, Heron SF, Eakin CM, Skirving WJ, Christensen T, Strong AE, Li J (2013) NOAA coral reef watch 50 km satellite sea surface temperature-based decision support system for coral bleaching management. US Dept Commer NOAA Tech Memo:63.

Loya Y, Sakai K, Yamazato K, Nakano Y, Sambali H, van Woesik R (2001) Coral bleaching: the winners and the losers. Ecol Lett 4:122–131.

Madin JS, Hughes TP, Connolly SR (2012) Calcification, Storm Damage and Population Resilience of Tabular Corals under Climate Change. PLoS One 7:e46637.

Magel JMT, Burns JHR, Gates RD, Baum JK (2019) Effects of bleaching-associated mass coral mortality on reef structural complexity across a gradient of local disturbance. Sci Rep 9:1–12.

Marshall PA, Baird AH (2000) Bleaching of corals on the Great Barrier Reef: Differential susceptibilities among taxa. Coral Reefs 19:155–163.

Matsuda SB, Huffmyer AS, Lenz EA, Davidson JM, Hancock JR, Przybylowski A, Innis T, Gates RD, Barott KL (2020) Coral Bleaching Susceptibility Is Predictive of Subsequent Mortality Within but Not Between Coral Species. Front Ecol Evol 8:1–14.

McClanahan T, Polunin N, Done T (2002) Ecological States and the Resilience of Coral Reefs. Conserv Ecol 6.

McClanahan TR (2014) Decadal coral community reassembly on an African fringing

reef. Coral Reefs 33:939–950.

McClanahan TR (2004) The relationship between bleaching and mortality of common corals. Mar Biol 144:1239–1245.

McCowan DM, Pratchett MS, Baird AH (2012) Bleaching susceptibility and mortality among corals with differing growth forms. In: *Proceedings of the 12th International Coral Reef Symposium*. Cairns, Australia, p 9–13.

Merow C, Dahlgren JP, Metcalf CJE, Childs DZ, Evans MEK, Jongejans E, Record S, Rees M, Salguero-Gómez R, McMahon SM (2014) Advancing population ecology with integral projection models: a practical guide. Methods Ecol Evol 5:99–110.

Metcalf CJE, McMahon SM, Salguero-Gómez R, Jongejans E (2013) IPMpack : an R package for integral projection models. Methods Ecol Evol 4:195–200.

Mieog JC, Van Oppen MJH, Cantin NE, Stam WT, Olsen JL (2007) Real-time PCR reveals a high incidence of Symbiodinium clade D at low levels in four scleractinian corals across the Great Barrier Reef: Implications for symbiont shuffling. Coral Reefs 26:449–457.

Mizerek TL, Baird AH, Madin JS (2018) Species traits as indicators of coral bleaching. Coral Reefs 37:791–800.

Montero-Serra I, Linares C, Doak DF, Ledoux JB, Garrabou J (2018) Strong linkages between depth, longevity and demographic stability across marine sessile species. Proc R Soc B Biol Sci 285.

Montero-Serra I, Garrabou J, Doak DF, Ledoux J, Linares C (2019) Marine protected areas enhance structural complexity but do not buffer the consequences of ocean warming for an overexploited precious coral. J Appl Ecol 56:1063–1074.

National Academies of Sciences, Engineering and M (2019) A Research Review of Interventions to Increase the Persistence and Resilience of Coral Reefs. National Academies Press.

Naughton P, Edwards C, Petrovic V, Kastner R, Kuester F, Sandin S (2015) Scaling the annotation of subtidal marine habitats. In: *Proceedings of the 10th International Conference on Underwater Networks & Systems*. Arlington, Virginia.

Nickols KJ, White JW, Malone D, Carr MH, Starr RM, Baskett ML, Hastings A, Botsford LW (2019) Setting ecological expectations for adaptive management of marine protected areas. J Appl Ecol 56:2376–2385.

NOAA Coral Reef Conservation Program (2018) US Coral Reef Monitoring Data Summary 2018. NOAA Tech Memo CRCP 31:224.

NOAA Coral Reef Watch (2018, updated daily) NOAA Coral Reef Watch Version 3.1 Daily Global 5km Satellite Coral Bleaching Degree Heating Week Product. Jan. 1, 2010 - Dec. 31, 2019. College Park, Maryland.

NOAA Pacific Islands Fisheries Science Center (PIFSC) (2016) NOAA/PIFSC Rapid Ecological Assessment (REA) Reef Fish Survey Locations: Main Hawaiian Islands. Distributed by the Pacific Islands Ocean Observing System (PacIOOS).

Noreen AME, Harrison PL, Van Oppen MJH (2009) Genetic diversity and connectivity in a brooding reef coral at the limit of its distribution. Proc R Soc B Biol Sci 276:3927–3935.

Obura DO (2001) Can Differential Bleaching and Mortality Among Coral Species Offer Useful Indicators for Assessment and Management of Reefs Under Stress? Bull Mar Sci 69:421–442.

Oliver TA, Palumbi SR (2011) Do fluctuating temperature environments elevate coral thermal tolerance? Coral Reefs 30:429–440.

Palumbi SR, Barshis DJ, Traylor-Knowles N, Bay RA (2014) Mechanisms of reef coral resistance to future climate change. New Ser 344:895–898.

Pandolfi JM, Bradbury RH, Sala E, Hughes TP, Bjorndal KA, Cooke RG, McArdle D, McClenachan L, Newman MJH, Paredes G, Warner RR, Jackson JBC (2003) Global Trajectories of the Long-Term Decline of Coral Reef Ecosystems. Science 301:955–958.

Petrovic V, Vanoni DJ, Richter AM, Levy TE, Kuester F (2014) Visualizing high resolution three-dimensional and two-dimensional data of cultural heritage sites. J Mediterr Archaeol Archaeom 14:93–100.

Pizarro O, Friedman A, Bryson M, Williams SB, Madin J (2017) A simple, fast, and repeatable survey method for underwater visual 3D benthic mapping and monitoring. Ecol Evol 7:1770–1782.

Polovina JJ, Howell EA, Abecassis M (2008) Ocean's least productive waters are expanding. Geophys Res Lett 35.

Precoda K, Baird A, Madsen A, Mizerek T, Sommer B, Su S, Madin J (2018) How does a widespread reef coral maintain a population in an isolated environment? Mar Ecol Prog Ser 594:85–94.

Putnam HM, Gates RD (2015) Preconditioning in the reef-building coral *Pocillopora damicornis* and the potential for trans-generational acclimatization in coral larvae under future climate change conditions. J Exp Biol 218:2365–2372.

Raymundo LJ, Maypa AP (2004) Getting Bigger Faster: Mediation of Size-Specific Mortality via Fusion in Juvenile Coral Transplants. Ecol Appl 14:281–295.

Riegl B, Johnston M, Purkis S, Howells E, Burt J, Steiner SCC, Sheppard CRC, Bauman A (2018) Population collapse dynamics in *Acropora downingi*, an Arabian/Persian Gulf ecosystem-engineering coral, linked to rising temperature. Glob Chang Biol 24:2447–2462.

Rodgers KS, Jokiel PL, Brown EK, Hau S, Sparks R (2015) Over a Decade of Change in Spatial and Temporal Dynamics of Hawaiian Coral Reef Communities. Pacific Sci 69:1–13.

Rodriguez C, Amir C, Gray A, Asbury M, Suka R, Lamirand M, Couch CS, Oliver T (2021) Extracting Coral Vital Rate Estimates at Fixed Sites Using Structure-from-Motion Standard Operating Procedures. US Dept Commer NOAA Tech Memo:90.

Romero-Torres M, Acosta A, Palacio-Castro AM, Treml EA, Zapata FA, Paz-García DA, Porter JW (2020) Coral reef resilience to thermal stress in the Eastern Tropical Pacific. Glob Chang Biol 26:3880–3890.

Ross M (2015) Environmental and Demographic Drivers of Hawaiian Reef Corals. Dissertation. University of Hawaii at Manoa. Manoa, Hawaii.

Roth L, Koksal S, van Woesik R (2010) Effects of thermal stress on key processes driving coral-population dynamics. Mar Ecol Prog Ser 411:73–87.

Safaie A, Silbiger NJ, McClanahan TR, Pawlak G, Barshis DJ, Hench JL, Rogers JS, Williams GJ, Davis KA (2018) High frequency temperature variability reduces the risk of coral bleaching. Nat Commun 2018 91 9:1–12.

Sale T, Marko P, Oliver T, Hunter C (2019) Assessment of acclimatization and subsequent survival of corals during repeated natural thermal stress events in Hawai'i. Mar Ecol Prog Ser 624:65–76.

Savage VM, Gillooly JF, Brown JH, Charnov EL, Charnov EL (2004) Effects of body size and temperature on population growth. Am Nat 163:429–41.

Scavo Lord K, Lesneski KC, Bengtsson ZA, Kuhn KM, Madin J, Cheung B, Ewa R, Taylor JF, Burmester EM, Morey J, Kaufman L, Finnerty JR (2020) Multi-Year Viability of a Reef Coral Population Living on Mangrove Roots Suggests an Important Role for Mangroves in the Broader Habitat Mosaic of Corals. Front Mar Sci 7:377.

Schlecker L, Page C, Matz M, Wright RM (2022) Mechanisms and potential immune tradeoffs of accelerated coral growth induced by microfragmentation. PeerJ.

Schoepf V, Grottoli AG, Levas SJ, Aschaffenburg MD, Baumann JH, Matsui Y, Warner ME (2015) Annual coral bleaching and the long-term recovery capacity of coral. Proc R Soc B Biol Sci 282:1–9.

Sheppard C, Harris A, Sheppard A (2008) Archipelago-wide coral recovery patterns since 1998 in the Chagos Archipelago, central Indian Ocean. Mar Ecol Prog Ser 362:109–117.

Skirving W, Marsh B, De La Cour J, Liu G, Harris A, Maturi E, Geiger E, Mark Eakin C (2020) CoralTemp and the Coral Reef Watch Coral Bleaching Heat Stress Product Suite Version 3.1. Remote Sens 12:1–10.

Stearns SC (1989) Trade-Offs in Life-History Evolution. Funct Ecol 3:259.

Storlazzi CD, van Ormondt M, Chen YL, Elias EPL (2017) Modeling fine-scale coral larval dispersal and interisland connectivity to help designate mutually-supporting coral reef marine protected areas: Insights from Maui Nui, Hawaii. Front Mar Sci 4:1–14.

Suka R, Asbury M, Couch C, Gray A, Winston M, Oliver T (2019) Processing Photomosaic Imagery of Coral Reefs Using Structure-from-Motion Standard Operating Procedures. US Dept Commer:54.

Sully S, van Woesik R (2020) Turbid reefs moderate coral bleaching under climate-

related temperature stress. Glob Chang Biol 26:1367–1373.

Szmant AM (1991) Sexual reproduction by the Caribbean reef corals *Montastrea annularis* and *M. cavernosa*. Mar Ecol Prog Ser 74:13–25.

Szmant AM, Gassman NJ (1990) The effects of prolonged 'bleaching' on the tissue biomass and reproduction of the reef coral *Montastrea annularis*. Coral Reefs 8:217–224.

Thomas L, López EH, Morikawa MK, Palumbi SR (2019) Transcriptomic resilience, symbiont shuffling, and vulnerability to recurrent bleaching in reef-building corals. Mol Ecol 28:3371–3382.

Thompson DM, van Woesik R (2009) Corals escape bleaching in regions that recently and historically experienced frequent thermal stress. Proc R Soc B Biol Sci 276:2893–2901.

Toh TC, Ng CSL, Peh JWK, Toh K Ben, Chou LM (2014) Augmenting the Post-Transplantation Growth and Survivorship of Juvenile Scleractinian Corals via Nutritional Enhancement. PLoS One 9:1–9.

Wiedenmann J, D'Angelo C, Smith EG, Hunt AN, Legiret FE, Postle AD, Achterberg EP (2012) Nutrient enrichment can increase the susceptibility of reef corals to bleaching. Nat Clim Chang 3:160–164.

Wilkinson C (2004) Status of Coral Reefs of the World: 2004. Townsville, Queensland.

Van Woesik R, Irikawa A, Anzai R, Nakamura T (2012) Effects of coral colony morphologies on mass transfer and susceptibility to thermal stress. Coral Reefs 31:633–639.

Wood SN (2011) Fast stable restricted maximum likelihood and marginal likelihood estimation of semiparametric generalized linear models. J R Stat Soc Ser B (Statistical Methodol 73:3–36.

Wooldridge SA (2014) Differential thermal bleaching susceptibilities amongst coral taxa: Re-posing the role of the host. Coral Reefs 33:15–27.

APPENDIX A

ADDITIONAL SITE INFORMATION

Supplementary Table 1. Latitude and longitude for the sixteen fixed sites in the Main Hawaiian Islands (MHI) and Papahānaumokuākea Marine National Monument in the Northwestern Hawaiian Islands (NWHI) used to assess coral population recovery in this study.

Site	Region	Latitude	Longitude
OAH_OCC_010	MHI	21.29	-157.90
OAH_OCC_005	MHI	21.48	-157.78
MAI_SIO_OL3	MHI	20.81	-156.60
MAI_OCC_002	MHI	20.87	-156.15
MAI_SIO_K01	MHI	20.94	-156.69
MAI_SIO_K02	MHI	20.94	-156.69
HAW_OCC_002	MHI	20.27	-155.90
HAW_OCC_010	MHI	19.24	-155.90
HAW_SIO_K08	MHI	19.44	-155.91
HAW_SIO_K10	MHI	19.64	-156.01
HAW_OCC_003	MHI	19.75	-155.06
KUR_OCC_010	KUR	28.39	-178.30
PHR_OCC_016	PHR	27.79	-176.00
LIS_OCC_005	LIS	26.04	-173.88
FFS_OCC_002	FFS	23.88	-166.29
FFS_OCC_014	FFS	23.79	-166.25

APPENDIX B

INTEGRAL PROJECT MODEL (IPM) PARAMETER ESTIMATES

Supplementary Table 2. Parameter estimates used in integral projection models (IPMs) of *Pocillopora*, *Montipora*, and *Porites* spp. in the Hawaiian archipelago. IPMs were created for each genus with all years and sites combined as well as for each site and year interval. The growth model slope (g.slp) and intercept (g.int) were calculated and model fits were chosen based on R^2 values. The survival model slope (s.slp) and intercept (s.int) were calculated for each combination of sites and years. Survival models were chosen based on Adjusted R^2 values.

Site	Sector Name	Inter-val	Genus Code	Region	Growth Transit-ions	Growth Intercept	Growth Slope	Growth Variance	Growth R2	Surv. Transit-ions	Surv. Intercept	Surv. Slope	Surv. R2
FFS_OCC_002	French Frigate	13-16	POSP	NWHI	9	0.262	0.518	0.020	0.807	164	-3.484	0.904	0.023
FFS_OCC_002	French Frigate	16-19	POSP	NWHI	16	0.120	0.781	0.013	0.883	132	-2.147	0.308	0.003
FFS_OCC_014	French Frigate	13-16	POSP	NWHI	22	0.031	0.986	0.012	0.991	30	-1.257	1.743	0.182
FFS_OCC_014	French Frigate	16-19	POSP	NWHI	21	-0.022	0.939	0.043	0.963	65	-2.454	1.475	0.260
HAW_OCC_002	HAW_HAMAKUA	16-19	POSP	MHI	316	0.045	0.874	0.033	0.916	460	0.495	0.494	0.019
HAW_OCC_002	HAW_HAMAKUA	16-19	MOSP	MHI	20	-0.038	0.919	0.028	0.903	35	0.008	0.550	0.016
HAW_OCC_003	HAW_PUNA	16-19	POSP	MHI	37	0.032	0.994	0.004	0.991	51	-4.234	3.587	0.573
HAW_OCC_003	HAW_PUNA	16-19	MOSP	MHI	19	0.221	0.890	0.019	0.940	24	-3.183	2.214	0.274

Site	Sector Name	Inter-val	Genus Code	Region	Growth Transit-ions	Growth Intercept	Growth Slope	Growth Variance	Growth R2	Surv. Transit-ions	Surv. Intercept	Surv. Slope	Surv. R2
HAW_OCC_010	HAW_KONA	16-19	POSP	MHI	118	0.046	0.950	0.018	0.945	214	-2.341	2.077	0.207
HAW_SIO_K08	HAW_KONA	15-17	POSP	MHI	39	0.009	0.878	0.064	0.861	86	-2.531	1.432	0.115
HAW_SIO_K08	HAW_KONA	17-19	POSP	MHI	35	0.206	0.931	0.016	0.966	43	-1.791	3.211	0.360
HAW_SIO_K10	HAW_KONA	15-17	POSP	MHI	66	0.029	0.862	0.078	0.839	128	-2.064	1.160	0.109
HAW_SIO_K10	HAW_KONA	17-19	POSP	MHI	60	0.253	0.902	0.022	0.959	72	-0.003	1.223	0.099
KUR_OCC_010	Kure	16-19	POCS	NWHI	46	0.344	0.877	0.002	0.992	46	26.566	0.000	Inf
KUR_OCC_010	Kure	16-19	POSP	NWHI	21	-0.003	0.950	0.023	0.915	65	-2.101	2.097	0.193
LIS_OCC_005	Lisianski	13-16	POSP	NWHI	25	0.167	0.917	0.021	0.932	42	-2.497	1.850	0.118
LIS_OCC_005	Lisianski	13-16	MOSP	NWHI	31	0.322	0.810	0.018	0.920	74	-2.274	1.285	0.073
LIS_OCC_005	Lisianski	16-19	MOSP	NWHI	36	0.128	0.958	0.015	0.932	46	-0.595	1.260	0.062
MAI_OCC_002	MAI_NE	16-19	POCS	MHI	25	0.437	0.828	0.004	0.985	36	4.618	-1.878	0.157
MAI_OCC_	MAI_NE	16-19	POSP	MHI	24	-0.007	0.937	0.028	0.900	38	0.723	-0.102	0.000

Site	Sector Name	Inter-val	Genus Code	Region	Growth Transit-ions	Growth Intercept	Growth Slope	Growth Variance	Growth R2	Surv. Transit-ions	Surv. Intercept	Surv. Slope	Surv. R2
002													
MAI_SIO_K01	MAI_LA HAINA	14-15	POSP	MHI	114	0.006	1.019	0.043	0.874	117	0.774	2.933	0.138
MAI_SIO_K01	MAI_LA HAINA	14-15	MOSP	MHI	61	0.049	0.965	0.112	0.805	90	-0.634	1.410	0.107
MAI_SIO_K01	MAI_LA HAINA	15-15	MOSP	MHI	48	-0.056	0.899	0.568	0.479	64	-0.353	1.560	0.178
MAI_SIO_K01	MAI_LA HAINA	15-15	POSP	MHI	108	-0.212	1.035	0.173	0.664	118	-1.076	3.695	0.289
MAI_SIO_K01	MAI_LA HAINA	15-16	POSP	MHI	95	0.127	0.927	0.107	0.715	107	-0.527	2.508	0.185
MAI_SIO_K01	MAI_LA HAINA	15-16	MOSP	MHI	34	0.299	0.880	0.101	0.810	45	-0.974	1.977	0.247
MAI_SIO_K01	MAI_LA HAINA	16-16	POSP	MHI	91	0.276	0.818	0.129	0.617	98	-1.313	3.906	0.264
MAI_SIO_K01	MAI_LA HAINA	16-16	MOSP	MHI	37	0.444	0.792	0.409	0.439	46	-1.009	2.289	0.252
MAI_SIO_K01	MAI_LA HAINA	16-17	POSP	MHI	90	-0.009	0.988	0.057	0.833	95	0.019	2.574	0.158
MAI_SIO_K01	MAI_LA HAINA	16-17	MOSP	MHI	41	0.441	0.701	0.244	0.536	43	2.776	0.170	0.002
MAI_SIO_K01	MAI_LA HAINA	17-18	POSP	MHI	86	0.044	0.936	0.045	0.866	97	-1.209	3.045	0.230

Site	Sector Name	Inter-val	Genus Code	Region	Growth Transit-ions	Growth Intercept	Growth Slope	Growth Variance	Growth R2	Surv. Transit-ions	Surv. Intercept	Surv. Slope	Surv. R2
MAI_SIO_K01	MAI_LAHAINA	17-18	MOSP	MHI	25	0.203	0.872	0.032	0.944	45	-1.265	1.113	0.092
MAI_SIO_K02	MAI_LAHAINA	17-18	POSP	MHI	141	0.123	0.885	0.038	0.881	177	-0.426	1.738	0.118
MAI_SIO_K02	MAI_LAHAINA	17-18	MOSP	MHI	27	0.407	0.637	0.090	0.663	37	-0.890	1.399	0.087
MAI_SIO_K02	MAI_LAHAINA	16-17	MOSP	MHI	20	0.294	0.809	0.063	0.822	35	-4.085	3.291	0.333
MAI_SIO_K02	MAI_LAHAINA	16-17	POSP	MHI	132	-0.029	1.014	0.039	0.888	170	-1.246	2.340	0.159
MAI_SIO_K02	MAI_LAHAINA	15-16	MOSP	MHI	20	0.037	0.993	0.036	0.928	29	-1.219	1.341	0.111
MAI_SIO_K02	MAI_LAHAINA	15-16	POSP	MHI	142	0.221	0.833	0.043	0.850	259	-1.544	1.737	0.162
MAI_SIO_K02	MAI_LAHAINA	14-15	POSP	MHI	169	0.083	0.940	0.069	0.807	245	-2.215	3.496	0.369
MAI_SIO_K02	MAI_LAHAINA	14-15	MOSP	MHI	23	0.160	0.883	0.117	0.716	69	-6.003	4.257	0.483
MAI_SIO_OL3	MAI_KIHEI	14-15	MOSP	MHI	129	0.081	0.930	0.131	0.804	226	-1.800	2.180	0.280
MAI_SIO_OL3	MAI_KIHEI	14-15	POSP	MHI	48	0.165	0.945	0.012	0.969	56	-0.772	2.914	0.406
MAI_SIO_	MAI_KI	15-15	MOSP	MHI	109	-0.174	0.987	0.517	0.523	146	-1.692	2.825	0.366

Site	Sector Name	Inter-val	Genus Code	Region	Growth Transit-ions	Growth Intercept	Growth Slope	Growth Variance	Growth R2	Surv. Transit-ions	Surv. Intercept	Surv. Slope	Surv. R2
OL3	HEI												
MAI_SIO_OL3	MAI_KIHEI	15-15	POSP	MHI	34	-0.449	0.789	0.881	0.187	51	-1.980	1.998	0.206
MAI_SIO_OL3	MAI_KIHEI	15-16	MOSP	MHI	99	0.041	0.924	0.192	0.719	124	-1.562	2.903	0.353
MAI_SIO_OL3	MAI_KIHEI	15-16	POSP	MHI	21	0.082	0.847	0.163	0.530	31	-5.248	4.915	0.518
MAI_SIO_OL3	MAI_KIHEI	16-16	MOSP	MHI	104	0.061	0.918	0.400	0.569	122	-0.332	2.164	0.264
MAI_SIO_OL3	MAI_KIHEI	16-16	POSP	MHI	27	0.630	0.677	0.090	0.590	28	1.948	0.944	0.024
MAI_SIO_OL3	MAI_KIHEI	16-17	MOSP	MHI	100	-0.048	0.999	0.134	0.813	137	-1.888	3.173	0.411
MAI_SIO_OL3	MAI_KIHEI	16-17	POSP	MHI	30	-0.069	1.065	0.037	0.924	37	-1.492	3.753	0.497
OAH_OCC_005	OAH_NE	16-18	POCS	MHI	22	0.317	0.871	0.007	0.842	25	-138.648	82.809	Inf
OAH_OCC_005	OAH_NE	16-18	POSP	MHI	50	0.222	0.914	0.020	0.949	57	-1.836	2.642	0.264
OAH_OCC_010	OAH_SOUTH	17-19	POCS	MHI	23	-0.127	1.056	0.022	0.747	29	-11.931	5.758	0.435
OAH_OCC_010	OAH_SOUTH	17-19	POSP	MHI	47	0.059	0.987	0.011	0.973	59	0.005	1.083	0.059

Site	Sector Name	Inter-val	Genus Code	Region	Growth Transit-ions	Growth Intercept	Growth Slope	Growth Variance	Growth R2	Surv. Transit-ions	Surv. Intercept	Surv. Slope	Surv. R2
PHR_OCC_016	Pearl & Hermes	16-19	POSP	NWHI	18	0.048	0.966	0.020	0.969	28	-1.238	1.795	0.250

Supplementary Table 3. Site-level stock recruitment estimates for each of the 16 fixed orthoprojection sites. For each site, a site-level stock recruitment parameter was calculated for each time interval and genus.

Site	Sector Name	Interval	Genus Code	Region	Site-level recruitment
FFS_OCC_002	French Frigate	13-16	MOSP	NWHI	0.017
FFS_OCC_002	French Frigate	13-16	POCS	NWHI	0.012
FFS_OCC_002	French Frigate	13-16	POSP	NWHI	0.016
FFS_OCC_002	French Frigate	16-19	MOSP	NWHI	0.026
FFS_OCC_002	French Frigate	16-19	POCS	NWHI	0.010
FFS_OCC_002	French Frigate	16-19	POSP	NWHI	0.037
FFS_OCC_014	French Frigate	13-16	MOSP	NWHI	0.005
FFS_OCC_014	French Frigate	13-16	POSP	NWHI	0.000
FFS_OCC_014	French Frigate	16-19	MOSP	NWHI	0.004
FFS_OCC_014	French Frigate	16-19	POSP	NWHI	0.000
HAW_OCC_002	HAW_HAMAKUA	16-19	MOSP	MHI	0.018
HAW_OCC_002	HAW_HAMAKUA	16-19	POCS	MHI	0.034
HAW_OCC_002	HAW_HAMAKUA	16-19	POSP	MHI	0.002
HAW_OCC_010	HAW_KONA	16-19	MOSP	MHI	0.025
HAW_OCC_010	HAW_KONA	16-19	POCS	MHI	NA
HAW_OCC_010	HAW_KONA	16-19	POSP	MHI	0.003
HAW_SIO_K08	HAW_KONA	15-17	POSP	MHI	0.000
HAW_SIO_K08	HAW_KONA	17-19	POSP	MHI	0.001
HAW_SIO_K10	HAW_KONA	15-17	POSP	MHI	0.000
HAW_SIO_K10	HAW_KONA	17-19	POSP	MHI	0.000
HAW_OCC_003	HAW_PUNA	16-19	MOSP	MHI	0.001
HAW_OCC_003	HAW_PUNA	16-19	POCS	MHI	0.000
HAW_OCC_003	HAW_PUNA	16-19	POSP	MHI	0.000
KUR_OCC_010	Kure	16-19	POCS	NWHI	0.000
KUR_OCC_010	Kure	16-19	POSP	NWHI	0.008
LIS_OCC_005	Lisianski	13-16	MOSP	NWHI	0.001
LIS_OCC_005	Lisianski	13-16	POSP	NWHI	0.001

Site	Sector Name	Interval	Genus Code	Region	Site-level recruitment
LIS_OCC_005	Lisianski	16-19	MOSP	NWHI	0.003
LIS_OCC_005	Lisianski	16-19	POSP	NWHI	0.001
MAI_SIO_OL3	MAI_KIHEI	14-15	MOSP	MHI	0.001
MAI_SIO_OL3	MAI_KIHEI	14-15	POCS	MHI	0.002
MAI_SIO_OL3	MAI_KIHEI	14-15	POSP	MHI	0.001
MAI_SIO_OL3	MAI_KIHEI	15-15	MOSP	MHI	0.001
MAI_SIO_OL3	MAI_KIHEI	15-16	MOSP	MHI	0.002
MAI_SIO_OL3	MAI_KIHEI	15-16	POSP	MHI	0.001
MAI_SIO_OL3	MAI_KIHEI	16-16	MOSP	MHI	0.002
MAI_SIO_OL3	MAI_KIHEI	16-16	POSP	MHI	0.011
MAI_SIO_OL3	MAI_KIHEI	16-17	MOSP	MHI	0.002
MAI_SIO_OL3	MAI_KIHEI	16-17	POSP	MHI	0.006
MAI_SIO_K01	MAI_LAHAINA	14-15	MOSP	MHI	0.002
MAI_SIO_K01	MAI_LAHAINA	14-15	POSP	MHI	0.001
MAI_SIO_K01	MAI_LAHAINA	15-15	MOSP	MHI	0.001
MAI_SIO_K01	MAI_LAHAINA	15-16	MOSP	MHI	0.004
MAI_SIO_K01	MAI_LAHAINA	15-16	POSP	MHI	0.001
MAI_SIO_K01	MAI_LAHAINA	16-16	MOSP	MHI	0.001
MAI_SIO_K01	MAI_LAHAINA	16-16	POSP	MHI	0.001
MAI_SIO_K01	MAI_LAHAINA	16-17	MOSP	MHI	0.001
MAI_SIO_K01	MAI_LAHAINA	16-17	POSP	MHI	0.002
MAI_SIO_K01	MAI_LAHAINA	17-18	MOSP	MHI	0.001
MAI_SIO_K01	MAI_LAHAINA	17-18	POSP	MHI	0.001
MAI_SIO_K02	MAI_LAHAINA	14-15	MOSP	MHI	0.001
MAI_SIO_K02	MAI_LAHAINA	14-15	POSP	MHI	0.008
MAI_SIO_K02	MAI_LAHAINA	15-16	MOSP	MHI	0.004
MAI_SIO_K02	MAI_LAHAINA	15-16	POSP	MHI	0.002
MAI_SIO_K02	MAI_LAHAINA	16-17	MOSP	MHI	0.003
MAI_SIO_K02	MAI_LAHAINA	16-17	POCS	MHI	0.015
MAI_SIO_K02	MAI_LAHAINA	16-17	POSP	MHI	0.005

Site	Sector Name	Interval	Genus Code	Region	Site-level recruitment
MAI_SIO_K02	MAI_LAHAINA	17-18	MOSP	MHI	0.008
MAI_SIO_K02	MAI_LAHAINA	17-18	POCS	MHI	0.017
MAI_SIO_K02	MAI_LAHAINA	17-18	POSP	MHI	0.008
MAI_OCC_002	MAI_NE	16-19	POCS	MHI	0.002
MAI_OCC_002	MAI_NE	16-19	POSP	MHI	0.008
OAH_OCC_005	OAH_NE	16-18	MOSP	MHI	0.003
OAH_OCC_005	OAH_NE	16-18	POSP	MHI	0.000
OAH_OCC_010	OAH_SOUTH	17-19	POCS	MHI	0.000
OAH_OCC_010	OAH_SOUTH	17-19	POSP	MHI	0.002
PHR_OCC_016	Pearl & Hermes	16-19	POSP	NWHI	0.001

Supplementary Table 4. Site-level stock recruitment estimates for each genus and region and the lower and upper confidence intervals (CI).

Genus Code	Region	Mean Site-Level Recruitment	5% CI	95% CI
MOSP	MHI	0.004	0.001	0.019
MOSP	NWHI	0.009	0.002	0.024
POCS	MHI	0.010	0.000	0.029
POCS	NWHI	0.007	0.001	0.012
POSP	MHI	0.003	0.000	0.008
POSP	NWHI	0.008	0.000	0.030

Supplementary Table 5. Sector-level stock recruitment and the lower and upper confidence intervals (CI) for every sector containing one of the 16 study sites. Sectors with no cover data are labeled 'Inf' for the mean recruitment. Sectors with no juvenile colonies have a mean recruitment value of 0.

Sector	Observation Year	Genus Code	Region	Mean Sector-Level Recruitment	5% CI	95% CI
HAW_HAMAKUA	2013	MOSP	MHI	0.027	-0.003	0.057
HAW_HAMAKUA	2013	POCS	MHI	0.002	0.000	0.004
HAW_HAMAKUA	2013	POSP	MHI	0.005	0.003	0.007
HAW_KONA	2013	MOSP	MHI	0.008	0.005	0.011
HAW_KONA	2013	POCS	MHI	0.003	0.002	0.005
HAW_KONA	2013	POSP	MHI	0.000	0.000	0.001
HAW_PUNA	2013	MOSP	MHI	0.001	0.000	0.002
HAW_PUNA	2013	POCS	MHI	0.001	0.000	0.001
HAW_PUNA	2013	POSP	MHI	0.001	0.000	0.002
MAI_KIHEI	2013	MOSP	MHI	0.000	0.000	0.001
MAI_KIHEI	2013	POCS	MHI	0.000	NA	NA
MAI_KIHEI	2013	POSP	MHI	0.000	0.000	0.000
MAI_NE	2013	MOSP	MHI	0.021	-0.014	0.057
MAI_NE	2013	POCS	MHI	0.002	-0.001	0.005
MAI_NE	2013	POSP	MHI	0.005	0.000	0.011
OAH_NE	2013	MOSP	MHI	0.002	0.001	0.003
OAH_NE	2013	POCS	MHI	0.002	0.001	0.003
OAH_NE	2013	POSP	MHI	0.002	0.001	0.002
OAH_SOUTH	2013	MOSP	MHI	0.004	0.001	0.008
OAH_SOUTH	2013	POCS	MHI	0.005	0.002	0.008
OAH_SOUTH	2013	POSP	MHI	0.003	0.002	0.004
HAW_KONA	2016	MOSP	MHI	0.020	0.011	0.028
HAW_KONA	2016	POCS	MHI	0.015	-0.003	0.033
HAW_KONA	2016	POSP	MHI	0.001	0.000	0.001
HAW_PUNA	2016	MOSP	MHI	0.002	0.001	0.004
HAW_PUNA	2016	POCS	MHI	0.007	0.001	0.012

Sector	Observation Year	Genus Code	Region	Mean Sector-Level Recruitment	5% CI	95% CI
HAW_PUNA	2016	POSP	MHI	0.002	0.000	0.004
MAI_KIHEI	2016	MOSP	MHI	0.001	0.000	0.002
MAI_KIHEI	2016	POCS	MHI	0.019	-0.011	0.050
MAI_KIHEI	2016	POSP	MHI	0.000	0.000	0.000
MAI_LAHAINA	2016	MOSP	MHI	0.073	0.029	0.117
MAI_LAHAINA	2016	POCS	MHI	0.000	NA	NA
MAI_LAHAINA	2016	POSP	MHI	0.001	0.000	0.001
MAI_NE	2016	MOSP	MHI	0.005	0.000	0.009
MAI_NE	2016	POCS	MHI	0.019	0.002	0.035
MAI_NE	2016	POSP	MHI	0.004	0.003	0.005
OAH_NE	2016	MOSP	MHI	0.002	0.001	0.003
OAH_NE	2016	POCS	MHI	0.004	0.000	0.008
OAH_NE	2016	POSP	MHI	0.001	0.001	0.001
OAH_SOUTH	2016	MOSP	MHI	0.013	0.003	0.022
OAH_SOUTH	2016	POCS	MHI	0.009	0.004	0.013
OAH_SOUTH	2016	POSP	MHI	0.006	0.002	0.011
HAW_HAMAKUA	2019	MOSP	MHI	0.011	0.003	0.019
HAW_HAMAKUA	2019	POCS	MHI	0.009	0.002	0.017
HAW_HAMAKUA	2019	POSP	MHI	0.004	0.001	0.006
HAW_KONA	2019	MOSP	MHI	0.029	0.015	0.044
HAW_KONA	2019	POCS	MHI	0.115	-0.095	0.325
HAW_KONA	2019	POSP	MHI	0.001	0.001	0.002
HAW_PUNA	2019	MOSP	MHI	0.037	0.013	0.060
HAW_PUNA	2019	POCS	MHI	0.013	0.005	0.020
HAW_PUNA	2019	POSP	MHI	0.007	0.003	0.011
MAI_KIHEI	2019	MOSP	MHI	0.002	0.000	0.005
MAI_KIHEI	2019	POCS	MHI	0.019	-0.006	0.044
MAI_KIHEI	2019	POSP	MHI	0.000	0.000	0.000
MAI_LAHAINA	2019	MOSP	MHI	0.001	0.000	0.002

Sector	Observation Year	Genus Code	Region	Mean Sector-Level Recruitment	5% CI	95% CI
MAI_LAHAINA	2019	POCS	MHI	0.017	-0.007	0.042
MAI_LAHAINA	2019	POSP	MHI	0.001	0.001	0.002
MAI_NE	2019	MOSP	MHI	0.235	0.091	0.380
MAI_NE	2019	POCS	MHI	0.002	-0.002	0.007
MAI_NE	2019	POSP	MHI	0.010	-0.001	0.020
OAH_NE	2019	MOSP	MHI	0.014	0.002	0.026
OAH_NE	2019	POCS	MHI	0.010	0.004	0.016
OAH_NE	2019	POSP	MHI	0.004	0.001	0.008
OAH_SOUTH	2019	MOSP	MHI	0.008	-0.001	0.017
OAH_SOUTH	2019	POCS	MHI	0.006	0.001	0.011
OAH_SOUTH	2019	POSP	MHI	0.005	0.002	0.009
French Frigate	2016	MOSP	NWHI	0.019	0.008	0.030
French Frigate	2016	POCS	NWHI	0.016	0.005	0.026
French Frigate	2016	POSP	NWHI	0.001	0.000	0.001
Kure	2016	MOSP	NWHI	Inf	NA	NA
Kure	2016	POCS	NWHI	0.002	0.001	0.003
Kure	2016	POSP	NWHI	0.005	0.002	0.007
Lisianski	2016	MOSP	NWHI	0.002	0.001	0.003
Lisianski	2016	POCS	NWHI	Inf	NA	NA
Lisianski	2016	POSP	NWHI	0.000	0.000	0.001
Pearl & Hermes	2016	MOSP	NWHI	0.112	-0.021	0.245
Pearl & Hermes	2016	POCS	NWHI	0.011	0.000	0.022
Pearl & Hermes	2016	POSP	NWHI	0.004	0.003	0.005

Supplementary Table 6. Population growth rates (λ) for every site, time interval and genus. Lambda values were calculated using the site-level, sector-level, and all-sectors stock recruitment methods and lower and upper confidence intervals (CI).

Site	Sector Name	Inter-val	Genus Code	Region	Site-Level	Sector-Level	5% CI Sector-Level	95% CI Sector Level	All-Sectors	5% CI All-Sectors	95% CI All-Sectors
FFS_OCC_002	French Frigate	13-16	POSP	NWHI	NA	NA	NA	NA	0.374	0.372	0.375
FFS_OCC_002	French Frigate	16-19	POSP	NWHI	0.504	0.488	0.487	0.488	0.490	0.488	0.491
FFS_OCC_014	French Frigate	13-16	POSP	NWHI	NA	NA	NA	NA	0.985	0.985	0.985
FFS_OCC_014	French Frigate	16-19	POSP	NWHI	0.658	0.658	0.658	0.658	0.658	0.658	0.658
HAW_OCC_002	HAW_HAMAKUA	16-19	POSP	MHI	NA	NA	NA	NA	0.871	0.869	0.872
HAW_OCC_002	HAW_HAMAKUA	16-19	MOSP	MHI	NA	NA	NA	NA	0.752	0.751	0.753
HAW_OCC_003	HAW_PUNA	16-19	POSP	MHI	NA	1.000	1.000	1.000	1.000	1.000	1.000
HAW_OCC_003	HAW_PUNA	16-19	MOSP	MHI	NA	0.926	0.925	0.926	0.927	0.925	0.928
HAW_OCC_010	HAW_KONA	16-19	POSP	MHI	NA	0.865	0.865	0.865	0.865	0.865	0.865
HAW_SIO_K08	HAW_KONA	15-17	POSP	MHI	NA	NA	NA	NA	0.495	0.495	0.495
HAW_SIO_K08	HAW_KONA	17-19	POSP	MHI	1.003	NA	NA	NA	1.033	1.013	1.043
HAW_SIO_K10	HAW_KONA	15-17	POSP	MHI	NA	NA	NA	NA	0.515	0.515	0.515
HAW_SIO_K10	HAW_KONA	17-19	POSP	MHI	0.983	NA	NA	NA	1.033	1.002	1.048
KUR_OCC_010	Kure	16-19	POCS	NWHI	NA	1.123	1.110	1.134	1.206	1.110	1.263
KUR_OCC_010	Kure	16-19	POSP	NWHI	NA	0.774	0.774	0.774	0.774	0.774	0.774

Site	Sector Name	Inter-val	Genus Code	Region	Site-Level	Sector-Level	5% CI Sector-Level	95% CI Sector Level	All-Sectors	5% CI All-Sectors	95% CI All-Sectors
LIS_OC C_005	Lisianski	13-16	POSP	NWHI	NA	NA	NA	NA	0.929	0.928	0.929
LIS_OC C_005	Lisianski	13-16	MOSP	NWHI	NA	NA	NA	NA	0.827	0.792	0.843
LIS_OC C_005	Lisianski	16-19	MOSP	NWHI	1.001	1.003	0.997	1.007	1.039	0.997	1.049
MAI_OC C_002	MAI_NE	16-19	POCS	MHI	NA	1.166	0.957	1.251	1.045	0.793	1.104
MAI_OC C_002	MAI_NE	16-19	POSP	MHI	NA	0.824	0.823	0.824	0.823	0.822	0.824
MAI_SI O_K01	MAI_LA HAINA	14-15	POSP	MHI	NA	NA	NA	NA	1.030	1.005	1.040
MAI_SI O_K01	MAI_LA HAINA	14-15	MOSP	MHI	NA	NA	NA	NA	0.949	0.937	0.955
MAI_SI O_K01	MAI_LA HAINA	15-15	MOSP	MHI	0.794	NA	NA	NA	0.853	0.770	0.882
MAI_SI O_K01	MAI_LA HAINA	15-15	POSP	MHI	0.913	NA	NA	NA	0.913	0.913	0.913
MAI_SI O_K01	MAI_LA HAINA	15-16	POSP	MHI	NA	NA	NA	NA	0.973	0.966	0.978
MAI_SI O_K01	MAI_LA HAINA	15-16	MOSP	MHI	0.967	NA	NA	NA	1.000	0.965	1.013
MAI_SI O_K01	MAI_LA HAINA	16-16	POSP	MHI	0.949	0.949	0.948	0.949	0.954	0.949	0.958
MAI_SI O_K01	MAI_LA HAINA	16-16	MOSP	MHI	1.097	1.582	1.369	1.719	1.164	0.964	1.222
MAI_SI O_K01	MAI_LA HAINA	16-17	POSP	MHI	0.971	0.971	0.971	0.971	0.971	0.971	0.972
MAI_SI O_K01	MAI_LA HAINA	16-17	MOSP	MHI	0.962	1.411	1.237	1.527	1.079	0.949	1.122
MAI_SI O_K01	MAI_LA HAINA	17-18	POSP	MHI	0.914	NA	NA	NA	0.914	0.914	0.914
MAI_SI O_K01	MAI_LA HAINA	17-18	MOSP	MHI	0.711	NA	NA	NA	0.712	0.711	0.713
MAI_SI	MAI_LA	17-18	POSP	MHI	0.866	NA	NA	NA	0.865	0.865	0.866

Site	Sector Name	Inter-val	Genus Code	Region	Site-Level	Sector-Level	5% CI Sector-Level	95% CI Sector-Level	All-Sectors	5% CI All-Sectors	95% CI All-Sectors
O_K02	HAINA										
MAI_SIO_K02	MAI_LA HAINA	17-18	MOSP	MHI	0.719	NA	NA	NA	0.733	0.711	0.744
MAI_SIO_K02	MAI_LA HAINA	16-17	MOSP	MHI	0.829	0.831	0.830	0.833	0.829	0.829	0.829
MAI_SIO_K02	MAI_LA HAINA	16-17	POSP	MHI	0.972	0.972	0.972	0.972	0.972	0.972	0.972
MAI_SIO_K02	MAI_LA HAINA	15-16	MOSP	MHI	0.957	NA	NA	NA	0.958	0.957	0.958
MAI_SIO_K02	MAI_LA HAINA	15-16	POSP	MHI	0.748	NA	NA	NA	0.748	0.748	0.748
MAI_SIO_K02	MAI_LA HAINA	14-15	POSP	MHI	NA	NA	NA	NA	0.958	0.958	0.958
MAI_SIO_K02	MAI_LA HAINA	14-15	MOSP	MHI	NA	NA	NA	NA	0.865	0.865	0.865
MAI_SIO_OL3	MAI_KI HEI	14-15	MOSP	MHI	NA	NA	NA	NA	0.914	0.909	0.917
MAI_SIO_OL3	MAI_KI HEI	14-15	POSP	MHI	NA	NA	NA	NA	1.012	1.003	1.016
MAI_SIO_OL3	MAI_KI HEI	15-15	MOSP	MHI	0.850	NA	NA	NA	0.908	0.849	0.930
MAI_SIO_OL3	MAI_KI HEI	15-15	POSP	MHI	0.397	NA	NA	NA	0.404	0.393	0.413
MAI_SIO_OL3	MAI_KI HEI	15-16	MOSP	MHI	0.901	NA	NA	NA	0.911	0.900	0.917
MAI_SIO_OL3	MAI_KI HEI	15-16	POSP	MHI	NA	NA	NA	NA	0.751	0.751	0.751
MAI_SIO_OL3	MAI_KI HEI	16-16	MOSP	MHI	0.944	0.925	0.893	0.947	1.029	0.917	1.063
MAI_SIO_OL3	MAI_KI HEI	16-16	POSP	MHI	0.977	0.960	0.950	0.970	1.025	0.973	1.056
MAI_SIO_OL3	MAI_KI HEI	16-17	MOSP	MHI	0.954	0.953	0.953	0.954	0.958	0.953	0.960
MAI_SIO_OL3	MAI_KI HEI	16-17	POSP	MHI	0.902	0.888	0.887	0.888	0.892	0.889	0.895

Site	Sector Name	Inter-val	Genus Code	Region	Site-Level	Sector-Level	5% CI Sector-Level	95% CI Sector Level	All-Sectors	5% CI All-Sectors	95% CI All-Sectors
OAH_OCC_005	OAH_NE	16-18	POCS	MHI	NA	1.000	1.000	1.000	1.000	1.000	1.000
OAH_OCC_005	OAH_NE	16-18	POSP	MHI	NA	1.002	0.999	1.004	1.010	1.000	1.017
OAH_OCC_010	OAH_SOUTH	17-19	POCS	MHI	NA	NA	NA	NA	0.901	0.901	0.901
OAH_OCC_010	OAH_SOUTH	17-19	POSP	MHI	NA	NA	NA	NA	1.002	0.994	1.005
PHR_OCC_016	Pearl & Hermes	16-19	POSP	NWHI	NA	0.954	0.954	0.954	0.954	0.954	0.954

APPENDIX C

ALL THERMAL STRESS MODEL RESULTS

Supplementary Table 7. Multiple-regression model ANOVA table for *Porites* and *Montipora* corals with lambda as the response variable. *Denotes thermal stress factors that are significant at p < 0.05 and (Int) denotes interactions terms.

Model	Explanatory Variables	BIC	Num df	Adjusted R2	Regression ANOVA
Porites	Major_Freq _YR10, Severity_YR10	-15.854	4	0.272	p<0.05*
Porites	Major_Freq_YR10, Severity_AllPriorYears	-14.680	4	0.243	p<0.05*
Porites	Freq_YR10, Severity_YR10	-13.841	4	0.202	p<0.05*
Porites	Severity_AllPriorYears	-13.097	3	0.159	p<0.05*
Porites	Freq_YR10, Severity_YR10	-13.097	4	0.202	p<0.05*
Porites	Major_Freq_YR10	-13.044	3	0.136	p<0.05*
Porites	Severity_YR10	-12.873	3	0.132	p<0.05*
Porites	Freq_YR10, Severity_AllPriorYears	-12.406	4	0.183	p<0.05*
Porites	Freq_AllPriorYears, Severity_AllPriorYears	-11.416	4	0.156	p<0.05*
Porites	Major_Freq_YR10, Major_Severity_YR10	-10.598	4	0.133	0.056
Porites	Freq_YR10, Severity_YR10 (Int)	-10.527	5	0.194	p<0.05*
Porites	Major_Freq_AllPriorYears	-10.128	3	0.048	0.127
Porites	Freq_YR10	-9.483	3	0.028	0.188
Porites	Major_Severity_AllPriorYears	-8.849	3	0.0068	0.283
Porites	Major_Severity_YR10	-8.819	3	0.0058	0.289
Porites	Major_Freq_YR10, Major_Severity_YR10 (Int)	-8.678	5	0.143	0.073
Porites	Freq_AllPriorYears, Severity_AllPriorYears (Int)	-8.218	5	0.129	0.087
Porites	Freq_AllPriorYears	-8.195	3	-0.015	0.456
Porites	Major_Freq_AllPriorYears, Major_Severity_AllPriorYears	-7.882	4	0.050	0.19

Model	Explanatory Variables	BIC	Num df	Adjusted R2	Regression ANOVA
Porites	Major_Freq_AllPriorYears, Major_Severity_AllPriorYears (Int)	-5.456	5	0.045	0.249
Montipora	Freq_YR10	-19.696	3	-0.043	0.623
Montipora	Freq_AllPriorYears	-19.634	3	-0.047	0.664
Montipora	Severity_AllPriorYears	-19.522	3	-0.053	0.763
Montipora	Major_Freq_AllPriorYears	-19.472	3	-0.056	0.829
Montipora	Major_Freq_YR10	-19.464	3	-0.056	0.841
Montipora	Major_Severity _YR10	-19.426	3	-0.058	0.933
Montipora	Major_Severity _AllPriorYears	-19.426	3	-0.058	0.933
Montipora	Severity_YR10	-19.426	3	-0.058	0.934
Montipora	Major_Freq_AllPriorYears, Severity_AllPriorYears (Int)	-17.183	4	-0.084	0.742
Montipora	Major_Freq_YR10, Severity_AllPriorYears	-17.135	4	-0.086	0.757
Montipora	Freq_YR10, Severity_AllPriorYears	-16.900	4	-0.099	0.835
Montipora	Freq_AllPriorYears, Severity_AllPriorYears	-16.782	4	-0.107	0.878
Montipora	Freq_AllPriorYears, Severity_AllPriorYears	-16.782	4	-0.107	0.878
Montipora	Freq_YR10, Severity_YR10	-16.762	4	-0.108	0.885
Montipora	Major_Freq_AllPriorYears, Major_Severity_AllPriorYears	-16.533	4	-0.121	0.975
Montipora	Major_Freq_YR10, Major_Severity_YR10	-16.524	4	-0.122	0.979
Montipora	Major_Freq_YR10, Major_Severity_YR10 (Int)	-15.369	5	-0.089	0.682
Montipora	Freq_YR10, Severity_YR10 (int)	-14.162	5	-0.161	0.915
Montipora	Freq_AllPriorYears, Severity_AllPriorYears (Int)	-13.929	5	-0.175	0.955

Model	Explanatory Variables	BIC	Num df	Adjusted R2	Regression ANOVA
Montipora	Major_Freq_AllPriorYears, Major_Severity_AllPriorYears (Int)	-13.711	5	-0.189	0.985